Department of Neuroscience
Karolinska Institutet, Stockholm, Sweden

WHITE MATTER CONNECTIONS

Developmental neuroimaging studies of the associations between genes, brain and behavior

Fahimeh Darki

Karolinska Institutet

Stockholm 2014

Published by Karolinska Institutet.
Printed by Larserics Digital Print AB

ISBN 978-91-7549-625-2

WHITE MATTER CONNECTIONS

DEVELOPMENTAL NEUROIMAGING STUDIES OF THE ASSOCIATIONS BETWEEN GENES, BRAIN AND BEHAVIOR

THESIS FOR DOCTORAL DEGREE (Ph.D.)

By

Fahimeh Darki

Principal Supervisor:
Professor Torkel Klingberg
Karolinska Institutet
Department of Neuroscience
Division of Cognitive Neuroscience

Co-supervisor(s):
Professor Tie-Qiang Li
Karolinska University Hospital
Department of Medical Physics

Opponent:
Doctor Robert F. Dougherty
Stanford University
Stanford Center for Cognitive and Neurobiological Imaging

Examination Board:
Docent Stefan Skare
Karolinska Institutet
Department of Clinical Neuroscience

Professor Stefan Samuelsson
Linköping University
Department of Behavioural Sciences and Learning

Professor Fredrik Ullén
Karolinska Institutet
Department of Neuroscience
Division of Cognitive Neuroscience

You cannot hope to build a better world without improving the individuals.
To that end each of us must work for his own improvement,
and at the same time share a general responsibility for all humanity,
our particular duty being to aid those to whom we think we can be most useful.

Marie Curie

To my beloved mother and father

ABSTRACT

Development of cognitive abilities across childhood and adulthood parallels brain maturation in typically developing samples. Cognitive abilities such as reading and working memory have been linked to neuroimaging measures in relevant brain regions. Though the correlations between inter-individual brain differences and their related cognitive abilities are well established, the cause of this inter-individual variability is still not fully known. This thesis aims to understand the neural bases of the inter-individual variability in reading ability by studying the associations between dyslexia susceptibility genes and white and gray matter brain structures, and determine whether the measures of associated regions correlate with variability in reading ability. Moreover, it aims to identify the brain measures that correlate with concurrent measures of working memory and those that are predictive of future working memory, using a longitudinal cohort of typically developing children and young adults.

Studies I and II: Three genes, *DYX1C1*, *DCDC2* and *KIAA0319*, have been previously associated with dyslexia, neuronal migration, and ciliary function. We investigated whether the polymorphisms within these genes would affect variability in white and gray matter brain structures. Rs3743204 (*DYX1C1*), rs793842 (*DCDC2*), and rs6935076 (*KIAA0319*) were associated with left temporo-parietal white matter volume connecting middle temporal cortex to angular and supramarginal gyri as well as lateral occipital cortex. Rs793842 was significantly associated with thickness of left parietal areas and the lateral occipital cortex. Both white and gray matter measures correlated with current reading ability, but only white matter predicted future reading.

Study III: We aimed to investigate whether *MRPL19/C2ORF3* dyslexia genes, found to be correlated with verbal and non-verbal IQ, have a significant influence on white matter brain structures. Rs917235 showed a significant association with white matter volume in bilateral posterior parts of the corpus callosum and the cingulum, with connections to parietal, occipital and temporal cortices that are involved in both language and general cognitive abilities.

Study IV: *ROBO1* is a dyslexia gene that has been associated with axonal guidance and midline crossing. We assessed whether the polymorphisms within this gene have an influence on structure of the corpus callosum. Rs7631357 was associated with probability of connections within the fibers extending through the body of corpus callosum to parietal brain regions. The results fit well with previous reports on the role of Robo1 in axonal path finding in mice.

Study V: Working memory has been associated with greater brain activity, thinner cortex, and white matter maturation in cross-sectional studies of children and young adults. Here, we aimed to investigate the role of differences in brain structure and function in the development of working memory. We assessed the concurrent and predictive relationships between working memory performance and neuroimaging measures in the fronto-parietal and fronto-striatal networks important for working memory. Working memory performance correlated with brain activity in frontal and parietal regions, cortical thickness in parietal cortex, and white matter volume of fronto-parietal and fronto-striatal tracts. White matter microstructure and brain activity in the caudate predicted future working memory.

This work highlights the impact of imaging genetics research, revealing important associations between genes, brain and behavior. The results identify the neural mechanism underlying two cognitive abilities, reading and working memory. Specifically, the findings identify the important role of white matter in driving the development of working memory and reading ability, connecting the related cortical areas, as well as bridging the gap between genes and behavior.

LIST OF PUBLICATIONS

I. **Darki F.**, Peyrard-Janvid M., Matsson H., Kere J., Klingberg T. (2012). Three dyslexia susceptibility genes, *DYX1C1*, *DCDC2*, and *KIAA0319*, affect temporo-parietal white matter structure. *Biol Psychiatry*. 15;72(8):671-6.

II. **Darki F.**, Peyrard-Janvid M., Matsson H., Kere J., Klingberg T. *DCDC2* polymorphism is associated with left temporoparietal gray and white matter structures during development, *J Neurosci.*, in press.

III. Scerri T.S., **Darki F.**, Newbury D.F., Whitehouse A.J., Peyrard-Janvid M., Matsson H., Ang Q.W., Pennell C.E., Ring S., Stein J., Morris A.P., Monaco A.P., Kere J., Talcott J.B., Klingberg T., Paracchini S. (2012). The dyslexia candidate locus on 2p12 is associated with general cognitive ability and white matter structure. *PLoS One*. 7(11):e50321.

IV. **Darki F.***, Massinen S.*, Salmela E., Matsson H., Peyrard-Janvid M., Klingberg T., Kere J. Human *ROBO1* regulates white matter structure in corpus callosum. under review.
* Authors contributed equally

V. **Darki F.**, Klingberg T. (2014). The role of fronto-parietal and fronto-striatal networks in the development of working memory: a longitudinal study. *Cereb. Cortex*; doi: 10.1093/cercor/bht352.

CONTENTS

LIST OF ABBREVIATIONS

MRI	Magnetic resonance imaging
CSF	Cerebrospinal fluid
DTI	Diffusion tensor imaging
FA	Fractional anisotropy
ROI	Region of interest
fMRI	Functional magnetic resonance imaging
BOLD	Blood-oxygen-level dependent
DYX1C1	*D*yslexia susceptibility 1 candidate 1
DCDC2	Doublecortin domain containing 2
C2ORF3	GC-rich sequence DNA-binding factor 2
MRPL19	Mitochondrial ribosomal protein L19
ROBO1	Roundabout homolog 1
PET	Positron emission tomography
ADHD	Attention Deficit Hyperactivity Disorder
A	Adenine
T	Thymine
C	Cytosine
G	Guanine
SNP	Single nucleotide polymorphism
FOV	Field of view
TR	Repetition time
TE	Echo time
VBM	Voxel-based morphometry
DARTEL	Diffeomorphic anatomical registration through exponentiated lie algebra
MNI	Montreal Neurological Institute
FDR	False discovery rate
TBSS	Tract-Based Spatial Statistics

1 INTRODUCTION

1.1 IMAGING GENETICS

Imaging genetics studies explore how genetic variations lead to inter-individual differences in brain structure and function, which in turn influences behavior and cognitive function. Imaging genetics studies resemble genetic association studies in their attempt to identify associations between genetic markers and brain phenotypes such as structure, chemistry and function. Despite that both imaging genetics studies and association studies following similar approaches in terms of data analyses, the phenotypes in imaging genetics are not necessarily disease symptoms, such as psychological and behavioral disorders. In imaging genetics analyses the phenotypes can be the brain measures of healthy individuals and the risk allele is associated with the end distribution of a continuum of normal brain structure or function.

1.1.1 Genetics

Successful sequencing of the human genome in combination with advances in molecular and behavioral genetics studies provides new opportunities to investigate the function of genes. Molecular genetics researchers aim to identify gene functions and expression-levels based on genetic effects on the cells physiology, morphology or level of expression. Behavioral genetics studies, on the other hand, have attempted to determine the link between genes and behavior, as well as the clinical or psychiatric symptoms. To bridge the gap between the molecular level and the behavioral outcome, the neuroimaging techniques have been used as intermediate phenotypes in imaging genetics studies.

1.1.2 Neuroimaging

Neuroimaging techniques provide in-vivo information for investigating the anatomy and function of the brain. Magnetic resonance imaging (MRI) is the most common neuroimaging technique which is safe and it provides high resolution images with good contrast. MRI uses strong magnetic field and two radiofrequency coils, the transmitter and receiver. It works based on radio waves which are non-ionizing and harmless, especially, in longitudinal studies that require repeated scanning.

T1-weighted imaging is a structural imaging sequence that provides proper contrast between different tissues in the brain, including gray matter, white matter and cerebrospinal fluid (CSF). The typical spatial resolution of the structural MRI data is approximately 1 mm^3, though it can be acquired with smaller voxel sizes. Structural MRI data is suitable for anatomical segmentation. Neuroimaging analysis toolboxes segment the structural data into gray matter, white matter and CSF; and they measure the volume of the segmented regions. Thickness, surface and curvature of the cortex can also be computed using structural imaging analysis tools.

Diffusion tensor imaging (DTI) is also a non-invasive imaging technique that is sensitive to diffusion of water molecules. Diffusion or random displacement of molecules is a physical phenomenon that occurs naturally. In isotropic environments,

diffusion is free and equal in all directions. However, in biological tissues such as white matter, diffusion is restricted by some obstacles including cell membranes, myelin sheaths and some macromolecules. Diffusion of water molecules in white matter is faster along the axons rather than the perpendicular directions. Thus, mapping the magnitude and direction of diffusion gives some information about the microstructure and architecture of white matter fibers. DTI uses tensor models to map the diffusion in brain voxels. Tensor is a 3×3 matrix and is a mathematical model of ellipsoid, which estimates the magnitude and direction of diffusion with three eigenvalues and three eigenvectors. Several quantitative indices including mean diffusivity (MD), fractional anisotropy (FA), axial diffusivity (AD) and radial diffusivity (RD) are computed from the tensors' estimated parameters. FA is the most common index and it ranges from 0 when there is no preferred direction for diffusion to 1 when the preferred direction is along one axis. The preferred direction is called the principal eigenvector and its estimated direction is a base for white matter fiber tracking or tractography. Tractography is a technique that creates three-dimensional visualizations of white matter tracts and can be performed by several tracking algorithms. Fiber tracking commonly starts from a seed or region of interest (ROI) and it follows the direction of the principal eigenvector in order to find the connectivity between different regions. DTI provides details about white matter microstructure and architecture both quantitatively and visually that can be used as phenotypes for imaging genetics studies.

In addition to the MRI techniques that collect information about brain structure and anatomy, functional MRI (fMRI) gives information about function of the brain. fMRI measures the blood-oxygen-level dependent (BOLD) signal based on the fact that blood flow and oxygen consumption increase in an active region. BOLD contrast is the difference in magnetization of oxygenated and deoxygenated blood. Based on different tasks presented in MRI scanner, different regions in the brain become active and BOLD signal is collected. Functional information of the active regions can be used as phenotypes by imaging genetics researchers.

1.1.3 Longitudinal imaging genetics

Most imaging genetics studies have been performed within a restricted age range and commonly during adulthood. However, the brain continues to restructure itself across the lifespan and genetic effects are likely dissimilar in different times during development (Johnson et al., 2009; Zhang et al., 2011). Thus, it is very important to identify the developmental brain changing patterns and to study whether the influence of genetic markers on brain structure or function is driven by their interaction with age or the genes have a static effect across different ages. Longitudinal imaging genetics studies provide information regarding how genetic markers affect the brain throughout development.

1.2 CHILDHOOD DEVELOPMENT

Childhood development refers to the development of biological, psychological and cognitive changes that commence after birth and continue through to adolescence. In children, cognitive development and brain maturation take place in parallel (Casey et al., 2000; Sowell et al., 2001; Spear, 2000). The developmental changes are likely to be

genetically driven (Johnson et al., 2009; Zhang et al., 2011), but also are influenced by environmental factors and inter-individuals experiences (Lewis, 2005).

1.2.1 Development of the brain

The cells that give rise to the cortex form the neural tube and subventricular zone in the third gestational week. The formation of neurons that will build the brain, known as neurogenesis, is a process that continues until the fifth month of gestation, with the exception of the hippocampus, which has been shown to produce neurons even in adulthood. After neurogenesis, a process called neuronal migration brings different types of neurons to their appropriate location so that the neurons can interact properly. Once the neurons reach their final positions, dendrites start growing to synapse with other cells, and axons start extending to reach their targets. The process of sending axons to reach their targets is called axonal guidance or axon pathfinding. All these stages are genetically programmed but are also influenced by the maternal environment (Kolb & Gibb, 2011).

The processes of dendritic formation and synaptogenesis are genetically set and continue to occur after birth. These processes are also guided by environmental cues and experiences. The number of dendrites and synapses peaks between the first and second year of life, due to the uncertainty in the number of neurons that will reach their proper cortical location (Kolb & Gibb, 2011). After that the extra and unwanted connections are eliminated by cell death and synaptic pruning. The effect of cell loss and synaptic pruning makes the cortex thinner around age two and continues through adulthood. This biological process can be detected by changes in thickness and volume of cortex during development (Giedd et al., 1999; Pfefferbaum et al., 1994).

Myelination of white matter axons is the last stage in brain development and begins after the axonal production and after the formation and maturation of oligodendrocytes (Thomas et al., 2000) during the fifth month of gestation. Life span postmortem studies have established that the myelination continues to progress up to the third and fourth decades of life (Barkovich et al., 2005; Benes, 1989; Yakovlev & Lecours, 1967). The quantitative indices of DTI (i.e., FA and MD) together with the morphological indices of white matter (i.e., white matter volume) are neural measures that can detect the developmental variations of white matter. Although these indices do not specifically measure the biological changes in the brain, they show the relative differences during development.

Typical brain development after birth is a dynamic process of maturation of both gray and white matter throughout childhood and adolescence, which coincides with the normal development of cognitive functions (Goddings et al., 2014; Nagy et al., 2004; Olesen et al., 2003; Squeglia et al., 2013; Tamnes et al., 2013). Longitudinal brain volumetric studies have shown that white matter increases across age range while gray matter volume peaks differently among different regions and then decreases after around 6-7 years of age (Giedd et al., 1999; Lenroot et al., 2007; Shaw et al., 2008; Sowell et al., 2004; Wierenga et al., 2014). These could be explained by continuous myelination as well as reduction in synaptic density during adolescence (Huttenlocher & Dabholkar, 1997; Yakovlev & Lecours, 1967).

1.2.1.1 Development of white matter

In the development of white matter, two main phases can be defined (Dubois et al., 2013). The first stage occurs during the last phase of human gestation, and involves the formation of the neural networks with the connection of long and short fibers connecting different parts of the brain. In this phase a large number of glial cells including astrocytes, oligodendrocytes and microglia are also formed in the brain. The second stage is the maturation of the connected fibers during infancy and childhood by myelination. It provides an effective and efficient transfer of information between the cortical and subcortical regions.

White matter volume increases with age throughout childhood and adulthood with more rapid changes in younger ages (Giedd et al., 1999; Lebel & Beaulieu, 2011; Lebel et al., 2008; Tamnes et al., 2010). FA is related to microstructural properties of white matter such as axonal diameter, density, packing and myelination (Beaulieu, 2002; Concha et al., 2010; Paus, 2010; Wedeen et al., 2005). It increases rapidly with age and then increases at a slower rate until it reaches a plateau in adulthood (Barnea-Goraly et al., 2005; Giorgio et al., 2008; Schmithorst et al., 2002). MD has a reverse trajectory, as it first decreases rapidly with increasing age and then the rate slows down until it reaches stability (Lebel et al., 2012).

1.2.1.2 Development of gray matter

Gray matter volume maturation demonstrates an inverted U-shaped trajectory across the lifespan with different peak in different brain regions (Giedd et al., 1999; Gogtay et al., 2004; Pfefferbaum et al., 1994). Gray matter loss during development has been reported as early as age 4 to 8 years in lower-order functional areas such as parietal and somatosensory regions (Giedd et al., 1999; Gogtay et al., 2004). Loss then occurs in the temporal lobes and dorsolateral prefrontal cortex. The regions involved in higher-order functions (e.g. spatial attention and language skills) such as parietal lobes peak around the age of 11 to 13 years. The latest maturation occurs in the regions involved in advanced executive functions and reasoning, for example in the prefrontal cortex and the posterior temporal regions (Gogtay et al., 2004). The gray matter loss may be the result of cortical dendrite pruning or it could be due to the parallel increase in the volume of white matter.

Besides the decrease in gray matter volume, cortical regions become thinner with age in most of the cortical areas (Sowell et al., 2004; Tamnes et al., 2010), excluding Broca's and Wernicke regions, which have been reported to increase in thickness during development (Sowell et al., 2004).

1.2.2 Cognitive development

Cognitive abilities, including memory, reasoning, information processing, problem-solving, perceptual skills and language, develop from childhood to adolescence. Working memory, known as the ability to keep a limited amount of information in mind and to manipulate and work with the information during a short period of time (Baddeley, 1992), is an essential factor for a variety of cognitive skills such as reading, mathematics and problem-solving (Bayliss et al., 2005; Gathercole et al., 2006;

Swanson & Beebe-Frankenberger, 2004). Working memory capacity develops across age with a particularly rapid increase in younger ages (Gathercole et al., 2004; Luciana & Nelson, 1998).

The increase in working memory capacity occurs in parallel with neurodevelopmental processes in the brain, including axonal and synaptic density elimination (Bourgeois & Rakic, 1993; Huttenlocher & Dabholkar, 1997; LaMantia & Rakic, 1990) as well as myelination (Paus et al., 1999; Yakovlev & Lecours, 1967).

1.2.3 Brain-behavior relationships during development

Several neuroimaging studies have examined the associations between cognitive abilities and brain functional and structural measures, since both brain and cognitive functions mature during typical childhood development.

1.2.3.1 Brain-working memory relationship

Functional MRI scans of children and young adults have consistently identified some activated brain areas during performance on visuospatial working memory task, a component of working memory that let us hold and manipulate information about locations and places in our brain. These regions include parietal cortex and dorsolateral prefrontal cortex containing the superior and the middle frontal gyri (Casey et al., 1995; Dumontheil et al., 2011; Klingberg et al., 2002; Thomas et al., 1999). It has been shown that the activation of these regions increases with age through childhood to adolescence and the functional measures are correlated with an individual's working memory capacity measured outside the scanner (Crone et al., 2006; Klingberg et al., 2002; Kwon et al., 2002; Scherf et al., 2006). The caudate nucleus is a subcortical area that is activated during performance of a working memory task in nonhuman primates (Levy et al., 1997), children (Klingberg et al., 2002; Ziermans et al., 2012), and adults (Postle et al., 2000).

Cortical thickness in the frontal and parietal areas has also been shown to correlate with working memory capacity measured outside the scanner (Tamnes et al., 2013; Tamnes et al., 2010; Østby et al., 2011). In addition to the functional and structural measures of gray matter, a positive correlation has been reported between the maturation of white matter pathways connecting these regions with working memory capacity during childhood development (Nagy et al., 2004; Olesen et al., 2003; Vestergaard et al., 2011; Østby et al., 2011).

1.2.3.2 Brain-reading relationship

Reading, an ability to extract meaning from a written text, involves different brain regions depending on which specific aspect of reading skill is needed. For instance, fMRI studies show the involvement of Broca's area and frontal areas in language production, grapheme-phoneme decoding and rhyme judgments (Frith et al., 1995; Price et al., 1997; Shaywitz et al., 1995), and the recruitment of the left supramarginal gyrus, angular gyrus and the left temporal areas in reading comprehension, phonological and semantic processing (Binder et al., 2009; Noonan et al., 2013; Price et al., 1997; Turken & Dronkers, 2011).

Several brain imaging studies have demonstrated correlations between white matter structure and reading ability among typically developing children and young adults (Beaulieu et al., 2005; Deutsch et al., 2005; Klingberg et al., 2000; Nagy et al., 2004; Niogi & McCandliss, 2006). Furthermore, white matter microstructural differences in the left temporo-parietal region could differentiate between normal and poor readers (Klingberg et al., 2000). Structural deviations in gray matter volume (Kronbichler et al., 2008; Silani et al., 2005; Vinckenbosch et al., 2005) and white matter microstructure (Deutsch et al., 2005; Klingberg et al., 2000; Niogi & McCandliss, 2006; Silani et al., 2005) have been reported in language and reading-related regions in individuals with reading disability. Moreover, different patterns of activity in the left temporo-parietal and occipito-temporal cortical areas have been shown among children with reading disability compared with normal readers (McCandliss et al., 2003; Paulesu et al., 2001; Richlan et al., 2011; Shaywitz et al., 2004; Shaywitz et al., 2002).

1.2.3.3 Neural mechanism underlying a behavioral ability

Behavioral abilities such as reading and working memory have been linked to neuroimaging measures in the relevant brain regions. Though the correlations between inter-individual brain differences and their related cognitive abilities are well established, the biological mechanisms underlying this inter-individual variability are still not fully known. The neuroimaging methods cannot clearly distinguish whether the performance related increase in white matter volumes or FA values results from the increase in axons diameter, organization or myelination. The direct effect of cell loss and synaptic density on the measures of cortex including gray matter volume, cortical thickness and area are also not fully explored. Additionally, the relationship between brain activity and the microstructure of white matter pathways is not still clearly explained by neuroimaging studies (Zatorre et al., 2012), though it is known by in-vitro studies that neuronal activity can induce oligodendrocyte differentiation and myelin formation (Demerens et al., 1996; Stevens et al., 1998).

Finding a direct link between brain measures and underlying biological processes in the human brain is not as straightforward as animal histological-imaging analyses (Lerch et al., 2011; Zatorre et al., 2012). The neuroimaging measures do not specifically measure the biological changes in the brain, however, they show the relative differences during development and they also reveal the inter-individual differences in relation to behavior.

One way of exploring the neural mechanism underlying a behavior is doing imaging genetics study. Knowing the function of a gene from animal models at the cellular level together with knowing the association of that candidate gene with behavior provides evidences to explore the effect of the gene on human brain and to link it to behavior. Imaging genetics studies bridge the gap between gene and behavior by finding the underlying neural mechanism that drives the inter-individual differences in behavior.

The other way of finding the neural mechanism underlying a behavioral ability is doing a longitudinal study. Using a longitudinal dataset, one can assess the inter-

individual brain differences in relation to a behavioral ability cross-sectionally. On the other hand, one can longitudinally investigate which brain measures predict future behavioral ability. This provides information regarding whether the functional or structural brain variability is the basis for inter-individual differences in a behavior or a skill.

1.3 GENETIC INFLUENCES ON DEVELOPMENT

1.3.1 Heritability of brain measures

Brain measures including both global and local measures are highly heritable. Total brain volume (Posthuma et al., 2000; Schmitt et al., 2007), total gray matter and white matter volumes (Pol et al., 2006) and white matter microstructure (Chiang et al., 2009) are heritable, and their heritability varies across lifespan (Batouli et al., 2014).

The heritability of brain measures differs regionally within different local areas. The volume and thickness of frontal areas and postcentral gyrus are highly (65– 97%) heritable, while the heritability of the density of hippocampus, amygdala and parahippocampal gyrus is less (40– 69%) (Pol et al., 2006; Thompson et al., 2001; Wright et al., 2002).

1.3.2 Heritability of cognitive abilities

Cognitive abilities, including working memory capacity and reading ability, are highly heritable. The heritability of working memory has been reported to be 43-65%, while word reading is 50-83% heritable (Ando et al., 2001; Schulte-Körne et al., 2007; van Leeuwen et al., 2009).

Although these cognitive skills are heritable and they improve throughout normal development, the biological and neuronal mechanisms underlying their development are still not fully understood. The brain structural and functional networks related to these cognitive skills are under the influence of genes (Baaré et al., 2001; Jamadar et al., 2011; Meda et al., 2008; Pfefferbaum et al., 2001; Pol et al., 2006; Thompson et al., 2001). Thus, imaging genetics studies have attempted to determine the effect of genetic markers on brain measures and to link them to behavior.

1.4 DYSLEXIA, A NEURODEVELOPMENTAL HERITABLE DISORDER

Dyslexia, or reading disability, is a common neurodevelopmental learning disorder exhibited in 5 to 17% of school-age children without any significant evidence of impaired intelligence, motivation, education or sensory abilities (Shaywitz et al., 1992; Shaywitz et al., 1990). Dyslexic individuals experience difficulties in reading fluently and more specifically with word decoding, recognition, spelling and reading comprehension (Lyon, 2003). Since a dyslexia diagnosis requires defining a cutoff on a continuous variable of reading ability, dyslexia has been referred to the lower end distribution of the continuum by researchers (Shaywitz et al., 1992).

Previous behavioral-genetic twin studies have shown that reading disability share genetic variability with IQ (DeFries & Alarcón, 1996; Fisher & DeFries, 2002). The heritability of the reading disability was reported higher among the subjects with higher IQ than those with lower IQ (Olson et al., 1999). A more recent article showed correlations between IQ, working memory and reading ability and revealed that the correlations are explained by common set of genes (van Leeuwen et al., 2009). They suggested possible way to classify children with reading disabilities: children who have low IQ and consequently have less reading ability; children who have normal IQ with problems in coding either phonemically or verbally; and children with low IQ and problems with coding phonemically and verbally. The last group may suffer from more difficulties in reading than the other two (van Leeuwen et al., 2009).

1.4.1 Dyslexia susceptibility genes

Dyslexia, as a developmental learning disability, is a heritable (40–84%) and familial disorder (Astrom et al., 2007; DeFries et al., 1987; Eicher & Gruen, 2013). Linkage studies (Démonet et al., 2004; Fisher & DeFries, 2002; McGrath et al., 2006) have linked the risk of dyslexia to nine loci (DYX1-DYX9). Six candidate genes- including *DYX1C1* on chromosome 15q21 within DYX1 locus; *DCDC2* and *KIAA0319* within the DYX2 locus on chromosome 6p21; *C2ORF3* and *MRPL19* in the DYX3 locus on chromosome 2p16-p15; and *ROBO1* on chromosome 3p12-q12 within the DYX5 locus have been associated with dyslexia and most of them have been replicated in several studies (Carrion-Castillo et al., 2013; Cope et al., 2005; Eicher et al., 2014; Massinen et al., 2009; Meng et al., 2005; Schumacher et al., 2006; Taipale et al., 2003).

Three of these candidate genes (*DYX1C1*, *DCDC2* and *KIAA0319*) are the most replicated and have been previously associated with neuronal migration and axon guidance during development of the neocortex in animal experiments (Gabel et al., 2010; Peschansky et al., 2010; Szalkowski et al., 2012; Wang et al., 2006). *DYX1C1* and *DCDC2* have also been associated with ciliary growth and function (Chandrasekar et al., 2013; Massinen et al., 2011). The primary cilia are organelles consisting of an array of microtubules, which act as the probes of the developing cell. They transduce information about the extracellular environment via surface receptors and influence the functioning of developmental signaling pathways (Marshall & Nonaka, 2006).

While very little is known regarding the role of *C2ORF3* and *MRPL19* at the cellular level, the role of *ROBO1* in axonal guidance and crossing the midline has been established in several studies (Andrews et al., 2006; López-Bendito et al., 2007; Unni et al., 2012).

1.4.1.1 *DYX1C1*

The first link between genes and reading disability was found on chromosome 15 (Smith et al., 1983) and was later replicated using markers on the DYX1 locus, i.e. the marker located in 15q21 (Bates et al., 2007; Chapman et al., 2004; Grigorenko et al., 2000). The dyslexia candidate gene, *DYX1C1*, was first discovered in a Finnish family study (Nopola-Hemmi et al., 2000), which showed that the *DYX1C1* gene was disturbed by chromosome 15 breakpoint. *DYX1C1* gene codes for a 420 amino acid protein with three protein–protein interaction domains (Taipale et al., 2003).

Although several studies have replicated the association of *DYX1C1* with dyslexia (Brkanac et al., 2007; Marino et al., 2007), some studies have failed to replicate this finding (Bellini et al., 2005; Tran et al., 2013).

The rodent knock-down studies of Dyx1c1 have shown abnormal migrations of neurons in neocortex (Adler et al., 2013; Currier et al., 2011; Wang et al., 2006). The abnormal increase in the migration of neurons has also been found in the knockdown samples in human neuroblastoma cells (Tammimies et al., 2013). In addition to neuronal migration, the role of *DYX1C1* in regulating cilia growth and motility in zebrafish has been reported (Chandrasekar et al., 2013).

1.4.1.2 *DCDC2*

DCDC2, located in DYX2 locus, is another dyslexia candidate gene that has been associated with reading disability in multiple studies (Meng et al., 2005; Newbury et al., 2011; Schumacher et al., 2006). This gene encodes a protein containing two doublecortin domains. The disrupted neuronal migration has been reported in Dcdc2 knock-down rats (Adler et al., 2013; Meng et al., 2005). *DCDC2* has also been implicated in cilia function and growth (Ivliev et al., 2012; Massinen et al., 2011).

1.4.1.3 *KIAA0319*

KIAA0319 is the other gene in DYX2 locus that has been found in association with dyslexia (Cope et al., 2005; Deffenbacher et al., 2004; Francks et al., 2004). Similar to *DYX1C1* and *DCDC2*, *KIAA0319* has been associated with neuronal migration in developmental neocortex (Adler et al., 2013; Paracchini et al., 2006; Peschansky et al., 2010).

1.4.1.4 *MRPL19 and C2ORF3*

DYX3 candidate locus on chromosome 2 (2p12–16) has been linked to dyslexia and reading disability in both dyslexic samples and general population (Fisher et al., 2002; Kaminen et al., 2003; Petryshen et al., 2002). Two candidate genes in this locus, *MRPL19* and *C2ORF3,* are in strong linkage disequilibrium and are highly expressed in different regions of human brain (Anthoni et al., 2007). The level of expression of these genes is highly correlated with the other dyslexia candidate genes. Although these genes have been associated with dyslexia and reading related traits, little is known about the function of these genes in animal and human brains.

1.4.1.5 *ROBO1*

ROBO1 gene in the DYX5 locus has also been associated with dyslexia (Hannula-Jouppi et al., 2005). Some polymorphisms in *ROBO1* have been linked to performance on short-term memory tasks, but not with reading ability (Bates et al., 2011). *ROBO1* gene is highly expressed in the developing brain (Lamminmäki et al., 2012). This gene encodes a protein with an axonal guidance role during cellular migration and axonal navigation, and it is implicated in midline crossing of axons between brain hemispheres.

1.4.2 Neuroimaging studies of dyslexia

Several functional studies have consistently reported the dysfunction of the left language networks including the temporo-parietal and the occipito-temporal cortical regions in individuals with reading disability compared with the normal readers (Démonet et al., 2004; Richlan et al., 2011; Shaywitz et al., 2004; Shaywitz et al., 2002). Reduced activity in the middle temporal gyrus, the inferior and superior temporal gyri and the middle occipital gyrus has been reported using positron emission tomography (PET) scans in dyslexic individuals from three different countries (Paulesu et al., 2001). These findings suggest a universal neural basis for developmental dyslexia regardless of the differences in language networks due to different writing systems. Reduction in gray matter density of the left middle temporal gyrus has also been reported in the same samples (Silani et al., 2005). Furthermore, structural studies have consistently reported white matter structural changes in the left temporo-parietal regions among children and young adults with poor reading ability (Klingberg et al., 2000; Niogi & McCandliss, 2006) compared with normal readers.

The neural mechanisms underlying the normal variability of reading ability (Beaulieu et al., 2005; Deutsch et al., 2005; Klingberg et al., 2000; Niogi & McCandliss, 2006) is similar to those underlie reading disability (Klingberg et al., 2000). However, the cause of this variability is still not fully established. Knowing the involvement of dyslexia susceptibility genes in neuronal migration, ciliary function and midline crossing, it is interesting to see whether the polymorphisms in and within the candidate genes would affect variability of white matter structure in typically developing children and young adults and contribute to variability in their reading abilities.

2 AIMS AND HYPOTHESES

The general aim of this thesis was to study the associations between some specific candidate genes, neuroimaging measures and behavioral outcomes during development using a longitudinal sample of typically developing children and young adults. In addition to the investigation of the concurrent associations between brain and behavioral measures, we assessed whether the neuroimaging measures can predict future behavioral scores.

2.1 STUDY I

The aim of this study was to assess the associations of three dyslexia susceptibility genes (*DYX1C1*, *DCDC2* and *KIAA0319*) with white matter structure. Both the integrity and volume of white matter have been previously correlated with reading ability, but the cause of these relationships and the involvement of other factors are still not fully known. In this study, we hypothesized that whether the polymorphisms within the dyslexia genes influence the variability of white matter structure, since these genes are known to be involved in neuronal migration.

2.2 STUDY II

Knowing the role of dyslexia genes in neuronal migration and ciliary functions, we aimed to assess whether the variability of dyslexia related genetic markers would also be related to the thickness of the cortical regions found in study I. We also assessed the relationships between brain measures and reading scores. Moreover, we investigated which brain measures can predict future reading ability.

2.3 STUDY III

In study III, we aimed to investigate whether the dyslexia genes, *MRPL19* and *C2ORF3*, found to be correlated with broader cognitive traits such as verbal and non-verbal IQ, have a significant influence on white matter structures.

2.4 STUDY IV

ROBO1 is another dyslexia related gene that has been associated with axonal guidance and midline crossing during development. Considering the role of *ROBO1* in controlling the midline crossing of callosal axons in rats, we aimed to assess whether the polymorphisms within this gene have any significant effect on the structure of corpus callosum in the human brain.

2.5 STUDY V

Working memory capacity, an important factor in cognitive development, has been associated with higher activity, thinner cortex and white matter maturation in cross-sectional studies. In this study, we aimed to investigate the role of brain structural and functional differences in the development of working memory using a longitudinal dataset. We assessed the concurrent brain-brain and brain-behavior relationships. We also investigated whether brain structural and functional measures can predict future working memory ability.

3 METHODS

3.1 PARTICIPANTS

A sample of 380 typically developing children and young adults aged 6 to 25 years from the population registry in Nynäshamn, Sweden, were selected to participate in a large, behavioral longitudinal study, the Brain Child study. The sample recruitment was done randomly with equal gender distribution in nine age groups (6, 8, 10, 12, 14, 16, 18, 20, and 25 years). The exclusion criteria were first language other than Swedish, vision or hearing impairment, or neurological or neuropsychiatric disorders with exception of dyslexia or Attention Deficit Hyperactivity Disorder (ADHD). Out of 380 individuals, 335 participated in behavioral and genetic testing. Based on available parents' reports, in 88.7% of the cases, both the participants and their parents were born in Sweden, 9.3% had at least one parent born outside of Sweden but within Europe, and the remaining 2% had one or both parents born outside of Europe. Informed consent was provided by the participants or the parents of children aged below 18 years old. The study was approved by the local ethics committee of the Karolinska University Hospital, Stockholm, Sweden.

Out of 335 participants in the Brain Child study, 90 were selected randomly to participate in the MRI assessments including T1-weighted structural imaging, fMRI, and DTI. The longitudinal data collections for both behavioral and imaging assessments were conducted on three occasions: 2007, 2009 and 2011.

3.2 BEHAVIORAL ASSESSMENTS

All individuals, participated in the longitudinal Brain Child study, were behaviorally assessed using a set of reading, math, working memory and attention tests. Reading was assessed using two tests: reading comprehension and word chains. Visuospatial working memory was also tested using a computerized grid task.

3.2.1 Assessment of reading comprehension

A reading comprehension task was administered either individually or in groups of two to 20 participants in a classroom setting. To measure reading comprehension, narrative and expository texts from the Progress in International Reading Literacy Trend Study (PIRLS 2001 T) and The International Association for the Evaluation of Educational Achievement Reading Literacy Study 1991 were employed. Seventy-seven items were used to form reading comprehension tests for four age groups from 8 to 25 years. An item response theory (IRT) analysis (Bond & Fox, 2001) was used to achieve an ability score for each subject.

3.2.2 Assessment of word decoding

Since reading comprehension was not only specific to language skills and it involved a range of other cognitive processes, including attention and working memory, we also administrated a second test of word decoding, called "word chains". This was

similar to the English Woodcock Johnson Word-ID test, in which the subjects had 72 sets of written words to read, each consisting of three words with different length between two and eight letters and without spaces in between. The task was to read as many words as possible during a two minutes period and mark with a pencil where the spaces should occur, i.e. identify the three words appearing in each set. The score was based on the number of words that has been marked correctly (Woodcock, 1987).

3.2.3 Assessment of visuospatial working memory

Visuospatial working memory was assessed individually using a computerized grid task from the Automated Working Memory Assessment (AWMA) battery (Alloway, 2007). A number of dots in a 4×4 grid were displayed sequentially for 1000 msec, with a 500 msec interval. The task was to remember the location and the order of the dots. The first level of the test was with one dot and six trials. By giving four correct responses, it continued to the next level with one more dot. By three wrong answers on one level, the test was terminated. The visuospatial working memory score was computed based on the number of correct trials.

3.3 GENOTYPING

For all 335 individuals participated in the Brain Child study, the material for DNA extraction was collected in the form of blood from finger tips or saliva. The DNA sequence is a double helical chain of four nucleotide bases including Adenine (A), Thymine (T), Cytosine (C) and Guanine (G). Normally T is paired with A and C is paired with G. Any variation that occurs commonly (more than 1% of the population) at a single location on a DNA sequence is called single nucleotide polymorphism (SNP).

In our Brain child study, 76 candidate SNPs located in or close vicinity of the genes related to language, learning and memory were genotyped using matrix-assisted laser desorption/ionization-time of flight mass spectrometry with iPlex Gold assays. This technique finds the differences in DNA and genotypes the SNPs into three possible combinations of two alleles, for example: CC, CT, and TT.

Based on our hypotheses for the studies presented in this thesis, the dyslexia related genes, *DYX1C1*, *DCDC2*, *KIAA0319*, *MRPL12*, *C2ORF3* and *ROBO1* were selected. The association of 13 SNPs located in or in close vicinity of the three dyslexia susceptibility genes: *DYX1C1* (rs3743204, rs3743205 and rs17819126); *DCDC2* (rs793842, rs793862, rs807701, rs2328819, rs2792682, rs7751169 and rs9460974); *KIAA0319* (rs4504469, rs6935076 and rs2143340) with white matter volume was assessed in Study I. The effect of the three SNPs associated with white matter volume (rs3743204, rs793842, and rs6935076), on cortical thickness was investigated in study II. For study III, we investigated the effect of seven SNPs (rs3088180, rs4853169, rs917235, rs6732511, rs714939, rs17689640 and rs17689863) located at the *MRPL19/C2ORF3* locus on white matter volume. In study IV, genotyping of *ROBO1* was performed on the Affymetrix Genome-wide Human SNP array 6.0, including more than 906600 SNPs and more than 946000 probes for detecting copy

number variations. For the first phase of the study, 20 SNPs (rs3773216, rs9875094, rs3773232, rs1457659, rs416551, rs7629522, rs162870, rs162871, rs162262, rs162429, rs7631406, rs12497294, rs6770483, rs9835692, rs9876238, rs4856291, rs4856447, rs12488868, rs6768880, rs9830013) were tagged to capture the common genetic variation in the area. The association study to white matter volume was done on these 20 SNPs and two of the SNPs (rs17396958 and rs1393375) showed significant associations. Then in the second phase, 28 SNPs within and between the two haplotype blocks of these two SNPs were chosen (rs6770755, rs7651370, rs7631357, rs4564923, rs6548621, rs9832405, rs7637338, rs6548628, rs9853895, rs9820160, rs7432676, rs9309825, rs13071586, rs13072324, rs6771681, rs7618126, rs7432306, rs6548650, rs7644521, rs1995402, rs17380584, rs11917376, rs11706346, rs1393360, rs1502298, rs10511118, rs1502305, and rs10511119).

3.4 BRAIN IMAGING AND ANALYSES

Multimodal brain imaging including T1-weighted structural imaging, fMRI, and DTI were acquired using a 1.5 T Siemens scanner (Siemens, Erlangen, Germany) on 90 participants, three times with two years gap between each scan. The multimodal brain images were then analyzed with different image processing methods and statistical image analysis techniques.

3.4.1 Structural brain imaging

T1-weighted spin echo scans were collected using a three-dimensional magnetization prepared rapid gradient echo (MP-RAGE) sequence with repetition time (TR) = 2300 msec, echo time (TE) = 2.92 msec, field of view (FOV) of 256 × 256 mm^2, 256 × 256 matrix size, 176 sagittal slices, and 1 mm^3 isotropic voxel size. Generalized auto-calibrating partially parallel acquisition (GRAPPA) with acceleration factor of two was also used to speed up the acquisition.

The structural images were then processed with two different methods. The first technique was voxel-based morphometry (VBM), which segmented the brain into gray matter, white matter and CSF. The white matter segmented images where then analyzed with the whole brain exploratory voxel-wise analysis as well as the ROI based analysis. The second technique was cortical thickness measurement that implemented in FreeSurfer software (https://surfer.nmr.mgh.harvard.edu) and measured the thickness of cortex in several defined ROIs (Reuter et al., 2012).

3.4.1.1 Structural brain analysis

Diffeomorphic Anatomical Registration Through Exponentiated Lie Algebra (DARTEL) (Ashburner, 2007) was performed on the structural data collected across all three rounds, to align all the structural data and segment them into gray and white matter. All scans first iteratively were aligned to their common average template and then they were segmented into gray and white matter as well as CSF based on the prior probability map for each tissue type and the intensity information of the images. The intensity at each voxel of the segmented images presented the probability of being gray or white matter. The segmented images were then modulated by multiplying by the

values in the deformation matrix of normalization. Modulation corrected for changes in volume caused by normalization. The modulated images were then registered to Montreal Neurological Institute (MNI) template and smoothed with a Gaussian kernel size of 8 mm.

3.4.1.2 Cortical thickness measurement

Cortical thickness of the structural dataset was estimated using automatic longitudinal stream in FreeSurfer (Reuter et al., 2012). The thickness of the cortex was measured by constructing models for the boundary between gray and white matter. First, a within-subject template was created for each subject using inverse consistent registration (Reuter & Fischl, 2011; Reuter et al., 2010). Then, several processing steps (Dale et al., 1999; Fischl & Dale, 2000) including skull removing, template transformation and atlas registration were performed. Images were later segmented to white matter, gray matter, and pial, based on intensity and neighborhood voxel restrictions. The distance between the white and the pial was computed as the thickness at each location of cortex.

3.4.2 Functional brain imaging and processing

T2*-weighted functional images were carried out using a gradient echo planar imaging (EPI) sequence with TR = 3000 ms, TE = 50 ms, FOV of 220 × 220 mm^2, 64 × 64 matrix size, and 4.5 mm of slice thickness. The same imaging sequence was repeated for the second and third rounds of the study. Participants performed 10 minutes of visuospatial working memory task in the scanner (Dumontheil et al., 2011). In this task, a number of dots were presented sequentially in a 4×4 grid and the task was to remember the location and the order of dots.

Functional images were first pre-processed by slice timing and motion correction in SPM5. Then the images were aligned and normalized to the MNI template and finally were high-pass (140 s) filtered and smoothed with a 12 mm Gaussian kernel.

Second-level analysis was performed using SPM5 for group analysis of the working memory contrast images using the flexible factorial design by considering subject and round of the scans as factors. After correcting for the effect of age and gender, the main working memory contrast was found at a false discovery rate (FDR), threshold of $p < 0.05$, to identify regions that were recruited during task performance. The activation map of main working memory contrast (thresholded at FDR < 0.000001) was then split into smaller ROIs with a center around a single local maximum. ROIs were defined so that the regions did not overlap, and together they covered the majority of the working memory related activations. Average of BOLD contrast within the defined ROIs was then computed for further statistical analyses.

3.4.3 DTI and fiber tracking

Diffusion weighted imaging was acquired with two different parameters. The one used to collect DTI data in all three rounds of data collection was with a FOV of 230 × 230 mm^2, matrix size of 128 × 128, 19 slices with 6.5 mm thickness, and b-value of 1000 sec/mm^2 in 20 gradient directions. The other one was acquired with a FOV of 230 × 230 mm^2, matrix size of 128 × 128, 40 slices, 2.5 mm of slice thickness, and b-value of

1000 sec/mm^2 in 64 gradient directions, at the third round of data collection of the longitudinal study. This was an additional sequence to increase the resolution of the DTI scans and consequently improve the tractography results.

Eddy current and head motions were corrected with affine registration for all diffusion-weighted images to a reference volume using FSL software (http://fsl.fmrib .ox.ac.uk/fsl/fslwiki). Diffusion tensor parameters were then estimated for each voxel, and subsequently the DTI and FA data were constructed. To align all FA images, nonlinear registration was carried out using Tract-Based Spatial Statistics, TBSS v1.2, (http://fsl.fmrib.ox.ac.uk/fsl/fslwiki/TBSS) on both longitudinal DTI data and the data collected only at round 3. This alignment was also used to find the common pathways traced by fiber tracking methods. Two different fiber tracking methods (streamline and probabilistic fiber tracking) were performed in our studies.

3.4.3.1 Streamline fiber tracking

Deterministic streamline is one of the fiber tracking techniques which uses the orientation information of the estimated diffusion to trace white matter fibers. Tracking starts from a seed point or seed region and streamlines propagate to the neighboring voxels with closest direction to the previous one until they reach the voxels with FA values less than predefined threshold.

Streamline tracking was performed in study I, II and III using ExploreDTI v4.7.3. (www.exploredti.com) to find white matter pathways passing through the white matter regions associated with dyslexia related genes. Fiber tracking was done at the individual's space for all subjects. The traced white matter pathways were then registered to the mean FA template using TBSS for non-FA images and then were binarized and averaged across all individuals. The tracts were finally thresholded at the group level by keeping the pathways that were available in 90% of the cases, in order to create a probability map of more probable white matter pathways among all individuals.

3.4.3.2 Probabilistic fiber tracking

The other fiber tracking technique is the probabilistic fiber tracking method which first models multiple fiber orientations at each voxel and then repetitively computes the streamlines staring from seed region and passing through the multiple orientations within the adjacent voxels. Summing up the estimated streamlines generates a probabilistic map which shows the distribution of the location of streamlines. This tracking method performs better and more accurate in crossing and branching fibers compared to the deterministic streamline tracking, since it estimates multiple orientations and provides a map of probability of connections.

In studies IV and V, probabilistic fiber tracking was performed on all individuals' high resolution DTI data (collected at the third round) using probtrackx tool of FMRIB's Diffusion Toolbox (FDT), v2.0 (http://fsl.fmrib.ox.ac.uk/fsl/fsl-4.1.9/fdt/fdt_probtrackx .html). The default parameters (5000 streamline samples, step length of 0.5 mm, and curvature threshold of 0.2) were used for the probabilistic fiber tracking. At the individual level, tracts were thresholded by 5% of the samples to remove the voxels

with low probability of connection (Leh et al., 2006). In the next step, all of the traced white matter pathways were aligned with TBSS method for non-FA images using the transformation matrices saved for each individual. The traced white matter pathways were then binarized and averaged across all subjects. To find the most probable white matter pathways across all individuals, the tracts were finally thresholded at the group level by keeping the pathways that were present in 90% of the cases.

For study IV, the body of corpus callosum was considered as a seed region and five different cortical ROIs including anterior frontal, superior frontal, parietal, temporal and occipital cortex were selected bilaterally as target regions. These cortical regions were defined based on the Harvard-Oxford cortical atlas. In this study, we segmented the corpus callosum into five sections and assessed whether the *ROBO1* SNPs were associated with FA or connectivity probability of the white matter pathways, separately in each segment of corpus callosum.

For study V, we aimed to trace fronto-parietal and fronto-striatal pathways. For fronto-parietal connections, fiber tracking initiated from the superior frontal and the target region was set as an inclusion mask of intra-parietal regions to include only the pathways that pass through these regions. For fronto-striatal pathway, the left and right caudate were the seed regions and bilateral superior frontal areas were considered as inclusion masks.

3.5 STATISTICAL ANALYSES

Several statistical analyses were performed for several purposes: 1) to explore the association between white matter volume and dyslexia related genes; 2) to find the link between brain measures and behavior; and 3) to investigate whether any certain brain measures can predict future cognitive ability.

3.5.1 Whole brain exploratory analysis

Whole brain exploratory analysis was performed in studies I, II, and III, to find the white matter specific regions associated with variations in dyslexia related genes. For study I, all of the 13 SNPs of *DYX1C1*, *DCDC2*, and *KIAA0319*, and for study III, all the 7 SNPs of *MRPL12* and *C2ORF3* were entered separately as a main factor in a flexible factorial design second-level SPM analysis, which included both the individual images with and without repeated measures. This analysis was corrected for the effect of age, gender, handedness and total white matter volume. Gene interactions with age and gender were also added to the model.

3.5.2 ROI based analysis

For study II, IV and V, the ROI based analysis was performed. In study II, thickness of cortex was measured for the cortical ROIs. Then the mixed linear model in SPSS statistics 21.0 software was applied to see whether any of the dyslexia SNPs has significant effect on cortical thickness. In study IV, probability of connections in different segments of the corpus callosum was computed and tested for significant associations with *ROBO1* SNPs.

In study V, functional and structural ROI-based measures in fronto-striatal and fronto-parietal networks were assessed for cross-sectional and prediction based correlations between brain-brain and brain-working memory measures. Mean values of working memory related BOLD contrast and cortical thickness were extracted from functionally active cortical regions during visuospatial working memory task performance. The white matter volume and FA were also computed from the white matter pathways traced by probabilistic fiber tracking of fronto-parietal and fronto-striatal tracts.

3.5.2.1 Cross-sectional Analysis

In all studies, concurrent correlations between brain and behavior measures (cross-sectional analyses) were performed using the mixed linear model in SPSS 21.0 software with Restricted Maximum Likelihood (REML) method, considering three longitudinal repeated measures. In dyslexia related studies, reading ability was set as dependent variable. For study V, working memory performance was the dependent variable. Brain measures were covariates of interest. Moreover, age, gender, and handedness were considered as covariates.

3.5.2.2 Longitudinal Analysis

For prediction analyses, correlations between current to future measures were tested by similar mixed linear model. In this case, we considered two repeated measures. For the first measures, round one and two values were observed as current and future variables, respectively. And for the second measures, round two and three were considered as current and future values. The model was corrected for the effect of gender as well as age at baseline. In studies II and V, we tested whether brain measures can predict future reading ability and working memory performance, respectively.

4 RESULTS

4.1 STUDY I

4.1.1 Dyslexia susceptibility genes, *DYX1C1*, *DCDC2*, and *KIAA0319* and white matter

In the assessment of the associations of 13 dyslexia related SNPs within *DYX1C1*, *DCDC2* and *KIAA0319* genes with white matter volume, three SNPs -rs3743204 (*DYX1C1*), rs793842 (*DCDC2*), and rs6935076 (*KIAA0319*)- significantly were associated with variations in white matter volumes ($p < 0.0038$, at cluster level, corrected for multiple comparisons of 13 SNPs). In this analysis, the flexible factorial design of second level SPM5 analysis was performed on two repeated measures (round 1 and 2) of white matter segmented images. All of the three mentioned SNPs were associated with white matter volume in the left temporo-parietal area (Fig. 1A and B) and they partially overlapped with each other (Fig. 1D). Rs3743204 (*DYX1C1*) had an extra cluster in the similar region in right hemisphere. Table 1 lists the MNI coordinates of the peak voxels as well as the p-values at the cluster level.

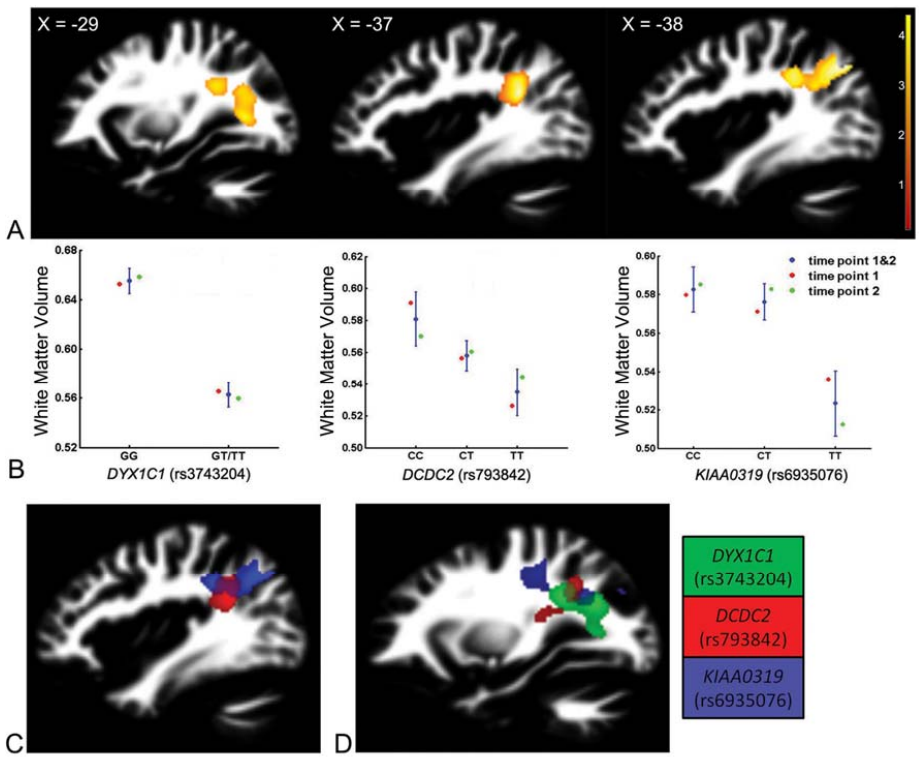

Figure 1: (A) Main effect of three SNPs within *DYX1C1*, *DCDC2*, and *KIAA0319* genes on white matter structure in left temporo-parietal area. (B) White matter volume distribution for genotypes of each SNP (error bars: ± 1 SEM). (C, D) Overlap between the significant regions.

Table 1: Coordinates for the effect of SNPs on white matter.

SNP (gene)	P-value at cluster level	Z score	x, y, z (MNI)
rs3743204 (*DYX1C1*)	3.10×10^{-3}	3.85	-15, -54, 16
	5.43×10^{-4}	3.70	13, -35, 30
rs793842 (*DCDC2*)	1.51×10^{-3}	4.23	-37, -49, 23
rs6935076 (*KIAA0319*)	5.51×10^{-4}	4.10	-38, -69, 38

Out of these three SNPs, only rs3743204 (*DYX1C1*) had a significant gene × age interaction (p = 0.0018) in the same region that showed the main effect in the left hemisphere (Fig. 2).

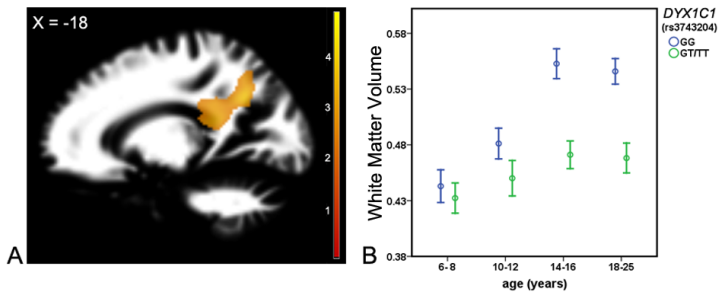

Figure 2: The *DYX1C1* (rs3743204) interaction with age in left hemisphere. (B) White matter volume variations and genotypes in the different age groups (error bars: ± 1 SEM).

4.1.2 Behavioral associations

Mean white matter volumes in three clusters associated with dyslexia SNPs were significantly correlated with reading comprehension scores ($p < 0.00009$) as well as word chain scores ($p < 0.0001$), with greater white matter volume associated with better reading ability. After correction for the effect of age, gender, and handedness, the correlations remained significant for both reading comprehension ($p < 0.004$) and word chain scores ($p < 0.002$). There was no significant correlation between these SNPs and reading comprehension or word chain scores, considering two rounds of the longitudinal data (Fig. 3).

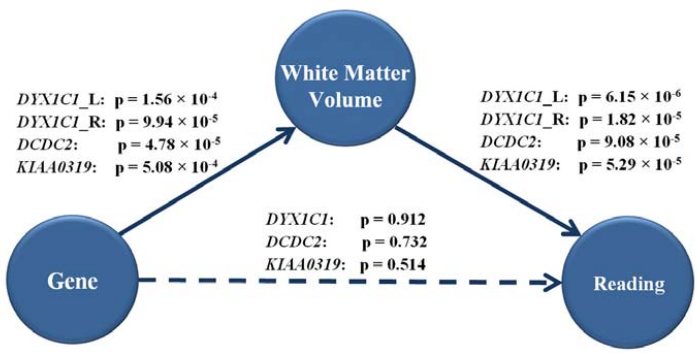

Figure 3: Associations between dyslexia genes, white matter volume, and reading comprehension scores. *DYX1C1*_L and *DYX1C1*_R denote the clusters found for rs3743204, in the left and the right hemispheres, respectively.

4.1.3 Fiber tracking

The overlap area of the SNP associated regions was found mainly in the left superior longitudinal fasciculus and the posterior part of corpus callosum according to John Hopkins Probabilistic Atlas. This region was used as a seed ROI for streamline fiber tracking on 30 randomly selected subjects. Fig. 4A shows the fiber tracking result of one individual. To obtain a probability map of those tractography results, all 30 tract maps were transformed back into a common space, converted into a binary image before being averaged across all individuals (Fig. 4B). The fibers passing through SNP associated region were found to be part of temporo-parietal and corpus callosum tracts. After overlaying the tracts to the Harvard-Oxford cortical atlas, we found that the fibers connected the left middle temporal cortex to the left angular and supramarginal gyri (Fig. 4C). The inter-hemispheric pathways also connected superior parietal lobules and superior division of lateral occipital cortex, bilaterally. The endpoints of the fibers were consistent with the areas previously reported by (Paulesu et al., 2001) for middle temporal cortex and by (Richlan et al., 2011) for inferior parietal lobule, as shown in Fig. 4D.

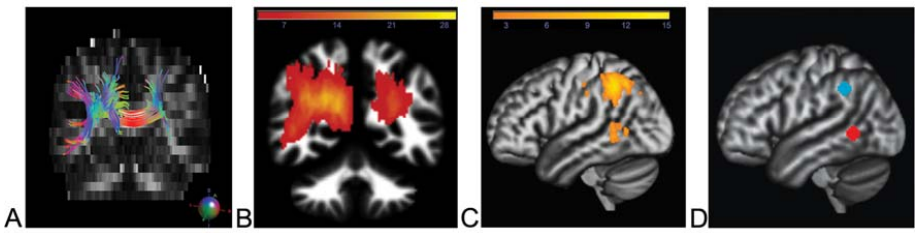

Figure 4: (A) A sample of fiber tracking result of one individual (red, green, and blue fibers show left–right, anterior–posterior, and inferior–superior directions, respectively). (B) Overlay of fiber tracking from 30 individuals. Color bar shows the number of individuals with overlapping connections. (C) The cortical regions most consistently connected are the left middle temporal sulcus and left supramarginal and angular gyri. (D) ROIs drown by the radius of 5 mm at the centers of −60, −56, 0 for middle temporal and −38, −48, 40 for inferior parietal cortex (Paulesu et al., 2001; Richlan et al., 2011).

4.2 STUDY II

4.2.1 Genetic associations with white matter volume

In study II, we repeated the similar analysis as study I to assess the association of three dyslexia related SNPs, rs793842 (*DCDC2*), rs6935076 (*KIAA0319*), and rs3743204 (*DYX1C1*) with white matter volume, this time by including all three time-points of the entire dataset. We found the same significant association with white matter volume for these SNPs. The rs6935076 and rs3743204 significant clusters were bilateral, while the rs793842 cluster was located in the left hemisphere. The peak MNI coordinates, size of the clusters, and FDR-corrected p-values at cluster level are listed in Table 2. Fig. 5A shows the clusters found significant for association of each SNP, and Fig. 5B illustrates the residual distribution of mean white matter volume in each significant region for the related genotypes after correction for age, gender and handedness.

The overlapping region of these clusters was quite similar to study I. Even after fiber tracking on our high resolution DTI data, we found the same pathways connected to the same cortical regions (Fig. 5C) according to their overlap with Harvard-Oxford cortical structural atlas. Fig. 5D shows these cortical regions labeled with different colors for the left middle temporal cortex, left supramarginal and angular gyri as well as the bilateral superior parietal lobules and the lateral occipital cortex.

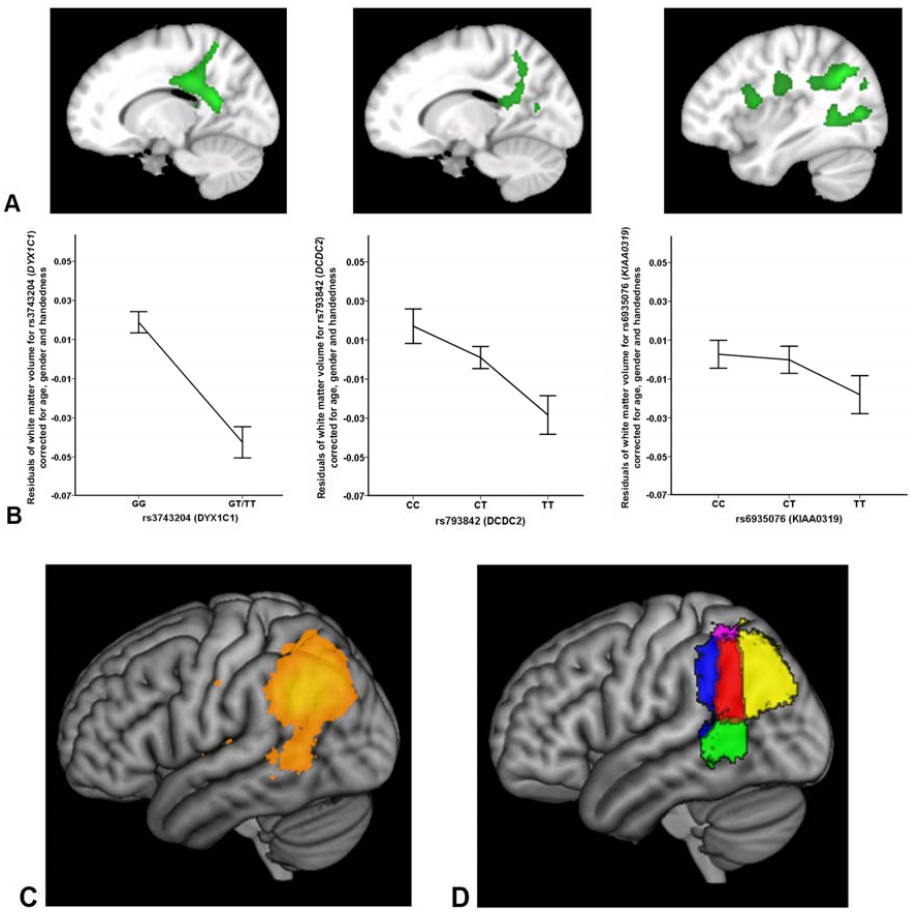

Figure 5: Main effect of three SNPs from *DYX1C1*, *DCDC2*, and *KIAA0319* genes on white matter structure. (A) White matter clusters showing significant association between SNPs and white matter volume, shown in sagittal sections. (B) Distribution of residual from mean white matter volume in each significant region across different genotypes after correction for age, gender and handedness (error bars: ±1 SEM). (C) After fiber tracking, the cortical regions most consistently connected to the middle temporal sulcus, supramarginal and angular gyri and lateral occipital cortex (D) Overlapped white matter pathways with Harvard-Oxford cortical structural atlas and labeled with different colors; Red for left angular, blue for left supramarginal gyrus, green for left middle temporal cortex, yellow for lateral occipital and purple for superior parietal cortex.

Table 2 Coordinates for the main effect of SNPs on white matter.

SNP	Gene	$P_{FDR\text{-}corrected}$ Cluster-level	Cluster size	Peak Voxel	
				Z	x, y, z (MNI)
rs3743204	***DYX1C1***	1.28×10^{-10}	9804	4.11	-16, -54, 18
rs793842	***DCDC2***	8.19×10^{-5}	3353	4.24	-28, -70, 33
rs6935076	***KIAA0319***	3.33×10^{-10}	8195	5.32	-34, -58, 31
		3.32×10^{-10}	8285	4.01	36, -28, 37

4.2.2 Genetic associations with cortical thickness

In the assessment of the main effect of the three SNPs on cortical thickness of left and right cortical ROIs, we found significant effect (Fig. 6A) for the association of rs793842 (*DCDC2*) with the cortical thickness of left supramarginal ($F_{2,\ 86.96} = 5.05$, $p = 2.68\times10^{-4}$), left angular gyrus ($F_{2,\ 88.78} = 5.12$, $p = 0.008$) and left lateral occipital cortex ($F_{2,\ 84.21} = 11.96$, $p = 2.70\times10^{-5}$). There was no significant association with either the middle temporal region or with the right cortical areas. The cortex found significantly thicker for T-allele carriers, who had lower white matter volume (Fig. 5A). The rs793842 × age interaction was also significant for thickness of left supramarginal gyrus ($F_{2,\ 114.78} = 7.61$, $p = 0.001$), as shown in Fig 6B.

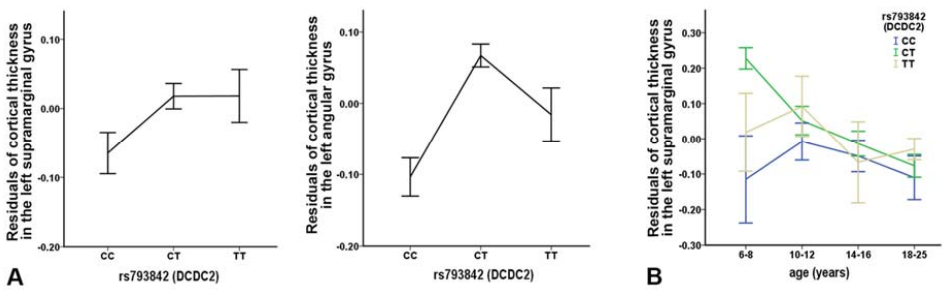

Figure 6: (A) Cortical thickness of left supramarginal and angular gyri across rs793842 (*DCDC2*) genotypes, after correction for age, gender and handedness. All three time-points are collapsed together. (B) Rs793842 × age interaction for the residuals from mean cortical thickness of left supramarginal gyrus across four different age groups after correction for gender and handedness (error bars: ±1 SEM).

4.2.3 Rs793842 (*DCDC2*) associated with reading ability

Out of three SNPs, rs793842 (*DCDC2*) significantly associated with reading comprehension scores ($F_{2,\ 50.02} = 4.66$, $p = 0.014$). Reading scores was less for T-allele carriers who also had lower white matter volume in the left temporo-parietal area, and thicker cortex in the left parietal and occipital areas. This association was not significant in study I, where we had two repeated measures. No genetic association was found for a test of single-word reading, the word chain test ($p = 0.608$). Moreover, the rs793842 × age interaction was not significant.

4.2.4 Relationships between brain measures and reading ability

The correlations between reading comprehension and white matter volumes in all three SNP-associated regions found significant ($p < 5.00\times10^{-5}$), even after correction for age ($p < 0.001$). Reading comprehension scores were also associated with cortical thickness in parietal and occipital regions, including left supramarginal ($F_{1,\ 128.28} = 8.45$, $p = 4.32\times10^{-3}$), right supramarginal ($F_{1,\ 152.68} = 16.14$, $p = 9.2\times10^{-5}$), left angular ($F_{1,\ 137.73} = 8.59$, $p = 3.95\times10^{-3}$), right angular ($F_{1,\ 144.97} = 21.72$, $p = 7.0\times10^{-6}$) gyri as well as the left and right lateral occipital cortex ($F_{1,\ 111.81} = 7.51$, $p = 7.15\times10^{-3}$ and $F_{1,\ 130.28} = 20.41$, $p = 1.4\times10^{-5}$, respectively). These correlations did not remain significant after the effect of age was removed.

The word chain scores were correlated with the white matter volumes ($p < 10^{-6}$) as well as the cortical measures in all bilateral cortical ROIs ($p < 0.036$ for middle temporal cortex, $p < 0.001$ for supramarginal, $p < 1.64\times10^{-4}$ for angular gyrus and $p < 1.0\times10^{-5}$ for lateral occipital cortex). The cortical measures did not remain significant after the effect of age was removed, whereas the relationships between white matter volumes and word chain scores remained significant ($p < 0.010$) after correcting for age.

4.2.5 Regional specificity to reading

In order to assess whether these brain measures are specific to reading or they are under the influence of working memory ability, the correlations between brain measures and reading ability were corrected for individual's working memory scores. White matter volumes in the SNP associated regions remained significant for both reading comprehension ($p < 0.001$) and word chain ($p < 1.57\times10^{-4}$) after working memory was entered as covariate. The cortical thickness in the left temporal and parietal areas remained significant ($p < 0.012$) for word chain (but not for reading comprehension) after correction for working memory ability. This revealed that the cortical ROIs were specific to reading, since the word chain was more related to the word decoding and phonological processing rather than reading comprehension which involves working memory.

4.2.6 Predicting future reading ability

White matter volumes in the SNP associated regions significantly predicted future reading comprehension ($p < 4.60\times10^{-5}$) and word chain ($p < 0.003$) measures. The volumes of white matter remained a significant predictor only for reading comprehension two years later, even after correcting for age ($p < 0.001$) or reading ($p < 0.041$) at baseline.

In order to quantify the amount of information gained from knowing the related SNPs and brain measures compared to the information gained from knowing the baseline reading comprehension scores in predicting future reading, we compared two following models in which age, gender and handedness are identical; Model 1: reading2 = $\beta_1\times$age + $\beta_2\times$gender + $\beta_3\times$handedness + $\beta_4\times$reading1, $r^2 = 0.617$ ($r = 0.785$); Model 2: reading2 = $\beta_1\times$age + $\beta_2\times$gender + $\beta_3\times$handedness + $\beta_4\times$gene + $\beta_5\times$white matter + $\beta_6\times$cortical thickness, $r^2 = 0.613$ ($r = 0.783$). The results showed that genetic information and brain measures at baseline ($r^2 = 0.613$) are approximately as informative as knowing baseline reading ability ($r^2 = 0.617$) in predicting future reading.

In another analysis, we assessed how much of the variance in reading scores can be explained by the brain measures. Using three different models, we found that reading at baseline explained 8.4% more variance than the model predicted by age, gender and handedness ($r^2 = 0.533$). Adding SNPs and structural measures (both white matter volume and cortical thickness) explained another 5.9 % of unique variance about future reading comprehension.

4.2.7 Independent effect of *DCDC2* on white and gray matter structures

Volume of left temporo-parietal pathways correlated with the cortical thickness of left angular gyrus ($p = 0.004$), supramarginal ($p = 0.048$), and middle temporal cortex ($p = 0.039$) after correction for gender and handedness. First, we kept developmental aspect of brain maturation by not removing the effect of age. Then in another analysis, we corrected for the effect of age to see whether the relationship between white matter volume and cortical thickness is age-dependent. After correcting for age the correlation was not significant. The associations of *DCDC2* SNP with white matter volume and cortical thickness were also significant after the effect of age was removed. This revealed the independent effect of *DCDC2* SNP on white matter volume and cortical thickness and showed that this association was not dependent to the developmental relationship between white and gray matter structural variations.

4.3 STUDY III

4.3.1 Dyslexia MRPL19/C2ORF3 locus and general cognitive ability

In this study, 19 SNPs within *MRPL19/C2ORF3, KIAA0319, DCDC2, ATP2C2* and *CMIP* genes were assessed for association with verbal IQ (VIQ) and performance IQ (PIQ) in the Avon Longitudinal Study of Parents and Children (ALSPAC) cohort (Golding et al., 2001). Significant association with VIQ ($p < 0.001$) was found for rs714939 (*MRPL12/C2ORF3* locus) and rs6935076 (*KIAA0319*). Rs714939 showed a significant association with PIQ ($p = 0.006$). After covarying out the reading ability, only rs714939 remained significantly associated with VIQ. G-allele was associated with low performance. A same trend of association was also found for rs917235 within *MRPL19/C2ORF3* locus.

4.3.2 Dyslexia *MRPL19/C2ORF3* locus and white matter

The effect of seven *MRPL19/C2ORF3* SNPs (rs3088180, rs4853169, rs917235, rs6732511, rs714939, rs17689640 and rs17689863) on white matter volume was assessed. Among those SNPs, only rs917235 showed significant association with variation in white matter volume ($p = 1.27\times10^{-3}$ at cluster level of $p < 0.01$) for bilateral posterior part of the corpus callosum and the cingulum (Fig. 7A). G-allele, already shown to be associated with lower IQ, was associated with lower white matter volume. The significant cluster in the posterior corpus callosum was then used as a seed region for streamline fiber tracking. Figs. 7B and C show a sample of fiber tracking for one individual and the probability map of 30 randomly selected subjects, respectively. The pathways passed through this ROI connected the right postcentral gyrus, superior parietal lobule, precuneous, lateral occipital cortex and fusiform gyrus to analogous areas in the left hemisphere (Fig. 7D).

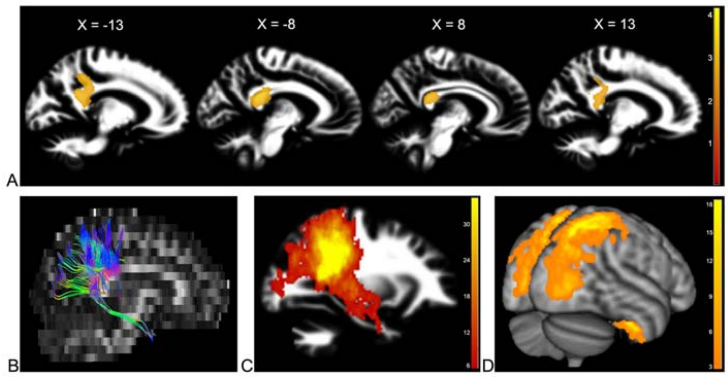

Figure 7: (A) Main association of rs917235 with white matter volume at MNI coordinates of X = −13, −8, 8, and 13 mm relative to midline. (B) A sample of fiber tracking from one individual whows the fibers passing through the rs917235 associated region. (C) Overlay of fiber tracking from 30 randomly selected individuals. The color bar is a count for the number of subjects. (D) Cortical end-points of white matter pathways showing that the fibers connect right postcentral gyrus, superior parietal lobule, precuneous, occipital cortex and temporal fusiform gyrus to the analogous left regions.

4.4 STUDY IV

4.4.1 *ROBO1* genetic associations with white matter volume

In study IV, we first exploratory assessed whether common SNPs anywhere within the *ROBO1* gene would associate with volume of white matter anywhere in the brain. Out of 20 selected SNPs, two SNPs (rs17396958 and rs1393375) were significantly associated with white matter volume in posterior part of the corpus callosum ($p = 5.4\times10^{-6}$ and $p = 2.02\times10^{-5}$, respectively, at FDR-corrected cluster level of $p < 0.05$).

In the second phase, we selected 28 SNPs within and between the haplotype blocks of these two SNPs and then assessed which of these SNPs would associate with the volume of white matter. We masked the white matter with a binary image of the corpus callosum pathways found by probabilistic tracking of the entire corpus callosum. Five of the SNPs (Fig. 8) were associated with the volume of white matter in the right posterior part of corpus callosum, interconnecting the parietal and occipital cortical regions between two hemispheres. All significant clusters overlapped with each other ($p < 0.0018$, at FDR-corrected cluster level, correcting for multiple comparisons of 28 SNPs,). Table 3 lists the peak coordinates, the cluster size and the p-value of the clusters significantly associated with each of those five SNPs.

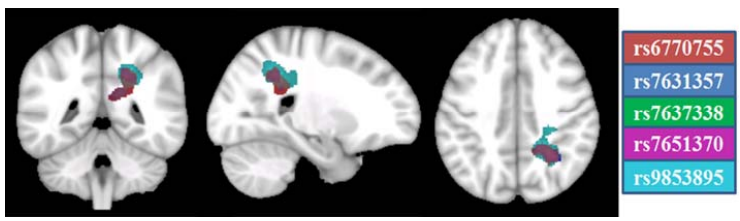

Figure 8: Five *ROBO1* SNPs showed significant effect on white matter volume in the right posterior part of the corpus callosum.

Table 3: Coordinates of the peak voxels for each cluster associated with each SNP.

	$P_{FDR\text{-}corrected}$ Cluster-level	Cluster size	Peak Voxel	
			Z	x, y, z (MNI)
rs6770755	5.49×10^{-5}	1701	6.43	37, -66, 30
rs7631357	1.40×10^{-3}	130	5.13	41, -65, 30
rs7637338	3.89×10^{-4}	78	4.58	42, -65, 25
rs7651370	6.40×10^{-5}	1326	6.03	37, -66, 30
rs9853895	4.89×10^{-5}	2182	5.79	29, -52, 38

4.4.2 Rs7631357 correlated with probability of connection to parietal areas

Two different indices (probability of connection and FA) were computed in the five segments of the corpus callosum (Fig. 9A). The averages of these indices were then analyzed for the associations of the five SNPs ($p < 0.002$, Bonferroni correction for 25 tests). One of the SNPs, rs7631357, was significantly associated with probability of connection of the body of corpus callosum to parietal areas ($p = 1.09 \times 10^{-5}$). FA values did not correlate with the genotype variations in any of these regions. Fig. 9B shows the logarithmic graph of the significant levels of the associations for each SNP and probabilities of connections to different cortical ROIs (Fig. 9B).

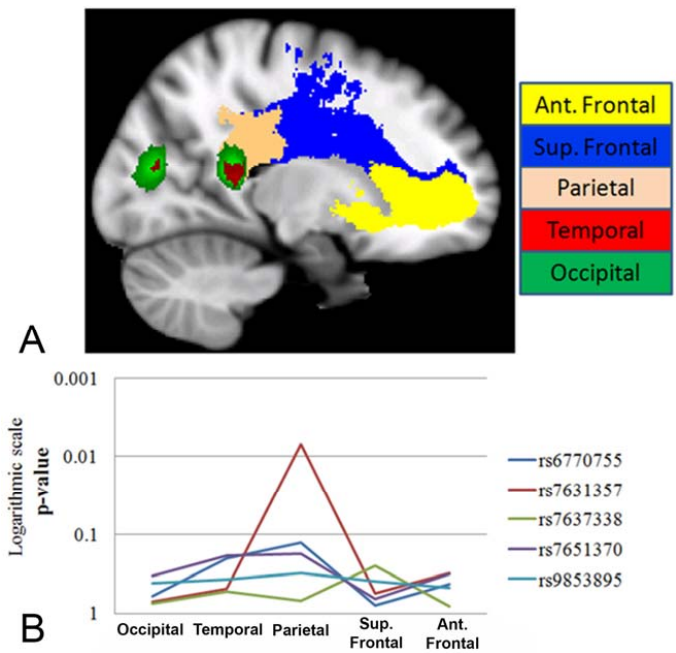

Figure 9: (A) Five different segments of corpus callosum segmented by the probabilistic fiber tracking of the body of corpus callosum with connections to anterior frontal, superior frontal, parietal, temporal and occipital cortex, bilaterally (shown by different colors in a sagittal section of the brain). (B) Logarithmic scale of the p-values for the associations between five significant SNPs and probability of connection in five different segments of the corpus callosum.

4.5 STUDY V

4.5.1 Fronto-parietal and fronto-striatal networks

To find the fronto-parietal and fronto-striatal pathways, the superior frontal and intra-parietal cortical regions (Fig. 10A), as well as the caudate nucleus (shown with light blue in Fig. 10C) were selected for probabilistic fiber tracking since they were active during the performance on a visuospatial working memory task in the scanner and the activity in these cortical regions correlated with working memory performance during development. The population map of the fronto-parietal tract as well as the fronto-striatal pathways are shown in Fig. 10B and C, for the right hemisphere.

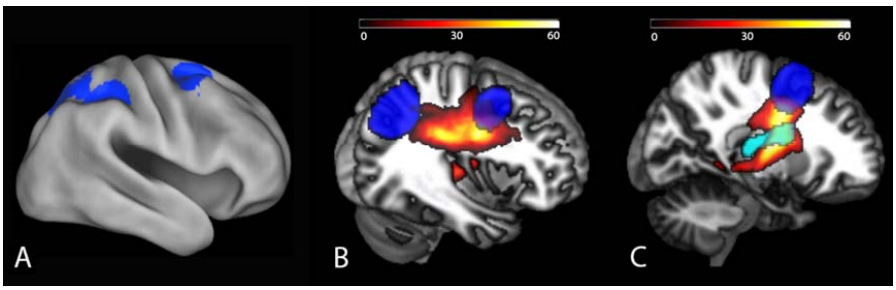

Figure 10: (A) Functionally active cortical regions (superior frontal, superior, and inferior parietal) during the performance on a visuospatial working memory task. (*B*) Population map of probabilistic fiber tracking of fronto-parietal pathway connecting superior frontal to intraparietal cortex. (*C*) Population map of the fronto-striatal pathway, connecting caudate (shown by light blue) to the superior frontal ROI. The color bars correspond to the number of subjects with available white mater pathways.

4.5.2 Cross-sectional analysis

Mean white matter volume and FA values were computed along the white matter pathways. BOLD contrast and cortical thickness were also extracted from functionally defined ROIs. The concurrent correlations between brain–working memory and brain–brain measures were tested by the mixed linear model, including three repeated measures. The model was first tested using gender and handedness as covariates. Then, in another analysis, the model was corrected for the effect of age to assess which of the concurrent relationships were age-independent.

4.5.2.1 Brain–working memory cross-sectional correlations

In the concurrent cross-sectional analysis of brain to working memory measures (Fig. 11), we found significant correlations between BOLD contrast in both frontal and parietal areas and current working memory capacity ($p < 4.2 \times 10^{-4}$). This correlation was not significant for the activity in the caudate nucleus ($p = 0.09$). The volume of white matter and FA values in both fronto-parietal and fronto-striatal tracts correlated with current working memory scores ($p < 1.7 \times 10^{-5}$ and $p < 7.4 \times 10^{-4}$, respectively). Cortical thinning of the parietal areas positively correlated with current working memory capacity ($p = 2.7 \times 10^{-3}$), whereas thickness in superior frontal ($p = 0.11$) and volume of caudate nucleus ($p = 0.86$) did not correlate with working memory scores.

Among all of those brain and working memory relationships, FA values of both fronto-parietal and fronto-striatal pathways ($p < 0.013$) as well as BOLD in the cortical ROIs ($p < 0.027$) and cortical thickness in superior frontal ($p = 0.020$) remained significant after the effect of age was removed.

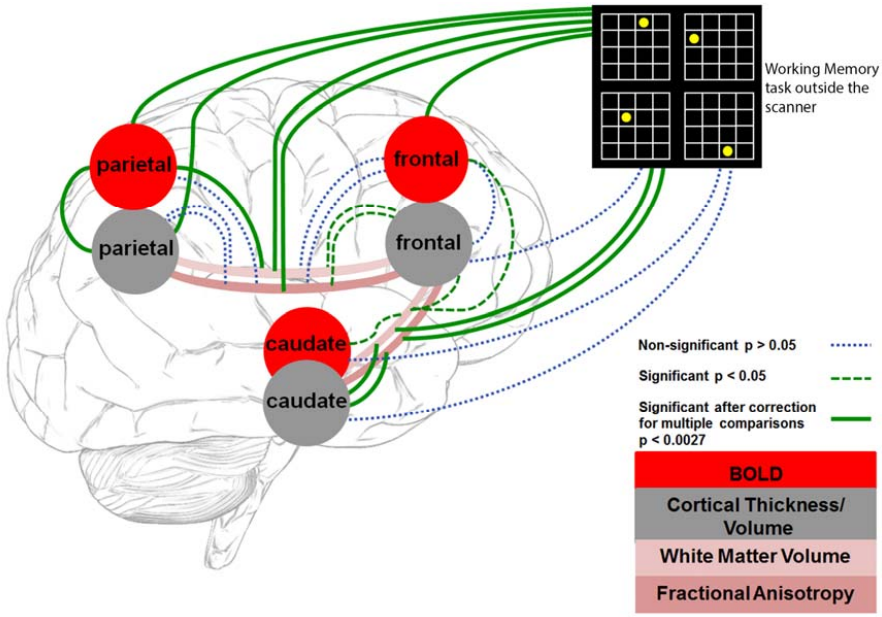

Figure 11: Cross-sectional analysis of correlations between brain–brain and brain–working memory after correction for gender and handedness. The correlations include all three rounds of the data for all variables. The dashed green and dotted blue lines show significant and non-significant correlations, respectively. The thick green lines are those that survived corrections for multiple comparisons.

4.5.2.2 Brain–brain cross-sectional correlations

In cross-sectional assessment of the brain-brain concurrent relationships, we found that the cortical thickness of the parietal ROIs correlated with BOLD contrast values in the corresponding regions ($p = 4.6 \times 10^{-4}$), while this correlation was not significant for the superior frontal ROI. The correlation between the volume of fronto-parietal pathway and the contrast values of parietal area was also significant ($p = 1.4 \times 10^{-3}$). Furthermore, volume of caudate correlated significantly with both white matter volume and FA of the fronto-striatal pathway ($p = 0.039$ and 0.003, respectively).

4.5.3 Longitudinal analysis of working memory capacity

From longitudinal assessment of working memory (Fig. 12), we found that future working memory capacity could be predicted by white matter structural measures in both fronto-parietal and fronto-striatal pathways (for white matter volume: $p < 0.01$ and for FA: $p < 6.6 \times 10^{-5}$). Moreover, BOLD contrast in the caudate significantly predicted future working memory performance ($p = 7.4 \times 10^{-3}$). After correcting for

age at baseline, FA values of both fronto-parietal and fronto-striatal pathways were still significant predictores for future working memory performance, $p < 6.8 \times 10^{-3}$.

We also analyzed the interaction with age in the prediction analyses. The only brain measure that showed significant interaction with age was the caudate activity ($p = 1.8 \times 10^{-4}$). Then, we divided the subjects into 2 groups based on their age (below and above 16 years old) to test the predictive ability of caudate activity in these 2 subsets. After correction for age and sex, the caudate activity significantly predicted future working memory capacity of younger subjects ($p = 9.0 \times 10^{-4}$).

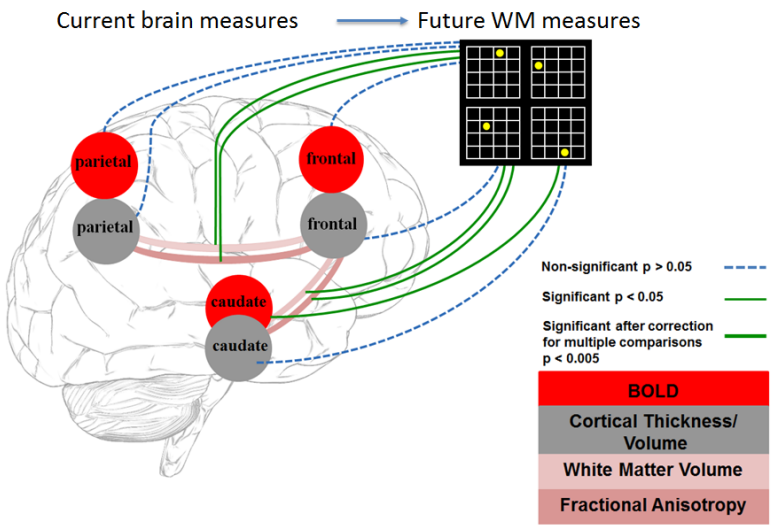

Figure 12: Prediction of future working memory capacity based on the measures collected two years earlier. The dashed green and dotted blue lines show the significant (even after corrections for multiple comparisons) and non-significant correlations, respectively, after correction for gender and handedness.

5 DISCUSSION

5.1 STUDIES I AND II- THE EFFECTS OF DYSLEXIA GENES, *DYX1C1*, *DCDC2* AND *KIAA0319* ON WHITE MATTER STRUCTURE AND CORTICAL THICKNESS

In study I, we first assessed the effect of three genes (*DYX1C1*, *DCDC2* and *KIAA0319*), previously associated with dyslexia and neuronal migration, on white matter structure in a longitudinal sample of typically developing children and young adults. Three polymorphisms within these genes, rs3743204 (*DYX1C1*), rs793842 (*DCDC2*) and rs6935076 (*KIAA0319*) were associated with the variability of white matter in the left temporo-parietal area. Using streamline fiber tracking, we found that the fibers passing through the SNP associated region connected the left middle temporal cortex to the left angular and supramarginal gyri as well as the lateral occipital cortex.

Then in study II, knowing the effect of these genes on neuronal migration, ciliary function and axonal growth, we investigated whether these polymorphisms have any significant effect on the variability of cortical thickness in the associated regions found by fiber tracking. Rs793842 within *DCDC2* was significantly associated with cortical thickness in the left angular and supramarginal gyri and the lateral occipital cortex. T-allele carriers, who also had lower white matter volume and lower reading comprehension scores, showed significantly thicker cortex compared to C-allele carriers.

5.1.1 Neuroimaging findings of impaired reading

The white matter regions associated with dyslexia genes are relatively close to the regions previously associated with reading ability (Beaulieu et al., 2005; Deutsch et al., 2005; Klingberg et al., 2000; Niogi & McCandliss, 2006). These studies have consistently shown a positive correlation between FA values of the left temporo-parietal area and reading ability among typically developing children and young adults. Poor readers could also be differentiated from normal readers through white matter integrity in the left temporo-parietal region (Klingberg et al., 2000). This is consistent with our findings which show significant associations between white matter volume of the temporo-parietal regions and reading comprehension as well as word chain scores.

Significant structural and functional differences in the middle temporal and inferior parietal regions have been reported in impaired readers compared with normal readers. The same regions have also been found to be less active in dyslexic subjects compared with controls (McCandliss et al., 2003; Paulesu et al., 2001; Richlan et al., 2011). Furthermore, gray matter volumetric differences in the middle temporal and inferior parietal regions have also been found in late-literates relative to illiterate individuals (Carreiras et al., 2009). In general, these regions have been reported to be involved in language comprehension and semantic processing using several functional neuroimaging studies (Binder et al., 2009; Noonan et al., 2013; Turken & Dronkers, 2011).

5.1.2 The role and function of dyslexia susceptibility genes

Three dyslexia genes, *DYX1C1*, *DCDC2* and *KIAA0319* are consistently associated with dyslexia across several independent studies (Cope et al., 2005; Couto et al., 2010; Massinen et al., 2009; Meng et al., 2005; Newbury et al., 2011; Paracchini et al., 2008; Schumacher et al., 2006; Venkatesh et al., 2013). The involvement of these genes in neuronal migration has also been established in rat knock-down experiments (Adler et al., 2013; Meng et al., 2005; Paracchini et al., 2006; Wang et al., 2006). Moreover, the malformation of neocortical and hippocampal cortex has been reported in *Dyx1c1* knocked-down rat (Rosen et al., 2007).

In addition to the role of dyslexia susceptibility genes in neuronal migration, two of these genes (*DYX1C1* and *DCDC2*) have been reported to affect the ciliary function (Chandrasekar et al., 2013; Massinen et al., 2011). It has been shown that the expression level of *DCDC2* regulates the ciliary length and signaling of the primary hippocampal neurons (Massinen et al., 2011). The role of *DYX1C1* in ciliary growth and motility has also been shown in a zebrafish model (Chandrasekar et al., 2013).

5.1.3 Imaging genetic studies of dyslexia related genes

Several imaging genetics studies have tried to find the effect of dyslexia susceptibility genes on human brain structure and function. In complement to animal and molecular studies, which aim to understand the molecular mechanism for developmental dyslexia, imaging genetics studies have attempted to use neuroimaging measures for understanding neural mechanisms underlying dyslexia. In an imaging genetics study, gray matter volumetric changes have been linked to a 2.4 kb deletion within *DCDC2* (Meda et al., 2008). Higher gray matter volumes in the occipito-parietal cortex, superior and middle temporal gyri, the intraparietal areas and the inferior and middle frontal gyri have been found for the heterozygous healthy subjects. *KIAA0319* has also been significantly associated with brain activation in superior temporal sulcus (Pinel et al., 2012). Functional brain measures in left inferior parietal lobe and right lateral occipito-temporal gyrus during a performance on reading tasks have been also linked to *DCDC2* polymorphism in a functional imaging study (Cope et al., 2012).

In studies I and II, we first focused on the association between white matter regions and dyslexia genes. Then, based on the fiber tracking of the SNP associated regions in the left temporo-parietal area, we identified the cortical ROIs to assess the associations of the candidate SNPs with cortical thickness. Due to the location of the seed region in left temporo-parietal area and possibly because of the limit of DTI and fiber tracking methods in tracking the crossing fibers, the tracts studied here were restricted to the pathways connecting the parietal, occipital and temporal areas. The occipito-temporal areas have also been reported as structurally and functionally abnormal in dyslexic individuals compared with healthy controls (Altarelli et al., 2013; Kronbichler et al., 2008; Silani et al., 2005; Vinckenbosch et al., 2005). These regions were significantly associated with other dyslexia related loci, *MRPL19/C2ORF3*, in study III.

5.1.4 Brain-behavior relationships

We found significant correlations between reading ability (reading comprehension and word chain scores) and volume of white matter volume in brain regions associated with the genetic variant of the dyslexia SNPs. We also found a significant association between reading ability and cortical thickness of temporal, parietal and occipital regions. These findings are in accordance with previous work regarding the correlations between reading and brain white/gray matter measures (Deutsch et al., 2005; Klingberg et al., 2000; Niogi & McCandliss, 2006). After removing the effect of age, only the white matter volume remained significant for both reading comprehension and word chain scores. This reveals that the relationship between white matter volume and reading ability is not only age-dependent, and other factors such as genetic markers are contributing in this correlation.

In order to assess whether these regions are specifically associated with reading or whether working memory capacity may act as a confounding factor, we corrected for working memory capacity in our sample. White matter volume in the dyslexia SNP associated regions remained significant in association with both reading comprehension and word chain after including working memory as covariate. Furthermore, cortical thickness in the left temporal and parietal areas remained significant for word chain (but not for reading comprehension) after correcting for working memory ability. This reveals that the cortical ROIs are specifically associated with reading, since the word chain is a test which is more related to the word decoding and phonological processing rather than reading comprehension which partly involves working memory.

In another set of analyses, we assessed which brain measure can predict future reading comprehension or word chain scores. White matter volume in the left temporo-parietal region was the only brain measure which significantly predicted future reading comprehension and word chain two years later even after correction for either age or reading at baseline. This suggests that white matter structure provides an essential neural basis for development of cognitive function, as previously shown for working memory which is in turn an essential factor for other cognitive skills (Ullman et al., 2014).

5.1.5 Gene, brain and behavior

In summary, we associated three SNPs within three dyslexia susceptibility genes, rs3743204 (*DYX1C1*), rs793842 (*DCDC2*) and rs6935076 (*KIAA0319*) with variability of left temporo-parietal white matter structure. One of these SNPs, rs793842 (*DCDC2*), has also been linked to the normal variations of cortical thickness in the left supramarginal and angular gyri as well as the lateral occipital cortex. This SNP was also associated with reading ability in our longitudinal sample of normal readers. The T-allele carriers had lower reading scores than C-allele carriers. White matter volume was also significantly lower for rs793842 T-allele carriers who had thicker cortex in left inferior parietal and lateral occipital areas.

To take into account the role of development in our imaging genetics study, we conducted the genetic association analyses as well as the brain-brain and brain-behavior

correlations with and without considering the effect of age. Fig. 13 shows the significant and non-significant associations with solid and dashed arrows, respectively.

DCDC2 associations with both white matter volume and cortical thickness were significant before and after correcting for age. Moreover, *DCDC2* association with reading was significant when the effect of age was removed. The SNP associations with brain measures as well as the correlations between brain measures and behavior were stronger than the genetic association with reading. This suggests that the brain measures are intermediate phenotypes mediating between genetic markers and reading.

Without correction for age, white matter volume of the brain regions associated with rs793842 was negatively correlated with cortical thickness of the parietal areas which have been associated with the same SNP. This emphasizes the parallel maturation of white and gray matter structures during development. Since the genetic associations were all significant after controlling for age, we also considered the white and gray matter structural relationships after correcting for age. This correlation did not remain significant. This suggests an independent effect of *DCDC2* on white matter and cortical thickness. This can be related to the role of *DCDC2* in ciliary function and signaling which affect neuronal migration and axonal outgrowth and in turn affects white and gray matter structures.

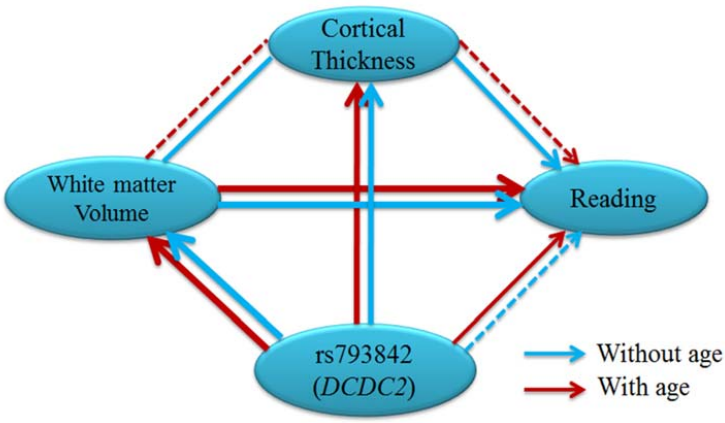

Figure 13: Associations between rs793842 (*DCDC2*), white matter volume, cortical thickness and reading comprehension considering three repeated measures of the longitudinal data, with age and without age as covariate in the model. All associations are corrected for gender and handedness.

5.2 STUDY III- THE EFFECT OF DYSLEXIA LOCUS *MRPL19/C2ORF3* ON WHITE MATTER STRUCTURES AND GENERAL COGNITIVE ABILITY

In study III, *MRPL19/C2ORF3* genetic markers on 2p12 locus were significantly associated with verbal and performance IQ in ALSPAC cohort (Golding et al., 2001). Even after using reading ability as a covariate, the association remained significant for this cohort and was replicated in four other independent samples. *MRPL19/C2ORF3* SNPs did not show any significant association with single-word reading.

In imaging genetics analysis of the candidate SNPs, one of the SNPs (rs917235) within *MRPL19* gene was significantly associated with white matter volume in posterior part of the corpus callosum and the cingulum. White matter volume in these regions was lower for G-allele carriers, who also had lower IQ in the behavioral analysis. Using streamline fiber tracking, we showed that the fibers passing through these regions connected the right postcentral gyrus, superior parietal area, precuneous, lateral occipital cortex and fusiform gyrus to their analogous areas in the left hemisphere. White matter structures with connections to the bilateral occipito-parietal areas have been correlated with measures of IQ in several neuroimaging studies (Chiang et al., 2009; Fjell et al., 2011; Schmithorst et al., 2005). Posterior part of the corpus callosum, an inter-hemispheric tract which connects large parts of the occipital, parietal and temporal lobes, has been previously associated with intelligence (Luders et al., 2011). Previous research also reported that normal and poor readers show significant differences in white matter structure within these regions (Dougherty et al., 2007; Frye et al., 2008; Hasan et al., 2012; Vandermosten et al., 2012).

The parietal, occipital and temporal cortices found by fiber tracking point to the areas involved in both language and general cognitive abilities. The intra parietal sulcus and superior parietal cortex are important neural correlates of reasoning and working memory performance (Jung & Haier, 2007; Koenigs et al., 2009; Olesen et al., 2004). The lateral occipital cortex and fusiform gyrus are involved in cognitive ability since they participate in visual elaboration and perception, recognition and imagination (Jung & Haier, 2007). The occipito-temporal areas have also been reported structurally different in dyslexic readers compared with normal controls (Altarelli et al., 2013; Kronbichler et al., 2008; Silani et al., 2005; Vinckenbosch et al., 2005). The role of these regions in both language and general cognitive ability has been previously established in several neuroimaging studies. However, the brain neural network and the cortical regions involved in cognitive functions are not limited to these regions and there are other regions underlying general cognitive abilities during childhood and adolescence.

5.3 STUDY IV- THE EFFECT OF *ROBO1* GENETIC MARKERS ON CORPUS CALLOSUM

In study IV, we found the association between five *ROBO1* SNPs and white matter volume in posterior part of the corpus callosum. One of the SNPs, rs7631357, was also associated with probability of connections within the fibers extending through the body of corpus callosum to the parietal regions. These findings fit well with previous reports of the role of Robo1 in axonal path finding in mice (Andrews et al., 2006).

The posterior part of corpus callosum interconnects the temporal, parietal and occipital cortices between two hemispheres with large, thick and heavily myelinated axons (Aboitiz et al., 1992). The posterior corpus callosum has been reported to be larger amongst dyslexic subjects in corpus callosum shape analysis studies (Duara et al., 1991; Duta, 2000; Hasan et al., 2012; Rumsey et al., 1997). The microstructure of the

posterior part of the corpus callosum has also been associated with reading skills (Dougherty et al., 2007; Frye et al., 2008).

ROBO1 has previously been shown to functionally affect midline crossing of auditory pathways in humans (Lamminmäki et al., 2012). In a rare Finnish family, there was a deficit in interaural interaction that correlated with the expression levels of *ROBO1*. Our results suggest that *ROBO1* may also regulate the midline crossing of callosal axons in general population.

5.4 STUDY V- ROLE OF FRONTO-PARIETAL AND FRONTO-STRIATAL NETWORKS IN WORKING MEMORY DEVELOPMENT

In this study, the relationships between working memory performance and brain structure and function in functionally defined fronto-parietal and fronto-striatal working memory networks were assessed. The analyses were conducted cross-sectionally and longitudinally in order to find the concurrent brain-brain and brain-behavior relationships as well as to investigate whether measures of brain structure or function can predict future working memory ability. The ROIs were defined based on the main effect of working memory performance during development (Dumontheil et al., 2011; Ziermans et al., 2012). Contrast map of the main effect of working memory during the performance on a visuospatial working memory task was used as a mask for extracting the brain activities of the superior frontal, intra-parietal and the caudate nucleus. Thickness of cortex in these regions was also measured. Mean white matter volume and FA values were also computed along the fronto-parietal and fronto-striatal pathways traced by probabilistic fiber tracking.

5.4.1 Concurrent brain-working memory and brain-brain relationships

Working memory capacity was significantly correlated with brain activity in frontal and parietal cortical regions, thickness of parietal area, and white matter structural and microstructural variability of the fronto-parietal and fronto-striatal tracts. Some other developmental neuroimaging studies have also shown a converging pattern of correlations between brain measures and working memory capacity. Maturation of white matter pathways connecting the frontal and parietal cortical areas has been reported to be positively correlated with visuospatial working memory capacity among children and young adults (Alexander et al., 1991; Nagy et al., 2004; Olesen et al., 2003; Vestergaard et al., 2011; Østby et al., 2011). Moreover, cortical thickness of the fronto-parietal cortical areas has been negatively associated with working memory capacity (Tamnes et al., 2013; Tamnes et al., 2010; Østby et al., 2011) as well as the reasoning ability (Shaw et al., 2006; Sowell et al., 2004; Wendelken et al., 2011) which highly correlates with working memory performance. In addition to structural differences associated with working memory differences, activation in the intra-parietal, superior frontal, and dorsolateral prefrontal cortices have also been positively linked to individual's working memory capacity during childhood and adolescence (Crone et al., 2006; Klingberg et al., 2002; Kwon et al., 2002; Olesen et al., 2007; Olesen et al., 2004; Scherf et al., 2006). The findings are similar to the structural differences found in children and adults suffering from ADHD. In individuals with

ADHD, the cortex has been reported thinner in frontal and parietal areas compared with controls. FA has also been found lower in ADHD cases (Makris et al., 2007; Makris et al., 2008). Since working memory is impaired in ADHD, the findings suggest that the anatomical deficits in ADHD can be linked to working memory impairment.

In our study, correlations between the concurrent brain and working memory measures revealed that white matter measures as well as the functional and structural measures of the cortical areas were the brain measures that could explain the inter-individual differences in working memory capacity. While the subcortical structural and functional measures did not correlate with working memory capacity during development.

Regarding the relationships between brain measures, we found a significant relationship between the fronto-parietal cortical measures and the white matter pathways connecting these regions. This is consistent with previous findings of the fronto-parietal network (Olesen et al., 2003; Østby et al., 2011). The concurrent correlations between brain measures showed that most of these measures are inter-related, though their relationships are under the influence of age.

5.4.2 Prediction of working memory capacity

Longitudinal analyses of the fronto-parietal and fronto-striatal networks revealed that white matter structural changes as well as the activity in caudate could predict future working memory capacity. However, in the study presented here, the cortical measures, which correlated with concurrent measures of working memory, could not predict the working memory capacity two years later.

Inter-individual variations in both volume and FA of the white matter pathways in working memory-related networks correlated with concurrent measures of working memory and predicted working memory capacity two years later. This emphasizes the important role of white matter neural basis and maturation in driving cognitive development.

Activation in caudate during a working memory task was also significantly predictive of future working memory capacity; however, it did not correlate with current working memory scores. There was also a significant interaction between caudate activity and age. The activity in caudate was a stronger predictor for future working memory capacity in younger children compared to older individuals.

The caudate nucleus has been reported active during working memory performance in nonhuman primates (Levy et al., 1997), children (Dumontheil et al., 2011; Klingberg et al., 2002; Ziermans et al., 2012) and adults (McNab & Klingberg, 2007). The caudate has also been associated with implicit learning and habit formation in some other studies (Graybiel, 2008; Packard & Knowlton, 2002). A study of nonhuman primates has shown that by changing the rule in the presentation of a delay task, the activation of the caudate would alter earlier than the activity of the cortical areas, and that cortical activity would correlate with behavior (Pasupathy & Miller, 2005). Moreover, a working memory training study has shown an increase in the activity of caudate and

thalamus after training (Olesen et al., 2004). Another training study has reported an increase in activity of caudate and that striatal activity predicted the working memory improvements after training (Dahlin et al., 2008). Two PET studies have reported the associations between D2 receptor density in caudate and the improvements in working memory performance after training (Bäckman et al., 2011), as well as the links between the density of cortical D1 receptor and the individual's working memory capacity (McNab & Klingberg, 2007). Both *DAT1* and *DRD2* genes are highly expressed in striatal area and both have been associated to the training related improvements in working memory (Brehmer et al., 2009; Söderqvist et al., 2012; Söderqvist et al., 2013). These studies suggest the key role of striatum in both cognitive development and working memory training-related improvements which can be related to the role of basal ganglia and caudate in learning (Graybiel, 2008; Packard & Knowlton, 2002).

6 CONCLUDING REMARKS, LIMITATIONS AND FUTURE DIRECTIONS

The main aim of this thesis was to assess the associations between genes, brain and behavior during typical development. We found the associations of dyslexia susceptibility genes with white matter structures. We then identified the cortical regions connected by the white matter pathways extending through the SNP associated regions. Variations in the thickness of these cortical areas were also correlated with variations of the genetic markers. Moreover, there were significant relationships between the brain and behavioral measures including reading and working memory scores. Among those, only the white matter measures correlated with the current behavioral measures and predicted the future behavioral outcomes. The findings emphasize the important role of white matter structure in driving cognitive development and bridging the gap between gene and behavior.

The longitudinal sample of 90 typically developing children and young adults provided a sufficient basis for studying these relationships and for investigating whether these associations are fixed during development or they interact with age. Three repeated observations of this longitudinal dataset provided more efficient and valid measures rather than a simple cross-sectional design for assessment of the concurrent associations between gene-brain and brain-behavior measures. Moreover, the two-year gap between each administration made it possible to assess the prediction ability of baseline measures in predicting future outcome measures at two years later.

Although the studies presented here benefited from the use of a large cohort of children and adolescence, the sample size was small for genetic studies. Thus, the results need to be replicated in independent samples. Moreover, the effect of environment and its interactions with genes were not considered in our studies due to the lack of appropriate environmental factors in the dataset (i.e., the socioeconomic status, reading ability of the parents, the amount of time that parents spend on reading at home, the amount of time they spend on helping the children with their homework, and other factors). Besides, the important effect of other genetic markers (i.e., the genes that affect white matter development) as well as the biological and environmental factors on the associations between genes, brain and behavior measures cannot be excluded.

The findings presented in this thesis were the associations between genetic markers, brain and behavior. The relationships between gene-white matter and white matter-reading found stronger than the link between gene-reading suggesting an intermediate role of white matter in bridging between genetic markers and behavioral outcomes. Moreover, white matter measures predicted future reading and working memory abilities. This suggests that white matter provides neural basis for development of these cognitive functions.

Regarding the imaging acquisition, the imaging sequences were kept as short as possible to make it tolerable for our pediatric sample. One of these sequences was DTI acquisition which was collected with 19 thick slices (6.5 mm) and 20 gradient

directions. The resolution of this DTI data was not optimal for voxel based analysis and fiber tracking. In third round of data collection, we included another DTI sequence with thinner slices (3.0 mm) and 64 gradient directions. This time, the subjects were older and they already had experience to stay still in the scanner. Tractography on this DTI data provided better fiber tracking results with both streamline and probabilistic fiber tracking. Tractography result of the high resolution DTI data was compared with the tracking of the low resolution DTI data. Although more fibers were detected by tractography of the high resolution data, fiber tracking results found quite consistent using both DTI datasets. In spite of this, we cannot exclude the possibility of finding other fibers extending through our ROIs if we had more informative dataset such as high angular resolution diffusion imaging (HARDI) or diffusion spectrum imaging (DSI). These imaging techniques are more sensitive to intra-voxel heterogeneities caused by different diffusion directions in crossing and branching fibers, and consequently provide more accurate fiber tracking results.

The studies presented here attempted to find the link between genes, brain and behavior and to find the neuronal mechanism underlying the inter-individual variability in cognitive abilities. On the other hand, the animal models help to understand the genetic and neuronal mechanisms at the cellular level. Combining animal imaging techniques with the histological analysis provide information to understand the link between the imaging measures and the cellular and molecular factors contributing the structural and functional variability in the brain.

7 ACKNOWLEDGMENTS

Thinking back to the last four years of my life makes me grateful for the privilege of doing research in such a prestigious university and in a highly inspiring lab, and being surrounded by brilliant minds and ideas of my supportive teachers, colleagues and friends. I would like to express my deepest appreciation to all the people how have been part it and made this a truly wonderful experience. I especially would like to say:

Thank you! to my brilliant supervisor, Torkel Klingberg. Thank you so much, Torkel, for trusting in me at the first place when you accepted me as a PhD student in your lab and letting me to experience new methods and extend my knowledge in the field of cognitive neuroscience. Thanks for your wise guidance, support, encouragement and inspiration throughout these four years. You have always been around with your intelligent advice, while you have let me to think and work independently. I highly admire your talent, intelligence, confidence as an outstanding supervisor who always knows about everything, listens to your questions and comes up with smart ideas and solutions. Thank you for being such supportive!

Thank you! to our inspiring collaborators and co-authors, Juha Kere, Myriam Peyrard-Janvid, Hans Matsson and Satu Massinen. Thank you all for your valuable collaboration, contribution, suggestions and comments on my articles. Thanks for sharing your wonderful ideas and for providing such an amazing genetic dataset that there is no end to dig into it!

Thank you! to my smart advisor, mentor and friend, Rita Almeida. Thank you, Rita, for all your support, care, encouragement, and enthusiasm not only to me but also to every one of us in the group. Indeed, thanks for being a caring Mom for the lab! I would never forget our travel to Seattle where I realized that how smart you are! And yes, it is absolutely true. You are brilliant!

Thank you to all my former and current lab mates: Iroise Dumontheil, Deepak Dash, Chantal Roggeman, Sissela Bergman Nutley, Stina Söderqvist, Tim Ziermans, Megan Spencer-Smith, Benjamin Garzon, Henrik Ullman, Charlotte Nymberg, Elin Lidman, Elin Helander, Elin Allzen, Federico Nemmi, and Margot Schel. I have been lucky to be surrounded by such wonderful, supportive, caring and kind colleagues and friends whose encouragements and supports have been truly valuable to me. Thanks for all the cheerful moments, chats, coffee breaks, launches, after works, conferences, parties, birthdays and lots of joys and cheers. A special thank you to Megan and Charlotte for careful reading and commenting on my thesis.

Thank you to Stockholm Brain Institute (SBI) for providing travel grants for the international conferences. Thank you to Fredrik Ullén and Louise Von Essen for organizing the SBI conferences, seminars and meeting. A special thanks to Jonathan Berrebi for taking care of our analyzing environment (BOLD, RETZ, and BERZ) and for being a technical support.

Thank you to all my Iranian friends, Sepideh, Farahnaz, Kambiz, Azadeh & Ehsan, Hamed, Haleh, Golnaz, Parisa, Sahar, Babak, Bahareh, Motasam, Reza, Zari, Yasi, Behrouz, Maryam & Arash. Thank you all for all the wonderful and joyful moments of chats, fikas, dinners, get togethers, picnics, playing games, reading poems, playing instruments, birthdays, surprises, concerts and other wonderful events.

Special thanks to my lovely friend, Sepideh. Thanks for being a true friend full of energy, happiness, care and support. Special thanks to my kind friends, Farahnaz and Kambiz, for all the wonderful moments of joy here in Stockholm, Netherlands and Iran.

Thank you to all my other supportive friends from all around the world, who have been always supportive throughout my PhD. Hanieh, Farahnaz, Somayeh, Farideh, Saeedeh, Ameneh, Maryam, Masoumeh, Mehrsima, Fereshteh and Raheleh, Miss you all!

Last but the most important and biggest thank you to my beloved ones, my mother, my father, my sisters, my brother and my sister-in-law. Thank you for your endless and unconditional love, support, care, joy and happiness. Love you!

8 REFERENCES

Aboitiz, F., Scheibel, A. B., Fisher, R. S., & Zaidel, E. (1992). Fiber composition of the human corpus callosum. *Brain research, 598*(1), 143-153.

Adler, W. T., Platt, M. P., Mehlhorn, A. J., Haight, J. L., Currier, T. A., Etchegaray, M. A., . . . Rosen, G. D. (2013). Position of Neocortical Neurons Transfected at Different Gestational Ages with shRNA Targeted against Candidate Dyslexia Susceptibility Genes. *PloS one, 8*(5), e65179.

Alexander, G. E., Crutcher, M. D., & DeLong, M. R. (1991). Basal ganglia-thalamocortical circuits: parallel substrates for motor, oculomotor,"prefrontal" and "limbic" functions. *Progress in brain research, 85*, 119-146.

Alloway, T. (2007). Automated Working Memory Assessment Manual. *Oxford: Harcourt.*

Altarelli, I., Monzalvo, K., Iannuzzi, S., Fluss, J., Billard, C., Ramus, F., & Dehaene-Lambertz, G. (2013). A Functionally Guided Approach to the Morphometry of Occipitotemporal Regions in Developmental Dyslexia: Evidence for Differential Effects in Boys and Girls. *The Journal of Neuroscience, 33*(27), 11296-11301.

Ando, J., Ono, Y., & Wright, M. J. (2001). Genetic structure of spatial and verbal working memory. *Behavior genetics, 31*(6), 615-624.

Andrews, W., Liapi, A., Plachez, C., Camurri, L., Zhang, J., Mori, S., . . . Richards, L. J. (2006). Robo1 regulates the development of major axon tracts and interneuron migration in the forebrain. *Development, 133*(11), 2243-2252.

Anthoni, H., Zucchelli, M., Matsson, H., Müller-Myhsok, B., Fransson, I., Schumacher, J., . . . Griesemann, H. (2007). A locus on 2p12 containing the co-regulated MRPL19 and C2ORF3 genes is associated to dyslexia. *Human molecular genetics, 16*(6), 667-677.

Ashburner, J. (2007). A fast diffeomorphic image registration algorithm. *Neuroimage, 38*(1), 95-113.

Astrom, R. L., Wadsworth, S. J., & DeFries, J. C. (2007). Etiology of the stability of reading difficulties: the longitudinal twin study of reading disabilities. *Twin Research and Human Genetics, 10*(03), 434-439.

Baaré, W. F., Pol, H. E. H., Boomsma, D. I., Posthuma, D., de Geus, E. J., Schnack, H. G., . . . Kahn, R. S. (2001). Quantitative genetic modeling of variation in human brain morphology. *Cerebral Cortex, 11*(9), 816-824.

Baddeley, A. (1992). Working memory. *Science, 255*(5044), 556-559.

Barkovich, A., Kuzniecky, R., Jackson, G., Guerrini, R., & Dobyns, W. (2005). A developmental and genetic classification for malformations of cortical development. *Neurology, 65*(12), 1873-1887.

Barnea-Goraly, N., Menon, V., Eckert, M., Tamm, L., Bammer, R., Karchemskiy, A., . . . Reiss, A. L. (2005). White matter development during childhood and adolescence: a cross-sectional diffusion tensor imaging study. *Cerebral Cortex, 15*(12), 1848-1854.

Bates, T. C., Luciano, M., Castles, A., Coltheart, M., Wright, M. J., & Martin, N. G. (2007). Replication of reported linkages for dyslexia and spelling and suggestive evidence for novel regions on chromosomes 4 and 17. *European Journal of Human Genetics, 15*(2), 194-203.

Bates, T. C., Luciano, M., Medland, S. E., Montgomery, G. W., Wright, M. J., & Martin, N. G. (2011). Genetic variance in a component of the language

acquisition device: ROBO1 polymorphisms associated with phonological buffer deficits. *Behavior genetics, 41*(1), 50-57.

Batouli, S. A. H., Trollor, J. N., Wen, W., & Sachdev, P. S. (2014). The heritability of volumes of brain structures and its relationship to age: A review of twin and family studies. *Ageing research reviews, 13*, 1-9.

Bayliss, D. M., Jarrold, C., Baddeley, A. D., & Leigh, E. (2005). Differential constraints on the working memory and reading abilities of individuals with learning difficulties and typically developing children. *Journal of Experimental Child Psychology, 92*(1), 76-99.

Beaulieu, C. (2002). The basis of anisotropic water diffusion in the nervous system–a technical review. *NMR in Biomedicine, 15*(7-8), 435-455.

Beaulieu, C., Plewes, C., Paulson, L. A., Roy, D., Snook, L., Concha, L., & Phillips, L. (2005). Imaging brain connectivity in children with diverse reading ability. *Neuroimage, 25*(4), 1266-1271.

Bellini, G., Bravaccio, C., Calamoneri, F., Cocuzza, M. D., Fiorillo, P., Gagliano, A., . . . Militerni, R. (2005). No evidence for association between dyslexia and DYX1C1 functional variants in a group of children and adolescents from Southern Italy. *Journal of molecular neuroscience, 27*(3), 311-314.

Benes, F. M. (1989). Myelination of cortical-hippocampal relays during late adolescence. *Schizophrenia Bulletin, 15*(4), 585.

Binder, J. R., Desai, R. H., Graves, W. W., & Conant, L. L. (2009). Where is the semantic system? A critical review and meta-analysis of 120 functional neuroimaging studies. *Cerebral Cortex, 19*(12), 2767-2796.

Bond, T. G., & Fox, C. M. (2001). *Applying the Rasch model: Fundamental measurement in the human sciences*: Lawrence Erlbaum Associates Publishers.

Bourgeois, J.-P., & Rakic, P. (1993). Changes of synaptic density in the primary visual cortex of the macaque monkey from fetal to adult stage. *The Journal of Neuroscience, 13*(7), 2801-2820.

Brehmer, Y., Westerberg, H., Bellander, M., Fürth, D., Karlsson, S., & Bäckman, L. (2009). Working memory plasticity modulated by dopamine transporter genotype. *Neuroscience letters, 467*(2), 117-120.

Brkanac, Z., Chapman, N. H., Matsushita, M. M., Chun, L., Nielsen, K., Cochrane, E., . . . Raskind, W. H. (2007). Evaluation of candidate genes for DYX1 and DYX2 in families with dyslexia. *American Journal of Medical Genetics Part B: Neuropsychiatric Genetics, 144*(4), 556-560.

Bäckman, L., Nyberg, L., Soveri, A., Johansson, J., Andersson, M., Dahlin, E., . . . Rinne, J. O. (2011). Effects of working-memory training on striatal dopamine release. *Science, 333*(6043), 718-718.

Carreiras, M., Seghier, M. L., Baquero, S., Estévez, A., Lozano, A., Devlin, J. T., & Price, C. J. (2009). An anatomical signature for literacy. *Nature, 461*(7266), 983-986.

Carrion-Castillo, A., Franke, B., & Fisher, S. E. (2013). Molecular genetics of dyslexia: an overview. *Dyslexia, 19*(4), 214-240.

Casey, B., Cohen, J. D., Jezzard, P., Turner, R., Noll, D. C., Trainor, R. J., . . . Rapoport, J. L. (1995). Activation of prefrontal cortex in children during a nonspatial working memory task with functional MRI. *Neuroimage, 2*(3), 221-229.

Casey, B., Giedd, J. N., & Thomas, K. M. (2000). Structural and functional brain development and its relation to cognitive development. *Biological psychology, 54*(1), 241-257.

Chandrasekar, G., Vesterlund, L., Hultenby, K., Tapia-Paez, I., & Kere, J. (2013). The Zebrafish Orthologue of the Dyslexia Candidate Gene DYX1C1 Is Essential for Cilia Growth and Function. *PloS one, 8*(5), e63123.

Chapman, N. H., Igo, R. P., Thomson, J. B., Matsushita, M., Brkanac, Z., Holzman, T., . . . Raskind, W. H. (2004). Linkage analyses of four regions previously implicated in dyslexia: confirmation of a locus on chromosome 15q. *American Journal of Medical Genetics Part B: Neuropsychiatric Genetics, 131*(1), 67-75.

Chiang, M.-C., Barysheva, M., Shattuck, D. W., Lee, A. D., Madsen, S. K., Avedissian, C., . . . De Zubicaray, G. I. (2009). Genetics of brain fiber architecture and intellectual performance. *The Journal of Neuroscience, 29*(7), 2212-2224.

Concha, L., Livy, D. J., Beaulieu, C., Wheatley, B. M., & Gross, D. W. (2010). In vivo diffusion tensor imaging and histopathology of the fimbria-fornix in temporal lobe epilepsy. *The Journal of Neuroscience, 30*(3), 996-1002.

Cope, N., Eicher, J. D., Meng, H., Gibson, C. J., Hager, K., Lacadie, C., . . . Gruen, J. R. (2012). Variants in the DYX2 locus are associated with altered brain activation in reading-related brain regions in subjects with reading disability. *Neuroimage*.

Cope, N., Harold, D., Hill, G., Moskvina, V., Stevenson, J., Holmans, P., . . . Williams, J. (2005). Strong Evidence That KIAA0319 on Chromosome 6p Is a Susceptibility Gene for Developmental Dyslexia. *The American Journal of Human Genetics, 76*(4), 581-591.

Couto, J. M., Livne-Bar, I., Huang, K., Xu, Z., Cate-Carter, T., Feng, Y., . . . Kerr, E. N. (2010). Association of reading disabilities with regions marked by acetylated H3 histones in KIAA0319. *American Journal of Medical Genetics Part B: Neuropsychiatric Genetics, 153*(2), 447-462.

Crone, E. A., Wendelken, C., Donohue, S., van Leijenhorst, L., & Bunge, S. A. (2006). Neurocognitive development of the ability to manipulate information in working memory. *Proceedings of the National Academy of Sciences, 103*(24), 9315-9320.

Currier, T. A., Etchegaray, M. A., Haight, J. L., Galaburda, A. M., & Rosen, G. D. (2011). The effects of embryonic knockdown of the candidate dyslexia susceptibility gene homologue< i> Dyx1c1</i> on the distribution of GABAergic neurons in the cerebral cortex. *Neuroscience, 172*, 535-546.

Dahlin, E., Neely, A. S., Larsson, A., Bäckman, L., & Nyberg, L. (2008). Transfer of learning after updating training mediated by the striatum. *Science, 320*(5882), 1510-1512.

Dale, A. M., Fischl, B., & Sereno, M. I. (1999). Cortical surface-based analysis: I. Segmentation and surface reconstruction. *Neuroimage, 9*(2), 179-194.

Deffenbacher, K. E., Kenyon, J. B., Hoover, D. M., Olson, R. K., Pennington, B. F., DeFries, J. C., & Smith, S. D. (2004). Refinement of the 6p21. 3 quantitative trait locus influencing dyslexia: linkage and association analyses. *Human genetics, 115*(2), 128-138.

DeFries, J., & Alarcón, M. (1996). Genetics of specific reading disability. *Mental Retardation and Developmental Disabilities Research Reviews, 2*(1), 39-47.

DeFries, J. C., Fulker, D. W., & LaBuda, M. C. (1987). Evidence for a genetic aetiology in reading disability of twins. *Nature, 329*(6139), 537-539.

Demerens, C., Stankoff, B., Logak, M., Anglade, P., Allinquant, B., Couraud, F., . . . Lubetzki, C. (1996). Induction of myelination in the central nervous system by electrical activity. *Proceedings of the National Academy of Sciences, 93*(18), 9887-9892.

Démonet, J.-F., Taylor, M. J., & Chaix, Y. (2004). Developmental dyslexia. *The Lancet, 363*(9419), 1451-1460.

Deutsch, G. K., Dougherty, R. F., Bammer, R., Siok, W. T., Gabrieli, J. D., & Wandell, B. (2005). Children's reading performance is correlated with white matter structure measured by diffusion tensor imaging. *Cortex, 41*(3), 354-363.

Dougherty, R. F., Ben-Shachar, M., Deutsch, G. K., Hernandez, A., Fox, G. R., & Wandell, B. A. (2007). Temporal-callosal pathway diffusivity predicts phonological skills in children. *Proceedings of the National Academy of Sciences, 104*(20), 8556-8561.

Duara, R., Kushch, A., Gross-Glenn, K., Barker, W. W., Jallad, B., Pascal, S., . . . Levin, B. (1991). Neuroanatomic differences between dyslexic and normal readers on magnetic resonance imaging scans. *Archives of neurology, 48*(4), 410-416.

Dubois, J., Dehaene-Lambertz, G., Kulikova, S., Poupon, C., Hüppi, P., & Hertz-Pannier, L. (2013). The early development of brain white matter: A review of imaging studies in fetuses, newborns and infants. *Neuroscience*.

Dumontheil, I., Roggeman, C., Ziermans, T., Peyrard-Janvid, M., Matsson, H., Kere, J., & Klingberg, T. (2011). Influence of the COMT Genotype on Working Memory and Brain Activity Changes During Development. *Biological psychiatry, 70*(3), 222-229.

Duta, N. (2000). Corpus callosum shape analysis: a comparative study of group differences associated with dyslexia, gender and handedness.

Eicher, J. D., & Gruen, J. R. (2013). Imaging-genetics in dyslexia: Connecting risk genetic variants to brain neuroimaging and ultimately to reading impairments. *Molecular genetics and metabolism, 110*(3), 201-212.

Eicher, J. D., Powers, N. R., Miller, L. L., Mueller, K. L., Mascheretti, S., Marino, C., . . . Smith, S. D. (2014). Characterization of the DYX2 locus on chromosome 6p22 with reading disability, language impairment, and IQ. *Human genetics*, 1-13.

Fischl, B., & Dale, A. M. (2000). Measuring the thickness of the human cerebral cortex from magnetic resonance images. *Proceedings of the National Academy of Sciences, 97*(20), 11050-11055.

Fisher, S. E., & DeFries, J. C. (2002). Developmental dyslexia: genetic dissection of a complex cognitive trait. *Nature Reviews Neuroscience, 3*(10), 767-780.

Fisher, S. E., Francks, C., Marlow, A. J., MacPhie, I. L., Newbury, D. F., Cardon, L. R., . . . Gayán, J. (2002). Independent genome-wide scans identify a chromosome 18 quantitative-trait locus influencing dyslexia. *Nature genetics, 30*(1), 86-91.

Fjell, A. M., Westlye, L. T., Amlien, I. K., & Walhovd, K. B. (2011). Reduced white matter integrity is related to cognitive instability. *The Journal of Neuroscience, 31*(49), 18060-18072.

Francks, C., Paracchini, S., Smith, S. D., Richardson, A. J., Scerri, T. S., Cardon, L. R., . . . Pennington, B. F. (2004). A 77-kilobase region of chromosome 6p22. 2 is associated with dyslexia in families from the United Kingdom and from the United States. *The American Journal of Human Genetics, 75*(6), 1046-1058.

Frith, C., Friston, K., Herold, S., Silbersweig, D., Fletcher, P., Cahill, C., . . . Liddle, P. (1995). Regional brain activity in chronic schizophrenic patients during the performance of a verbal fluency task. *The British Journal of Psychiatry, 167*(3), 343-349.

Frye, R. E., Hasan, K., Xue, L., Strickland, D., Malmberg, B., Liederman, J., & Papanicolaou, A. (2008). Splenium microstructure is related to two dimensions of reading skill. *Neuroreport, 19*(16), 1627.

Gabel, L. A., Gibson, C. J., Gruen, J. R., & LoTurco, J. J. (2010). Progress towards a cellular neurobiology of reading disability. *Neurobiology of disease, 38*(2), 173-180.

Gathercole, S. E., Alloway, T. P., Willis, C., & Adams, A.-M. (2006). Working memory in children with reading disabilities. *Journal of Experimental Child Psychology, 93*(3), 265-281.

Gathercole, S. E., Pickering, S. J., Ambridge, B., & Wearing, H. (2004). The structure of working memory from 4 to 15 years of age. *Developmental psychology, 40*(2), 177.

Giedd, J. N., Blumenthal, J., Jeffries, N. O., Castellanos, F. X., Liu, H., Zijdenbos, A., . . . Rapoport, J. L. (1999). Brain development during childhood and adolescence: a longitudinal MRI study. *Nature neuroscience, 2*(10), 861-863.

Giorgio, A., Watkins, K., Douaud, G., James, A., James, S., De Stefano, N., . . . Johansen-Berg, H. (2008). Changes in white matter microstructure during adolescence. *Neuroimage, 39*(1), 52-61.

Goddings, A.-L., Mills, K., Clasen, L., Giedd, J., Viner, R., & Blakemore, S.-J. (2014). Longitudinal MRI to assess effect of puberty on subcortical brain development: an observational study. *The Lancet, 383*, S52.

Gogtay, N., Giedd, J. N., Lusk, L., Hayashi, K. M., Greenstein, D., Vaituzis, A. C., . . . Toga, A. W. (2004). Dynamic mapping of human cortical development during childhood through early adulthood. *Proceedings of the national academy of sciences of the united states of america, 101*(21), 8174-8179.

Golding, J., Pembrey, M., & Jones, R. (2001). ALSPAC--the Avon Longitudinal Study of Parents and Children. I. Study methodology. *Paediatric and perinatal epidemiology, 15*(1), 74-87.

Graybiel, A. M. (2008). Habits, rituals, and the evaluative brain. *Annu. Rev. Neurosci., 31*, 359-387.

Grigorenko, E. L., Wood, F. B., Meyer, M. S., & Pauls, D. L. (2000). Chromosome 6p influences on different dyslexia-related cognitive processes: further confirmation. *The American Journal of Human Genetics, 66*(2), 715-723.

Hannula-Jouppi, K., Kaminen-Ahola, N., Taipale, M., Eklund, R., Nopola-Hemmi, J., Kääriäinen, H., & Kere, J. (2005). The axon guidance receptor gene ROBO1 is a candidate gene for developmental dyslexia. *PLoS Genetics, 1*(4), e50.

Hasan, K. M., Molfese, D. L., Walimuni, I. S., Stuebing, K. K., Papanicolaou, A. C., Narayana, P. A., & Fletcher, J. M. (2012). Diffusion tensor quantification and cognitive correlates of the macrostructure and microstructure of the corpus callosum in typically developing and dyslexic children. *NMR in Biomedicine, 25*(11), 1263-1270.

Huttenlocher, P. R., & Dabholkar, A. S. (1997). Regional differences in synaptogenesis in human cerebral cortex. *Journal of comparative Neurology, 387*(2), 167-178.

Ivliev, A. E., AC't Hoen, P., van Roon-Mom, W. M., Peters, D. J., & Sergeeva, M. G. (2012). Exploring the transcriptome of ciliated cells using in silico dissection of human tissues. *PloS one, 7*(4), e35618.

Jamadar, S., Powers, N., Meda, S., Gelernter, J., Gruen, J., & Pearlson, G. (2011). Genetic influences of cortical gray matter in language-related regions in healthy controls and schizophrenia. *Schizophrenia research, 129*(2), 141-148.

Johnson, M. B., Kawasawa, Y. I., Mason, C. E., Krsnik, Ž., Coppola, G., Bogdanović, D., . . . Šestan, N. (2009). Functional and evolutionary insights into human brain development through global transcriptome analysis. *Neuron, 62*(4), 494-509.

Jung, R. E., & Haier, R. J. (2007). The Parieto-Frontal Integration Theory (P-FIT) of intelligence: converging neuroimaging evidence. *Behavioral and Brain Sciences, 30*(02), 135-154.

Kaminen, N., Hannula-Jouppi, K., Kestilä, M., Lahermo, P., Muller, K., Kaaranen, M., . . . Nopola-Hemmi, J. (2003). A genome scan for developmental dyslexia confirms linkage to chromosome 2p11 and suggests a new locus on 7q32. *Journal of Medical Genetics, 40*(5), 340-345.

Klingberg, T., Forssberg, H., & Westerberg, H. (2002). Increased brain activity in frontal and parietal cortex underlies the development of visuospatial working memory capacity during childhood. *Journal of cognitive neuroscience, 14*(1), 1-10.

Klingberg, T., Hedehus, M., Temple, E., Salz, T., Gabrieli, J. D., Moseley, M. E., & Poldrack, R. A. (2000). Microstructure of temporo-parietal white matter as a basis for reading ability: evidence from diffusion tensor magnetic resonance imaging. *Neuron, 25*(2), 493-500.

Koenigs, M., Barbey, A. K., Postle, B. R., & Grafman, J. (2009). Superior parietal cortex is critical for the manipulation of information in working memory. *The Journal of Neuroscience, 29*(47), 14980-14986.

Kolb, B., & Gibb, R. (2011). Brain plasticity and behaviour in the developing brain. *Journal of the Canadian Academy of Child and Adolescent Psychiatry, 20*(4), 265.

Kronbichler, M., Wimmer, H., Staffen, W., Hutzler, F., Mair, A., & Ladurner, G. (2008). Developmental dyslexia: gray matter abnormalities in the occipitotemporal cortex. *Human brain mapping, 29*(5), 613-625.

Kwon, H., Reiss, A. L., & Menon, V. (2002). Neural basis of protracted developmental changes in visuo-spatial working memory. *Proceedings of the National Academy of Sciences, 99*(20), 13336-13341.

LaMantia, A., & Rakic, P. (1990). Axon overproduction and elimination in the corpus callosum of the developing rhesus monkey. *The Journal of Neuroscience, 10*(7), 2156-2175.

Lamminmäki, S., Massinen, S., Nopola-Hemmi, J., Kere, J., & Hari, R. (2012). Human ROBO1 regulates interaural interaction in auditory pathways. *The Journal of Neuroscience, 32*(3), 966-971.

Lebel, C., & Beaulieu, C. (2011). Longitudinal development of human brain wiring continues from childhood into adulthood. *The Journal of Neuroscience, 31*(30), 10937-10947.

Lebel, C., Gee, M., Camicioli, R., Wieler, M., Martin, W., & Beaulieu, C. (2012). Diffusion tensor imaging of white matter tract evolution over the lifespan. *Neuroimage, 60*(1), 340-352.

Lebel, C., Walker, L., Leemans, A., Phillips, L., & Beaulieu, C. (2008). Microstructural maturation of the human brain from childhood to adulthood. *Neuroimage, 40*(3), 1044-1055.

Leh, S. E., Johansen-Berg, H., & Ptito, A. (2006). Unconscious vision: new insights into the neuronal correlate of blindsight using diffusion tractography. *Brain, 129*(7), 1822-1832.

Lenroot, R. K., Gogtay, N., Greenstein, D. K., Wells, E. M., Wallace, G. L., Clasen, L. S., . . . Evans, A. C. (2007). Sexual dimorphism of brain developmental trajectories during childhood and adolescence. *Neuroimage, 36*(4), 1065-1073.

Lerch, J. P., Yiu, A. P., Martinez-Canabal, A., Pekar, T., Bohbot, V. D., Frankland, P. W., . . . Sled, J. G. (2011). Maze training in mice induces MRI-detectable brain shape changes specific to the type of learning. *Neuroimage, 54*(3), 2086-2095.

Lewis, M. D. (2005). Self-organizing individual differences in brain development. *Developmental Review, 25*(3), 252-277.

Levy, R., Friedman, H. R., Davachi, L., & Goldman-Rakic, P. S. (1997). Differential activation of the caudate nucleus in primates performing spatial and nonspatial working memory tasks. *The Journal of Neuroscience, 17*(10), 3870-3882.

López-Bendito, G., Flames, N., Ma, L., Fouquet, C., Di Meglio, T., Chedotal, A., . . . Marín, O. (2007). Robo1 and Robo2 cooperate to control the guidance of major axonal tracts in the mammalian forebrain. *The Journal of Neuroscience, 27*(13), 3395-3407.

Luciana, M., & Nelson, C. A. (1998). The functional emergence of prefrontally-guided working memory systems in four-to eight-year-old children. *Neuropsychologia, 36*(3), 273-293.

Luders, E., Thompson, P. M., Narr, K. L., Zamanyan, A., Chou, Y.-Y., Gutman, B., . . . Toga, A. W. (2011). The link between callosal thickness and intelligence in healthy children and adolescents. *Neuroimage, 54*(3), 1823-1830.

Lyon, G. R. (2003). Reading disabilities: Why do some children have difficulty learning to read? What can be done about it. *Perspectives, 29*(2), 17-19.

Makris, N., Biederman, J., Valera, E. M., Bush, G., Kaiser, J., Kennedy, D. N., . . . Seidman, L. J. (2007). Cortical thinning of the attention and executive function networks in adults with attention-deficit/hyperactivity disorder. *Cerebral Cortex, 17*(6), 1364-1375.

Makris, N., Buka, S. L., Biederman, J., Papadimitriou, G. M., Hodge, S. M., Valera, E. M., . . . Caviness, V. S. (2008). Attention and executive systems abnormalities in adults with childhood ADHD: A DT-MRI study of connections. *Cerebral Cortex, 18*(5), 1210-1220.

Marino, C., Citterio, A., Giorda, R., Facoetti, A., Menozzi, G., Vanzin, L., . . . Molteni, M. (2007). Association of short-term memory with a variant within DYX1C1 in developmental dyslexia. *Genes, Brain and Behavior, 6*(7), 640-646.

Marshall, W. F., & Nonaka, S. (2006). Cilia: tuning in to the cell's antenna. *Current biology, 16*(15), R604-R614.

Massinen, S., Hokkanen, M.-E., Matsson, H., Tammimies, K., Tapia-Páez, I., Dahlström-Heuser, V., . . . Swoboda, P. (2011). Increased expression of the dyslexia candidate gene DCDC2 affects length and signaling of primary cilia in neurons. *PloS one, 6*(6), e20580.

Massinen, S., Tammimies, K., Tapia-Páez, I., Matsson, H., Hokkanen, M.-E., Söderberg, O., . . . Treuter, E. (2009). Functional interaction of DYX1C1 with estrogen receptors suggests involvement of hormonal pathways in dyslexia. *Human molecular genetics, 18*(15), 2802-2812.

McCandliss, B. D., Cohen, L., & Dehaene, S. (2003). The visual word form area: expertise for reading in the fusiform gyrus. *Trends in cognitive sciences, 7*(7), 293-299.

McGrath, L. M., Smith, S. D., & Pennington, B. F. (2006). Breakthroughs in the search for dyslexia candidate genes. *Trends in molecular medicine, 12*(7), 333-341.

McNab, F., & Klingberg, T. (2007). Prefrontal cortex and basal ganglia control access to working memory. *Nature neuroscience, 11*(1), 103-107.

Meda, S. A., Gelernter, J., Gruen, J. R., Calhoun, V. D., Meng, H., Cope, N. A., & Pearlson, G. D. (2008). Polymorphism of DCDC2 reveals differences in cortical morphology of healthy individuals—a preliminary voxel based morphometry study. *Brain imaging and behavior, 2*(1), 21-26.

Meng, H., Smith, S. D., Hager, K., Held, M., Liu, J., Olson, R. K., . . . O'Reilly-Pol, T. (2005). DCDC2 is associated with reading disability and modulates neuronal

development in the brain. *Proceedings of the national academy of sciences of the united states of america, 102*(47), 17053-17058.
Nagy, Z., Westerberg, H., & Klingberg, T. (2004). Maturation of white matter is associated with the development of cognitive functions during childhood. *Journal of cognitive neuroscience, 16*(7), 1227-1233.
Newbury, D., Paracchini, S., Scerri, T., Winchester, L., Addis, L., Richardson, A. J., . . . Monaco, A. (2011). Investigation of dyslexia and SLI risk variants in reading- and language-impaired subjects. *Behavior genetics, 41*(1), 90-104.
Niogi, S. N., & McCandliss, B. D. (2006). Left lateralized white matter microstructure accounts for individual differences in reading ability and disability. *Neuropsychologia, 44*(11), 2178-2188.
Noonan, K. A., Jefferies, E., Visser, M., & Ralph, M. A. L. (2013). Going beyond inferior prefrontal involvement in semantic control: evidence for the additional contribution of dorsal angular gyrus and posterior middle temporal cortex. *Journal of cognitive neuroscience, 25*(11), 1824-1850.
Nopola-Hemmi, J., Taipale, M., Haltia, T., Lehesjoki, A.-E., Voutilainen, A., & Kere, J. (2000). Two translocations of chromosome 15q associated with dyslexia. *Journal of Medical Genetics, 37*(10), 771-775.
Olesen, P. J., Macoveanu, J., Tegnér, J., & Klingberg, T. (2007). Brain activity related to working memory and distraction in children and adults. *Cerebral Cortex, 17*(5), 1047-1054.
Olesen, P. J., Nagy, Z., Westerberg, H., & Klingberg, T. (2003). Combined analysis of DTI and fMRI data reveals a joint maturation of white and grey matter in a fronto-parietal network. *Cognitive Brain Research, 18*(1), 48-57.
Olesen, P. J., Westerberg, H., & Klingberg, T. (2004). Increased prefrontal and parietal activity after training of working memory. *Nature neuroscience, 7*(1), 75-79.
Olson, R. K., Datta, H., Gayan, J., & DeFries, J. C. (1999). A behavioral-genetic analysis of reading disabilities and component processes. *Converging methods for understanding reading and dyslexia*, 133-153.
Packard, M. G., & Knowlton, B. J. (2002). Learning and memory functions of the basal ganglia. *Annual review of neuroscience, 25*(1), 563-593.
Paracchini, S., Steer, C., Buckingham, L.-L., Morris, A., Ring, S., Scerri, T., . . . Golding, J. (2008). Association of the KIAA0319 dyslexia susceptibility gene with reading skills in the general population. *American Journal of Psychiatry, 165*(12), 1576-1584.
Paracchini, S., Thomas, A., Castro, S., Lai, C., Paramasivam, M., Wang, Y., . . . Scerri, T. (2006). The chromosome 6p22 haplotype associated with dyslexia reduces the expression of KIAA0319, a novel gene involved in neuronal migration. *Human molecular genetics, 15*(10), 1659-1666.
Pasupathy, A., & Miller, E. K. (2005). Different time courses of learning-related activity in the prefrontal cortex and striatum. *Nature, 433*(7028), 873-876.
Paulesu, E., Démonet, J.-F., Fazio, F., McCrory, E., Chanoine, V., Brunswick, N., . . . Frith, C. D. (2001). Dyslexia: cultural diversity and biological unity. *Science, 291*(5511), 2165-2167.
Paus, T. (2010). Growth of white matter in the adolescent brain: myelin or axon? *Brain and cognition, 72*(1), 26-35.
Paus, T., Zijdenbos, A., Worsley, K., Collins, D. L., Blumenthal, J., Giedd, J. N., . . . Evans, A. C. (1999). Structural maturation of neural pathways in children and adolescents: in vivo study. *Science, 283*(5409), 1908-1911.
Peschansky, V. J., Burbridge, T. J., Volz, A. J., Fiondella, C., Wissner-Gross, Z., Galaburda, A. M., . . . Rosen, G. D. (2010). The effect of variation in expression of the candidate dyslexia susceptibility gene homolog Kiaa0319 on neuronal

migration and dendritic morphology in the rat. *Cerebral Cortex, 20*(4), 884-897.

Petryshen, T., Kaplan, B., Hughes, M., Tzenova, J., & Field, L. (2002). Supportive evidence for the DYX3 dyslexia susceptibility gene in Canadian families. *Journal of Medical Genetics, 39*(2), 125-126.

Pfefferbaum, A., Mathalon, D. H., Sullivan, E. V., Rawles, J. M., Zipursky, R. B., & Lim, K. O. (1994). A quantitative magnetic resonance imaging study of changes in brain morphology from infancy to late adulthood. *Archives of neurology, 51*(9), 874-887.

Pfefferbaum, A., Sullivan, E. V., & Carmelli, D. (2001). Genetic regulation of regional microstructure of the corpus callosum in late life. *Neuroreport, 12*(8), 1677-1681.

Pinel, P., Fauchereau, F., Moreno, A., Barbot, A., Lathrop, M., Zelenika, D., . . . Dehaene, S. (2012). Genetic variants of FOXP2 and KIAA0319/TTRAP/THEM2 locus are associated with altered brain activation in distinct language-related regions. *The Journal of Neuroscience, 32*(3), 817-825.

Pol, H. E. H., Schnack, H. G., Posthuma, D., Mandl, R. C., Baaré, W. F., van Oel, C., . . . Amunts, K. (2006). Genetic contributions to human brain morphology and intelligence. *The Journal of Neuroscience, 26*(40), 10235-10242.

Posthuma, D., De Geus, E., Neale, M., Pol, H. H., Baare, W., Kahn, R., & Boomsma, D. (2000). Multivariate genetic analysis of brain structure in an extended twin design. *Behavior genetics, 30*(4), 311-319.

Postle, B. R., Zarahn, E., & D'Esposito, M. (2000). Using event-related fMRI to assess delay-period activity during performance of spatial and nonspatial working memory tasks. *Brain Research Protocols, 5*(1), 57-66.

Price, C. J., Moore, C., Humphreys, G., & Wise, R. (1997). Segregating semantic from phonological processes during reading. *Journal of cognitive neuroscience, 9*(6), 727-733.

Reuter, M., & Fischl, B. (2011). Avoiding asymmetry-induced bias in longitudinal image processing. *Neuroimage, 57*(1), 19-21.

Reuter, M., Rosas, H. D., & Fischl, B. (2010). Highly accurate inverse consistent registration: a robust approach. *Neuroimage, 53*(4), 1181-1196.

Reuter, M., Schmansky, N. J., Rosas, H. D., & Fischl, B. (2012). Within-subject template estimation for unbiased longitudinal image analysis. *Neuroimage*.

Richlan, F., Kronbichler, M., & Wimmer, H. (2011). Meta-analyzing brain dysfunctions in dyslexic children and adults. *Neuroimage, 56*(3), 1735-1742.

Rosen, G. D., Bai, J., Wang, Y., Fiondella, C. G., Threlkeld, S. W., LoTurco, J. J., & Galaburda, A. M. (2007). Disruption of neuronal migration by RNAi of Dyx1c1 results in neocortical and hippocampal malformations. *Cerebral Cortex, 17*(11), 2562-2572.

Rumsey, J. M., Nace, K., Donohue, B., Wise, D., Maisog, J. M., & Andreason, P. (1997). A positron emission tomographic study of impaired word recognition and phonological processing in dyslexic men. *Archives of neurology, 54*(5), 562-573.

Scherf, K. S., Sweeney, J. A., & Luna, B. (2006). Brain basis of developmental change in visuospatial working memory. *Journal of cognitive neuroscience, 18*(7), 1045-1058.

Schmithorst, V. J., Wilke, M., Dardzinski, B. J., & Holland, S. K. (2002). Correlation of white matter diffusivity and anisotropy with age during childhood and adolescence: a cross-sectional diffusion-tensor MR imaging study. *Radiology, 222*(1), 212.

Schmithorst, V. J., Wilke, M., Dardzinski, B. J., & Holland, S. K. (2005). Cognitive functions correlate with white matter architecture in a normal pediatric population: a diffusion tensor MRI study. *Human brain mapping, 26*(2), 139-147.

Schmitt, J. E., Eyler, L. T., Giedd, J. N., Kremen, W. S., Kendler, K. S., & Neale, M. C. (2007). Review of twin and family studies on neuroanatomic phenotypes and typical neurodevelopment. *Twin Research and Human Genetics, 10*(05), 683-694.

Schulte-Körne, G., Ziegler, A., Deimel, W., Schumacher, J., Plume, E., Bachmann, C., . . . Warnke, A. (2007). Interrelationship and familiality of dyslexia related quantitative measures. *Annals of human genetics, 71*(2), 160-175.

Schumacher, J., Anthoni, H., Dahdouh, F., König, I. R., Hillmer, A. M., Kluck, N., . . . Remschmidt, H. (2006). Strong genetic evidence of DCDC2 as a susceptibility gene for dyslexia. *The American Journal of Human Genetics, 78*(1), 52-62.

Shaw, P., Greenstein, D., Lerch, J., Clasen, L., Lenroot, R., Gogtay, N., . . . Giedd, J. (2006). Intellectual ability and cortical development in children and adolescents. *Nature, 440*(7084), 676-679.

Shaw, P., Kabani, N. J., Lerch, J. P., Eckstrand, K., Lenroot, R., Gogtay, N., . . . Rapoport, J. L. (2008). Neurodevelopmental trajectories of the human cerebral cortex. *The Journal of Neuroscience, 28*(14), 3586-3594.

Shaywitz, B. A., Shaywitz, S. E., Blachman, B. A., Pugh, K. R., Fulbright, R. K., Skudlarski, P., . . . Marchione, K. E. (2004). Development of left occipitotemporal systems for skilled reading in children after a phonologically-based intervention. *Biological psychiatry, 55*(9), 926-933.

Shaywitz, B. A., Shaywitz, S. E., Pugh, K. R., Mencl, W. E., Fulbright, R. K., Skudlarski, P., . . . Lyon, G. R. (2002). Disruption of posterior brain systems for reading in children with developmental dyslexia. *Biological psychiatry, 52*(2), 101-110.

Shaywitz, B. A., Shaywltz, S. E., Pugh, K. R., Constable, R. T., Skudlarski, P., Fulbright, R. K., . . . Katz, L. (1995). Sex differences in the functional organization of the brain for language.

Shaywitz, S. E., Escobar, M. D., Shaywitz, B. A., Fletcher, J. M., & Makuch, R. (1992). Evidence that dyslexia may represent the lower tail of a normal distribution of reading ability. *New England Journal of Medicine, 326*(3), 145-150.

Shaywitz, S. E., Shaywitz, B. A., Fletcher, J. M., & Escobar, M. D. (1990). Prevalence of reading disability in boys and girls. *JAMA: the journal of the American Medical Association, 264*(8), 998-1002.

Silani, G., Frith, U., Demonet, J.-F., Fazio, F., Perani, D., Price, C., . . . Paulesu, E. (2005). Brain abnormalities underlying altered activation in dyslexia: a voxel based morphometry study. *Brain, 128*(10), 2453-2461.

Smith, S. D., Kimberling, W. J., Pennington, B. F., & Lubs, H. A. (1983). Specific reading disability: identification of an inherited form through linkage analysis. *Science, 219*(4590), 1345-1347.

Sowell, E. R., Delis, D., Stiles, J., & Jernigan, T. L. (2001). Improved memory functioning and frontal lobe maturation between childhood and adolescence: a structural MRI study. *Journal of the International Neuropsychological Society, 7*(03), 312-322.

Sowell, E. R., Thompson, P. M., Leonard, C. M., Welcome, S. E., Kan, E., & Toga, A. W. (2004). Longitudinal mapping of cortical thickness and brain growth in normal children. *The Journal of Neuroscience, 24*(38), 8223-8231.

Spear, L. P. (2000). The adolescent brain and age-related behavioral manifestations. *Neuroscience & Biobehavioral Reviews, 24*(4), 417-463.

Squeglia, L. M., Jacobus, J., Sorg, S. F., Jernigan, T. L., & Tapert, S. F. (2013). Early Adolescent Cortical Thinning Is Related to Better Neuropsychological Performance. *Journal of the International Neuropsychological Society, 19*(09), 962-970.

Stevens, B., Tanner, S., & Fields, R. D. (1998). Control of myelination by specific patterns of neural impulses. *The Journal of Neuroscience, 18*(22), 9303-9311.

Swanson, H. L., & Beebe-Frankenberger, M. (2004). The Relationship Between Working Memory and Mathematical Problem Solving in Children at Risk and Not at Risk for Serious Math Difficulties. *Journal of Educational Psychology, 96*(3), 471.

Szalkowski, C. E., Fiondella, C. G., Galaburda, A. M., Rosen, G. D., LoTurco, J. J., & Fitch, R. H. (2012). Neocortical disruption and behavioral impairments in rats following in utero RNAi of candidate dyslexia risk gene Kiaa0319. *International Journal of Developmental Neuroscience, 30*(4), 293-302.

Söderqvist, S., Bergman Nutley, S., Peyrard-Janvid, M., Matsson, H., Humphreys, K., Kere, J., & Klingberg, T. (2012). Dopamine, working memory, and training induced plasticity: Implications for developmental research. *Developmental psychology, 48*(3), 836.

Söderqvist, S., Matsson, H., Peyrard-Janvid, M., Kere, J., & Klingberg, T. (2013). Polymorphisms in the Dopamine Receptor 2 Gene Region Influence Improvements during Working Memory Training in Children and Adolescents. *Journal of Cognitive Neuroscience in press*.

Taipale, M., Kaminen, N., Nopola-Hemmi, J., Haltia, T., Myllyluoma, B., Lyytinen, H., . . . Hannula-Jouppi, K. (2003). A candidate gene for developmental dyslexia encodes a nuclear tetratricopeptide repeat domain protein dynamically regulated in brain. *Proceedings of the National Academy of Sciences, 100*(20), 11553-11558.

Tammimies, K., Vitezic, M., Matsson, H., Le Guyader, S., Bürglin, T. R., Öhman, T., . . . Kere, J. (2013). Molecular Networks of DYX1C1 Gene Show Connection to Neuronal Migration Genes and Cytoskeletal Proteins. *Biological psychiatry, 73*(6), 583-590.

Tamnes, C. K., Walhovd, K. B., Grydeland, H., Holland, D., Østby, Y., Dale, A. M., & Fjell, A. M. (2013). Longitudinal working memory development is related to structural maturation of frontal and parietal cortices. *Journal of cognitive neuroscience, 25*(10), 1611-1623.

Tamnes, C. K., Østby, Y., Walhovd, K. B., Westlye, L. T., Due-Tønnessen, P., & Fjell, A. M. (2010). Neuroanatomical correlates of executive functions in children and adolescents: a magnetic resonance imaging (MRI) study of cortical thickness. *Neuropsychologia, 48*(9), 2496-2508.

Thomas, Spassky, N., Perez Villegas, E., Olivier, C., Cobos, I., Goujet-Zalc, C., . . . Zalc, B. (2000). Spatiotemporal development of oligodendrocytes in the embryonic brain. *Journal of neuroscience research, 59*(4), 471-476.

Thomas, K. M., King, S. W., Franzen, P. L., Welsh, T. F., Berkowitz, A. L., Noll, D. C., . . . Casey, B. (1999). A developmental functional MRI study of spatial working memory. *Neuroimage, 10*(3), 327-338.

Thompson, P. M., Cannon, T. D., Narr, K. L., Van Erp, T., Poutanen, V.-P., Huttunen, M., . . . Khaledy, M. (2001). Genetic influences on brain structure. *Nature neuroscience, 4*(12), 1253-1258.

Tran, C., Gagnon, F., Wigg, K., Feng, Y., Gomez, L., Cate-Carter, T., . . . Lovett, M. (2013). A family-based association analysis and meta-analysis of the reading

disabilities candidate gene DYX1C1. *American Journal of Medical Genetics Part B: Neuropsychiatric Genetics, 162*(2), 146-156.
Turken, U., & Dronkers, N. F. (2011). The neural architecture of the language comprehension network: converging evidence from lesion and connectivity analyses. *Frontiers in systems neuroscience, 5*.
Ullman, H., Almeida, R., & Klingberg, T. (2014). Structural maturation and brain activity predict future working memory capacity during childhood development. *The Journal of Neuroscience, 34*(5), 1592-1598.
Unni, D. K., Piper, M., Moldrich, R. X., Gobius, I., Liu, S., Fothergill, T., . . . Richards, L. J. (2012). Multiple Slits regulate the development of midline glial populations and the corpus callosum. *Developmental biology, 365*(1), 36-49.
van Leeuwen, M., van den Berg, S. M., Peper, J. S., Pol, H. E. H., & Boomsma, D. I. (2009). Genetic covariance structure of reading, intelligence and memory in children. *Behavior genetics, 39*(3), 245-254.
Vandermosten, M., Boets, B., Poelmans, H., Sunaert, S., Wouters, J., & Ghesquière, P. (2012). A tractography study in dyslexia: neuroanatomic correlates of orthographic, phonological and speech processing. *Brain, 135*(3), 935-948.
Wang, Y., Paramasivam, M., Thomas, A., Bai, J., Kaminen-Ahola, N., Kere, J., . . . Loturco, J. (2006). DYX1C1 functions in neuronal migration in developing neocortex. *Neuroscience, 143*(2), 515-522.
Wedeen, V. J., Hagmann, P., Tseng, W. Y. I., Reese, T. G., & Weisskoff, R. M. (2005). Mapping complex tissue architecture with diffusion spectrum magnetic resonance imaging. *Magnetic Resonance in Medicine, 54*(6), 1377-1386.
Wendelken, C., O'Hare, E. D., Whitaker, K. J., Ferrer, E., & Bunge, S. A. (2011). Increased functional selectivity over development in rostrolateral prefrontal cortex. *The Journal of Neuroscience, 31*(47), 17260-17268.
Venkatesh, S. K., Siddaiah, A., Padakannaya, P., & Ramachandra, N. B. (2013). Lack of association between genetic polymorphisms in ROBO1, MRPL19/C2ORF3 and THEM2 with Developmental Dyslexia. *Gene, 529*(2), 215-219.
Vestergaard, M., Madsen, K. S., Baaré, W. F., Skimminge, A., Ejersbo, L. R., Ramsøy, T. Z., . . . Jernigan, T. L. (2011). White matter microstructure in superior longitudinal fasciculus associated with spatial working memory performance in children. *Journal of cognitive neuroscience, 23*(9), 2135-2146.
Wierenga, L. M., Langen, M., Oranje, B., & Durston, S. (2014). Unique developmental trajectories of cortical thickness and surface area. *Neuroimage, 87*, 120-126.
Vinckenbosch, E., Robichon, F., & Eliez, S. (2005). Gray matter alteration in dyslexia: converging evidence from volumetric and voxel-by-voxel MRI analyses. *Neuropsychologia, 43*(3), 324-331.
Woodcock, R. W. (1987). *Woodcock reading mastery tests, revised*: American Guidance Service Circle Pines, MN.
Wright, I. C., Sham, P., Murray, R. M., Weinberger, D. R., & Bullmore, E. T. (2002). Genetic contributions to regional variability in human brain structure: methods and preliminary results. *Neuroimage, 17*(1), 256-271.
Yakovlev, P. I., & Lecours, A.-R. (1967). The myelogenetic cycles of regional maturation of the brain. *Regional development of the brain in early life*, 3-70.
Zatorre, R. J., Fields, R. D., & Johansen-Berg, H. (2012). Plasticity in gray and white: neuroimaging changes in brain structure during learning. *Nature neuroscience, 15*(4), 528-536.
Zhang, Y. E., Landback, P., Vibranovski, M. D., & Long, M. (2011). Accelerated recruitment of new brain development genes into the human genome. *PLoS biology, 9*(10), e1001179.

Ziermans, T., Dumontheil, I., Roggeman, C., Peyrard-Janvid, M., Matsson, H., Kere, J., & Klingberg, T. (2012). Working memory brain activity and capacity link MAOA polymorphism to aggressive behavior during development. *Translational psychiatry*, *2*(2), e85.

Østby, Y., Tamnes, C. K., Fjell, A. M., & Walhovd, K. B. (2011). Morphometry and connectivity of the fronto-parietal verbal working memory network in development. *Neuropsychologia, 49*(14), 3854-3862.

I

Three Dyslexia Susceptibility Genes, *DYX1C1*, *DCDC2*, and *KIAA0319*, Affect Temporo-Parietal White Matter Structure

Fahimeh Darki, Myriam Peyrard-Janvid, Hans Matsson, Juha Kere, and Torkel Klingberg

Background: Volume and integrity of white matter correlate with reading ability, but the underlying factors contributing to this variability are unknown.

Methods: We investigated single nucleotide polymorphisms in three genes previously associated with dyslexia and implicated in neuronal migration (*DYX1C1*, *DCDC2*, *KIAA0319*) and white matter volume in a cohort of 76 children and young adults from the general population.

Results: We found that all three genes contained polymorphisms that were significantly associated with white matter volume in the left temporo-parietal region and that white matter volume influenced reading ability.

Conclusions: The identified region contained white matter pathways connecting the middle temporal gyrus with the inferior parietal lobe. The finding links previous neuroimaging and genetic results and proposes a mechanism underlying variability in reading ability in both normal and impaired readers.

Key Words: Diffusion tensor imaging, dyslexia genes, general population, reading ability, single nucleotide polymorphism, SNP

Reading is a complex cognitive activity, requiring the recruitment of multiple brain regions. Insights into the neurobiology of reading are provided by neuroimaging studies of typical adult readers, development of reading in children, as well as by studies of developmental dyslexia, a specific reading disability exhibited in 5%–15% of the population (1,2). Anatomically, dyslexia has been associated with nested neurons, so-called ectopias, in language regions of both male and female subjects, which might relate to disturbed neuronal migration early in life (3,4). Functional neuroimaging studies have shown altered deviant activation in subjects with dyslexia, including lower activation of the left temporal, inferior parietal and occipito-temporal regions (5–7). Cortical thickness is also affected in similar regions (8).

Dyslexic individuals have also shown disturbances of white matter structure in the left temporo-parietal region (9). Interestingly, variability in white matter structure not only differentiates impaired from nonimpaired subjects but also correlates with variability in reading ability among typically developing children and adults (9–12). This shows that connectivity between language regions is crucial for reading. Secondly, these findings suggest that the same neural mechanisms could underlie both the normal variability in reading ability and dyslexia. However, the cause for this variability is not yet known. In this study, we hypothesized that polymorphisms in genes associated with dyslexia and implicated in neuronal migration in early brain development would affect variability of white matter structure in typically developing children and young adults and contribute to variability in reading ability.

A number of genes have been associated with dyslexia, and the three most consistently replicated genes are *DYX1C1*, *DCDC2*, and *KIAA0319* (13–18). Some previous studies have failed to replicate the association between *DYX1C1* and dyslexia in samples from the United Kingdom, Italy, United States, and India (19–22). However, it should be noted that the sample sizes used were relatively small, and differences exist in association test designs between original publications and replication attempts. All three genes are involved in neuronal migration, as seen in rat knock-down experiments (14,23,24). In the *DYX1C1* knock-down animal models, disturbances in neuronal migration lead to ectopias and changes in both gray and white matter structure. Recent studies have also suggested that polymorphisms in some of the *DYX1C1*, *KIAA0319*, and *DCDC2* genes are related to normal variability in reading ability (25–28) and to brain activation in language related-regions (29).

In this study, we genotyped 13 single nucleotide polymorphisms (SNPs), in or near the vicinity of three genes *DYX1C1*, *DCDC2*, and *KIAA0319* in a group of 76 randomly selected 6–25-year-old children and young adults. Volume of white matter was measured with a T1-weighted magnetic resonance sequence, and microstructure of white matter was investigated by diffusion tensor imaging (DTI). These measurements were then repeated 2 years later in 69 of the subjects. The use of a developmental sample and longitudinal design allowed us also to investigate whether any genetic effect was constant across age or whether it interacted with age. The former would suggest a very early effect on brain development only, whereas the latter would suggest an effect on the gradual maturation of white matter during childhood, such as myelination.

Methods and Materials

Participants

Seventy-six healthy Swedish-speaking children and young adults (age range 6 to 25 years, 41 male and 35 female subjects) without any evidence of neurological or psychological disorders were randomly selected from the population register in the city of Nynäshamn to participate (see [30,31] for further description of the cohort). On the basis of available parent reports, in most (89%) cases the participants and both of their parents were born in Sweden, 9% had at least one parent born outside of Sweden but within Europe, and the remaining 2% had one or both parents born outside of Europe. This study was approved by the local ethics committee of the Karolinska University Hospital. Written informed consent was obtained from each participant and the parents of those participants younger than 18 years old. On the basis of parent reports, one subject had dyslexia, and two were under investigation for dyslexia. The data from these subjects did not deviate significantly from the statistical analysis models (genetics vs. white matter and white matter vs. reading residuals, standardized residuals <2 SDs in both cases). Imaging and behavioral assessments were performed for all the participants and repeated two years later for 69 of them.

Image Acquisition and Processing

Three-dimensional structural T1-weighted imaging (magnetization-prepared rapid gradient echo sequence, repetition time =

From the Neuroscience Department (FD, TK), Karolinska Institutet, Stockholm; Department of Biosciences and Nutrition (MP-J, HM, JK), Karolinska Institutet, Huddinge; Science for Life Laboratory (JK), Karolinska Institutet, Solna, Sweden; and the Research Programs Unit (JK), Haartman Institute, University of Helsinki, and Folkhälsan Institute of Genetics, Helsinki, Finland.

Address correspondence to Torkel Klingberg, M.D., Ph.D., Department of Neuroscience, Karolinska Institutet, Retzius v. 8, Stockholm 171 76, Sweden; E-mail: torkel.klingberg@ki.se.

Received Oct 28, 2011; revised Apr 27, 2012; accepted May 4, 2012.

0006-3223/$36.00
http://dx.doi.org/10.1016/j.biopsych.2012.05.008

2300 msec, echo time = 2.92 msec) with a 256 × 256 mm field of view, 176 sagittal slices, and 1 mm^3 voxel size was carried out with a 1.5T Avanto scanner (Siemens Medical System, Inc., Erlangen, Germany) on the participants and repeated after two years for 69 subjects. GRAPPA parallel imaging technique with an acceleration factor of two was also employed to speed up the acquisition.

White matter segmentation was performed on the structural data with a Voxel-Based Morphometry tool available via SPM5 (www.fil.ion.ucl.ac.uk/spm/software/spm5) and followed by an alignment technique performed with the Diffeomorphic Anatomical Registration with Exponentiated Lie algebra (DARTEL) toolbox in SPM. This method iteratively aligned the white matter images from both timepoint 1 and timepoint 2 to their common average template. The modulated images were then spatially smoothed with a Gaussian kernel size of 8 mm and registered to Montreal Neurological Institute space. Because the DARTEL morphing was applied to tissue segmented images, output images were the tissue probability maps in which each voxel shows the probabilty of being locally expanded or contracted in each white matter structure.

Diffusion tensor imaging was acquired with a field of view of 230 × 230 mm^2, matrix size of 128 × 128, 19 slices with 6.5 mm thickness, and b-value of 1000 sec/mm^2 in 20 gradient directions. Eddy current and head motions were corrected with affine registration to a reference volume with FSL software (www.fmrib.ox.ac.uk/fsl/). The diffusion tensors were then computed for each voxel, and the DTI and fractional anisotropy (FA) data were constructed. Tract-Based Spatial Statistics, TBSS v1.2, (fsl.fmrib.ox.ac.uk/fsl/tbss/) was applied to align all FA images to the mean FA image. In this step, the TBSS inverse transformation method was used to find the region of interest (ROI) projected on the FA data of all individuals. Deterministic fibers were obtained from 30 randomly selected subjects by starting tractography from the ROI following the principal eigenvector direction with 1 mm steps, considering thresholds of .15 for FA values and 30 for angular degree, with ExploreDTI v4.7.3. (www.exploredti.com). These 30 subjects were selected randomly from the total imaging sample, and the distribution of their genotypes was not significantly different from the whole sample ($p > .32$ assessed by χ^2 test), so they represent the whole imaging sample. The computed tracts of all individuals were then transformed to the mean FA template with the same TBSS transformation matrices already used for each subject to mean normalization.

Behavioral Assessment

The reading comprehension task for this study was administered either individually or in groups of two to 20 participants in a classroom setting. To measure reading comprehension, narrative and expository texts from the Progress in International Reading Literacy Trend Study and The International Association for the Evaluation of Educational Achievement Reading Literacy Study 1991 were employed. Seventy-seven items were used to form reading comprehension tests for four age groups from 8 to 25 years old. An item response theory analysis was used to achieve an ability score for each subject.

Because reading comprehension encompasses a range of cognitive processes, including not only language-specific aspects but also attention and working memory, we also administrated a second test of word decoding, called "word chains." This is similar to the English Woodcock Johnson Word-ID test, in which the subjects read as many words as possible during a 2-min period and get a score on the basis of the number of correctly read words (32).

Genotyping

Material for DNA extraction was collected from all subjects in form of blood from finger tips or saliva. Genotyping of 13 SNPs located in or in close vicinity to the three genes—*DYX1C1*: rs3743204, rs3743205, and rs17819126; *DCDC2*: rs793842, rs793862, rs807701, rs2328819, rs2792682, rs7751169, and rs9460974; *KIAA0319*: rs4504469, rs6935076, and rs2143340—was performed with matrix-assisted laser desorption/ionization-time of flight mass spectrometry with iPlex Gold assays according to instructions of the manufacturer as follows: polymerase chain reaction assays and associated extension reactions were designed with the MassArray assay design 3.1 software (Sequenom; www.sequenom.com). Primers were acquired from Metabion GmbH (Planegg-Martinsried, Germany). Amplification reactions were run in a total volume of 5 μL with 10 ng of genomic DNA and 1 pmol of the amplification primer, 100 nmol/L of each deoxynucleotide triphosphate, 1.625 mmol/L of magnesium chloride, and .5 U of HotStarTaq DNA polymerase (Qiagen, Crawley, West Sussex, United Kingdom). Reactions were heated at 95°C for 15 min and thereafter subjected to 45 cycles of amplification (20 sec at 94°C, 30 sec at 56°C, 60 sec at 72°C) before a final extension of 3 min at 72°C. Unincorporated deoxyribonucleotide triphosphates were dephosphorylated by addition of .3 U shrimp alkaline phosphatase. Extension reactions were carried out in a total volume of 9 μL with .625–1.25 μmol/L extension primer, and the Iplex Gold Reagents Kit Clean primer extension products were analyzed by a MassARRAY mass spectrometer (Bruker Daltonik GmbH, Bremen, Germany). For peak identification, the SpectroT RT3.3.0/4.0 software (Sequenom) was used.

The genotyping of all SNPs studied here was originally performed in a larger sample of 335 individuals, of which 76 were randomly selected to participate in the magnetic resonance imaging. The SNPs were validated with DNA from a set of 14 trios (42 individuals) with genotype data available through the HapMap consortium. Furthermore, two independent scorers confirmed all genotypes and re-genotyping of 5% of the study samples resulted in 100% concordance. Concordance analyses with the HapMap data resulted in 100% concordance. The average genotyping success rate for all 13 SNPs reported here was 98.9%.

Statistical Analysis

All of the 13 SNPs were entered separately as a main factor in a flexible factorial design second-level SPM analysis (www.fil.ion.ucl.ac.uk/spm/software/spm5), which included both the individual images with and without repeated measures, to assess the variation of white matter volume with respect to genetic markers. This analysis was corrected for the effect of age, gender, handedness, and total white matter volume. Age × gene and gender × gene interaction effects were also added into the model. As a part of this exploratory analysis the significance level was corrected at the cluster level with nonstationary cluster extent correction (33). We corrected for multiple comparison of searching the entire white matter volume (with the threshold of $p < .05$) and, in addition, for the analysis of 13 SNPs (Bonferroni correction, with $p_{corrected} < .0038$). The 3dClustSim program of the AFNI toolkit (http://afni.nimh.nih.gov/afni) was used to determine the cluster size threshold by Monte-Carlo simulation (uncorrected significant level = .05, cluster significant level = .0038, cluster size threshold = 2285 voxels).

The significant regions were saved as binary ROIs and then entered in MarsBar SPM toolbox (http://marsbar.sourceforge.net) to compute the mean white matter volume. The mean values were then analyzed with linear mixed models in SPSS Statistics v. 20 (IBM Corporation, Somers, New York) to assess whether the white matter volume in these regions might correlate with the reading ability.

Results

After co-registering the imaging data to a common template, white matter volume was used as the dependent variable in a flexible factorial model with SPM5. This measure reflects signal intensity modulated

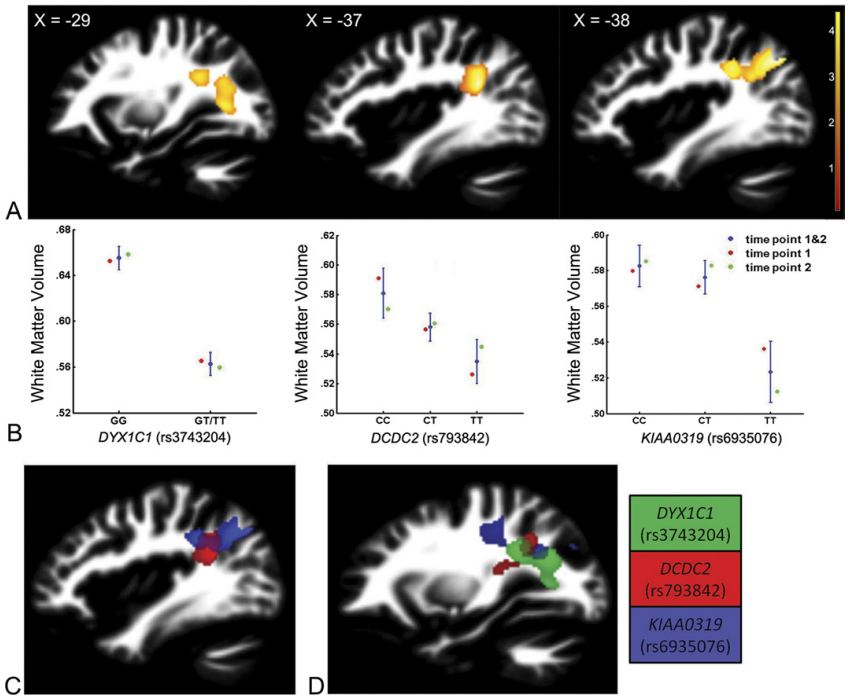

Figure 1. Main effect of three single nucleotide polymorphisms (SNPs) from the *DYX1C1*, *DCDC2*, and *KIAA0319* genes on white matter structure. **(A)** White matter clusters showing significant association between SNPs and white matter volume. All images are sagittal sections from the left tempo-parietal region. **(B)** White matter volume distribution for genotypes of each SNP (error bars: ± 1 SEM). **(C, D)** Overlap between the significant regions.

by local expansion or contraction of volume. A separate analysis was performed for each of the 13 SNPs to investigate whether any of these polymorphisms affected white matter volume. Age, gender, handedness, and total white matter volume were entered as covariates.

Genetic Associations

Three of the 13 SNPs, rs3743204 (*DYX1C1*), rs793842 (*DCDC2*), and rs6935076 (*KIAA0319*), had a significant effect on white matter volume (Bonferroni correction, with $p_{corrected} < .0038$ corrected for multiple comparison in each SPM analysis) (Figure 1A, B). Image analysis resulted in four significant clusters (Table 1). Three of the clusters, one of each associated with rs3743204, rs793842, and rs6935076, were all located in the left temporo-parietal region and partially overlapped with each other (Figure 1C, D). One additional cluster associated with rs3743204 was located in the similar location in right hemisphere (data not shown).

Table 1. Coordinates for the Effect of SNPs on White Matter

SNP	$p_{corrected}$ Cluster Level	*Z* Score	x, y, z (MNI)
rs3743204 (*DYX1C1*)	3.10×10^{-3}	3.85	−15, −54, 16
	5.43×10^{-4}	3.70	13, −35, 30
rs793842 (*DCDC2*)	1.51×10^{-3}	4.23	−37, −49, 23
rs6935076 (*KIAA0319*)	5.51×10^{-4}	4.10	−38, −69, 38

MNI, Montreal Neurological Institute; SNP, single nucleotide polymorphism.

White matter volume in these regions showed consistent association with rs3743204, rs793842, and rs6935076 at both time points of measurement, separated by 2 years (both $p < .011$) (Figure 1B). There was no significant gene × age interaction in these regions for rs793842 (*DCDC2*) or rs6935076 (*KIAA0319*), but for rs3743204 (*DYX1C1*) there was a gene × age interaction ($p = .0018$) in a region overlapping with the main effect area in the left hemisphere (Figure 2A). The interaction resulted in larger gene effect at higher ages (Figure 2B).

All analyses were corrected for the effect of white matter volume. In an additional analysis, we assessed the correlation of total white matter volume with all 3 SNPs. Rs3743204 significantly ($p = .003$) correlated with total white matter volume, after correction for age, gender, and handedness, showing the association of this SNP with white matter both locally and globally.

Tract Tracing

From DTI data we analyzed the connectivity of the white matter clusters identified by the genetic analysis. Although all significant clusters in the left hemisphere overlapped (Figure 1D), this overlap was found to be too small to generate consistent fiber tracking results from a large group of subjects. The second most consistent region was the overlap between clusters associated with *DCDC2* and *KIAA0319* (Figure 1C). This region was mainly located in the left superior longitudinal fasciculus and the corpus callosum according to the John Hopkins Probabilistic Atlas (www.fmrib.ox.ac.uk/fsl/data/atlas-descriptions.html#wm). We then identified tracts that passed through this ROI. For this purpose, the ROI was registered to the diffusion weighted image of each individual. Streamline fiber

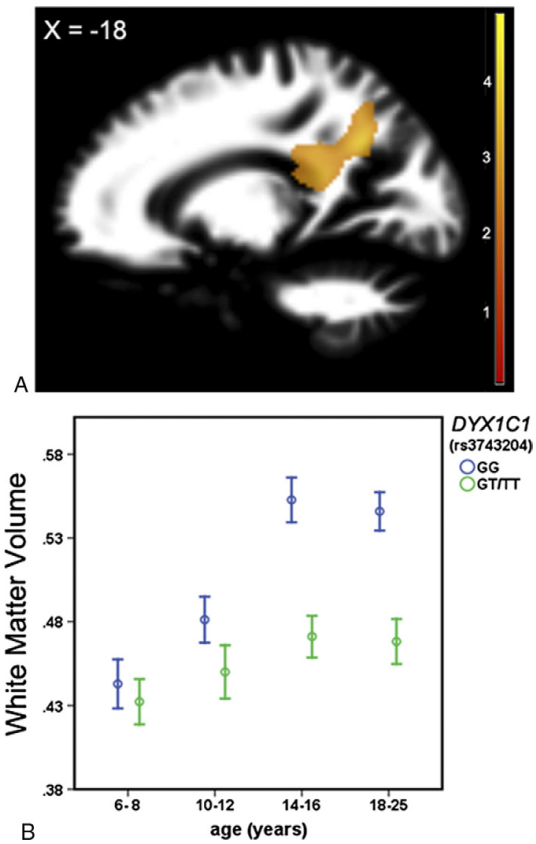

Figure 2. The *DYX1C1* (rs3743204) interaction with age. **(A)** Cluster found significant for age × rs3743204 interaction in left hemisphere. **(B)** White matter volume variations and genotypes in the different age groups (error bars: ± 1 SEM).

tracking was then performed on 30 randomly selected subjects (see Figure 3A for tracking of one individual). To have a probability map of those tractography results, all 30 tract maps were transformed back into a common space, converted into a binary image before being averaged across all individuals (Figure 3B). Finally, the probability map was overlaid on the Harvard-Oxford cortical atlas (www.cma.mgh.harvard.edu/fsl_atlas.html) to localize the cortical areas in which the tracts terminated (Figure 3C). The pathways passing through the ROI were found to be part of temporo-parietal and inter-hemispheric tracts. After "peeling off" the surface of the brain, we found that the temporo-parietal tracts connected the middle temporal gyrus to the left angular and supramarginal gyri. The endpoints of the fibers are consistent with the areas previously reported by Paulesu *et al.* (5) for middle temporal gyrus and by Richlan *et al.* (6) for inferior parietal lobule (Figure 3D). The inter-hemispheric pathways terminated mainly in the left and right superior parietal lobules and in the superior division of the lateral occipital cortex.

Behavioral Associations

The mean white matter volume in each significant cluster associated with each SNP was extracted for all subjects and then correlated with their reading scores using a mixed linear model.

First, the correlation between SNPs and white matter was confirmed, as first shown by the SPM analysis (with age, gender, handedness, and whole white matter volume as covariates). Second, white matter volume was found to be significantly correlated with reading scores (Figure 3E) in all clusters (all $p < .00009$), with greater white matter volume associated with better reading. Correlation between white matter volume, in all three clusters in left hemisphere, and reading scores survived the significant level after correcting for the effect of age, gender, and handedness ($p < .004$). In contrast, there was no significant correlation directly between these SNPs and reading scores with the same covariates.

The second reading test was "word chains" test, in which the subjects read as many words as possible during a 2-min period and received a score on the basis of the number of correctly read words (32). Again, white matter values correlated significantly with accuracy ($p < .0001$ for all tests), whereas there was no significant correlation between SNPs and accuracy. Correlation between white matter volume and accuracy remained significant after correcting for the effect of age, gender, and handedness ($p < .002$).

Discussion

Here we showed that polymorphisms in three genes previously associated with dyslexia and neuronal migration all affected white matter volume in the left temporo-parietal region of the brain. The three genetic associations pointed to the same overlapping region, with a high joint significance, and the effect remained across two different time points, 2 years apart. The results will require replication in an independent sample of individuals, because the sample size is considered small for a genetic study.

The genetic associations with white matter observed in this study are close to and partly overlapping with previously reported white matter regions associated with reading (9–12). Previous studies have been inconsistent with regard to the connectivity of reading-related white matter regions. For this study, we used tract tracing and analyzed voxel-wise consistency of location in a larger sample than in any of the previous studies in the literature. Although interindividual variability is large, we found that the most consistent connectivity was between the middle temporal gyrus/superior temporal sulcus and the supramarginal and angular gyri. These cortical areas are under-activated in subjects with dyslexia (5,6,34,35). Activity in these regions correlates with the development of reading in children (36), and they show volumetric changes in adults learning to read (37). The present study thus connects genetic findings with previous structural and functional neuroimaging studies of both normal and impaired readers.

Several previous studies have found associations between anterior–posterior connections and language function. However, there are reports of individuals with normal language function but an absence of long-ranging temporo-frontal connections (38). Our results emphasize the importance of temporo-parietal connectivity, but we cannot exclude the possibility that there might be additional frontal connectivity, not identified here due to low spatial resolution of the DTI data that the tract tracing was based on.

White matter volume could reflect the number or thickness of axons or the amount of myelination. In the present study, there was no interaction between age and the genetic polymorphisms for *DCDC2* or *KIAA0319*. This speaks against an effect on childhood brain maturation, such as myelination or increased axonal thickness, at least after 6 years of age. Instead it suggests an effect on early brain development, such as neuronal migration affecting the number of axons. For *DYX1C1*, there was both a main effect of gene and a gene × age interaction, possibly reflecting the participation of *DYX1C1* not only in early brain development but also in pathways that could affect later myelination (18).

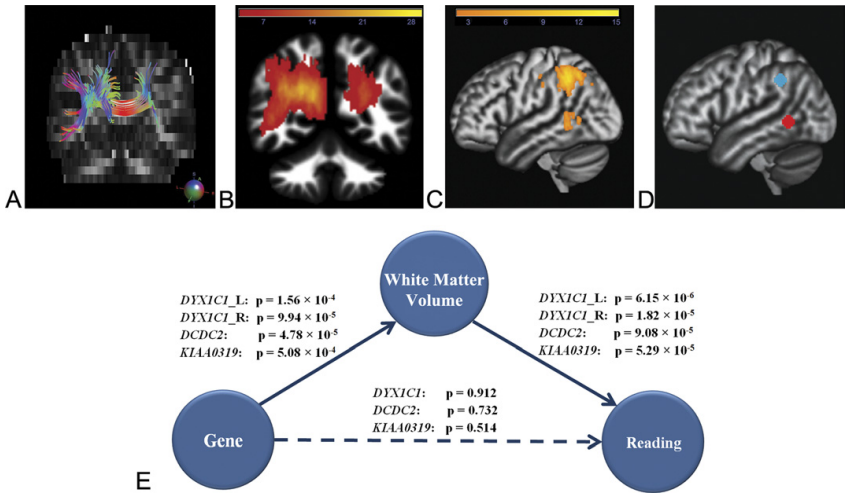

Figure 3. White matter connections and correlation to behavior. **(A)** Example of tract tracing results from one individual (red, green, and blue fibers show left–right, anterior–posterior, and inferior–superior directions, respectively). **(B)** Overlay of tract tracing from 30 individuals. The color bar shows the number of individuals with overlapping connections. **(C)** The cortical regions most consistently connected are the middle temporal gyrus/superior temporal sulcus inferiorly and supramarginal and angular gyrus superiorly. **(D)** Regions of interest drown by the radius of 5 mm at the centers of −60, −56, 0 (reported by Paulesu *et al.* [5] for middle temporal) and −38, −48, 40 (reported by Richlan *et al.* [6] for inferior parietal lobule). **(E)** Correlations between genes (SNPs), white matter volume, and reading (reading comprehension test). *DYX1C1*_L and *DYX1C1*_R denote the clusters found for rs3743204, in the left and the right hemispheres, respectively.

A very early impairment in dyslexia is suggested by analysis of event-related potentials showing that phonological deficits in subjects with hereditary risk for dyslexia can be detected as early as a few weeks after birth (39). Recent data show that the protein expressed by *DCDC2* localizes in neurons to the primary cilium and associates with proteins involved in establishing cell polarity, suggesting an effect on neuronal migration (40). Interestingly, the proteins expressed by *DYX1C1* and *DCDC2* also bind to each other (Tammimies K., Tapia-Paéz I., Kere J., personal communication, August 29, 2011). A common cellular pathway for these genes might explain the common cluster region seen at the neuroanatomical level.

It is still unclear why genes affecting neuronal migration would have such a regionally specific effect in the human brain. However, it is evident that the expression of *DCDC2* and *KIAA0319* vary widely from one brain region to another, and both are highly expressed in the temporal and parietal cortex (14). Future studies of white matter development from birth to age 6 might provide additional information about possible interactions between environment and genetic polymorphism.

The rs793842 (in *DCDC2*) SNPs has, to our knowledge, not previously been reported associated with dyslexia. However, recent reports have described associations of the SNPs rs6935076 (in the first intron of *KIAA0319*) and rs3743204 (in the first intron of *DYX1C1*) with variation in normal reading ability in a twin sample from Australia (25,41). In our study, the TT genotype of rs6935076 was associated with lower white matter volume. The combination of previous reports and new data suggest a correlation between worse reading performance and lower white matter volume. For rs3743204, association was found with both irregular and non-word reading in the Australian population cohort. In our study, the GG genotype of rs3743204 was associated with higher white matter volume, whereas the rare homozygous TT cannot be distinguished from heterozygotes.

Interestingly, two of the polymorphisms studied in this report, rs3743204 and rs3743205, are part of a haplotype of three SNPs associated specifically with female dyslexic subjects in a sample of 366 German trios (17). This might argue for an involvement of sex hormone signaling pathways in dyslexia, a hypothesis strengthened by the previously shown interaction of *DYX1C1* and estrogen receptors in primary neurons (18).

In utero knockdown of *Dyx1c1* and *Kiaa0319* expression in rat brain produce a defective neuronal migration (24,41–43). A follow-up study of adult rats after *Dyx1c1* knockdown revealed neocortical and hippocampal malformations similar to those first seen in human postmortem brains of dyslexic subjects (44). Furthermore, misplaced neurons (ectopias) with abnormal radial orientation were seen in neocortex and white matter. The reported disturbances in the rat brain model system suggest that neuronal migration provide one possible candidate pathway controlling the differences in white matter structure. Considering the association of SNPs within those three genes with variation of general reading ability (25,26,45), it is tempting to speculate that the DNA variants can produce subtle expression levels changes influencing white matter volume in the developing human brain.

In summary, this study connects previous findings from genetics and imaging studies of both normal and impaired readers. Here, we suggest a neuronal mechanism in which *DYX1C1*, *DCDC2*, and *KIAA0319*, three dyslexia susceptibility genes, affect brain connectivity between the temporal and parietal regions, which in turn affects variability in reading ability.

This work was supported by the Knut and Alice Wallenberg Foundation, The Swedish Research Council, and a Swedish Royal Bank Tercentennial Foundation grant in the program "Learning and Memory in Children and Young Adults" to TK and JK. We would like to thank Jens Gisselgård, Ylva Samuelsson, Douglas Sjöwall, Iroise Dumontheil, Stina Söderqvist, and Sissela Bergman Nutley for help with the study administration; Kerstin Eriksson and Tomas Jonsson for the scanning of the participants; Kristiina Tammimies, Ingegerd Fransson, and the Mutation Analysis Core Facility for genotyping.

The authors report no biomedical financial interests or potential conflicts of interest.

1. Shaywitz SE, Shaywitz BA, Fletcher JM, Escobar MD (1990): Prevalence of reading disability in boys and girls. *JAMA* 264:998–1002.
2. Shaywitz SE (1998): Dyslexia. *N Engl J Med* 338:307–312.
3. Galaburda AM, Sherman GF, Rosen GD, Aboitiz F, Geschwind N (1985): Developmental dyslexia: Four consecutive patients with cortical anomalies. *Ann Neurol* 18:222–233.
4. Humphreys P, Kaufmann WE, Galaburda AM (1990): Developmental dyslexia in women: Neuropathological findings in three patients. *Ann Neurol* 28:727–738.
5. Paulesu E, Démonet JF, Fazio F, McCrory E, Chanoine V, Brunswick N, *et al.* (2001): Dyslexia: Cultural diversity and biological unity. *Science* 291:2165–2167.
6. Richlan F, Kronbichler M, Wimmer H (2011): Meta-analyzing brain dysfunctions in dyslexic children and adults. *Neuroimage* 53:1735–1742.
7. Shaywitz BA, Shaywitz SE, Pugh KR, Mencl WE, Fulbright RK, Skudlarski P, *et al.* (2002): Disruption of posterior brain systems for reading in children with developmental dyslexia. *Biol Psychiatry* 52:101–110.
8. Silani G, Frith U, Demonet JF, Fazio F, Perani D, Price C, *et al.* (2005): Brain abnormalities underlying altered activation in dyslexia: A voxel based morphometry study. *Brain* 128:2453–2461.
9. Klingberg T, Hedehus M, Temple E, Salz T, Gabrieli JDE, Moseley ME, *et al.* (2000): Microstructure of temporo-parietal white matter as a basis for reading ability: Evidence from diffusion tensor magnetic resonance imaging. *Neuron* 25:493–500.
10. Beaulieu C, Plewes C, Paulson LA, Roy D, Snook L, Concha L, *et al.* (2005): Imaging brain connectivity in children with diverse reading ability. *Neuroimage* 25:1266–1271.
11. Deutsch GK, Dougherty RF, Bammer R, Siok WT, Gabrieli JDE, Wandell B (2005): Special issue children's reading performance is correlated with white matter structure measured by diffusion tensor imaging. *Cortex* 41: 354–363.
12. Niogi SN, McCandliss BD (2006): Left lateralized white matter microstructure accounts for individual differences in reading ability and disability. *Neuropsychologia* 44:2178–2188.
13. Cope N, Harold D, Hill G, Moskvina V, Stevenson J, Holmans P, *et al.* (2005): Strong evidence that KIAA0319 on chromosome 6p is a susceptibility gene for developmental dyslexia. *Am J Hum Genet* 76:581–591.
14. Meng H, Smith SD, Hager K, Held M, Liu J, Olson RK, *et al.* (2005): DCDC2 is associated with reading disability and modulates neuronal development in the brain. *Proc Natl Acad Sci U S A* 102:17053–17058.
15. Schumacher J, Anthoni H, Dahdouh F, König IR, Hillmer AM, Kluck N, *et al.* (2006): Strong genetic evidence of DCDC2 as a susceptibility gene for dyslexia. *Am J Hum Genet* 78:52–62.
16. Taipale M, Kaminen N, Nopola-Hemmi J, Haltia T, Myllyluoma B, Lyytinen H, *et al.* (2003): A candidate gene for developmental dyslexia encodes a nuclear tetratricopeptide repeat domain protein dynamically regulated in brain. *Proc Natl Acad Sci U S A* 100:11553–11558.
17. Dahdouh F, Anthoni H, Tapia-Paéz I, Peyrard-Janvid M, Schulte-Körne G, Warnke A, *et al.* (2009): Further evidence for DYX1C1 as a susceptibility factor for dyslexia. *Psychiatr Genet* 19:59–63.
18. Massinen S, Tammimies K, Tapia-Paéz I, Matsson H, Hokkanen ME, Söderberg O, *et al.* (2009): Functional interaction of DYX1C1 with estrogen receptors suggests involvement of hormonal pathways in dyslexia. *Hum Mol Genet* 18:2802–2812.
19. Cope NA, Hill G, Van Den Bree M, Harold D, Moskvina V, Green EK, *et al.* (2004): No support for association between dyslexia susceptibility 1 candidate 1 and developmental dyslexia. *Mol Psychiatry* 10:237–238.
20. Marino C, Giorda R, Lorusso ML, Vanzin L, Salandi N, Nobile M, *et al.* (2005): A family-based association study does not support DYX1C1 on 15q21. 3 as a candidate gene in developmental dyslexia. *Eur J Hum Genet* 13:491–499.
21. Meng H, Hager K, Held M, Page GP, Olson RK, Pennington BF, *et al.* (2005): TDT-association analysis of EKN1 and dyslexia in a Colorado twin cohort. *Hum Genet* 118:87–90.
22. Venkatesh SK, Siddaiah A, Padakannaya P, Ramachandra NB (2011): An examination of candidate gene SNPs for dyslexia in an Indian sample. *Behav Genet* 41:105–109.
23. Paracchini S, Thomas A, Castro S, Lai C, Paramasivam M, Wang Y, *et al.* (2006): The chromosome 6p22 haplotype associated with dyslexia reduces the expression of KIAA0319, a novel gene involved in neuronal migration. *Hum Mol Genet* 15:1659–1666.
24. Wang Y, Paramasivam M, Thomas A, Bai J, Kaminen-Ahola N, Kere J, *et al.* (2006): DYX1C1 functions in neuronal migration in developing neocortex. *Neuroscience* 143:515–22.
25. Bates TC, Lind PA, Luciano M, Montgomery GW, Martin NG, Wright MJ (2009): Dyslexia and DYX1C1: Deficits in reading and spelling associated with a missense mutation. *Mol Psychiatry* 15:1190–1196.
26. Lind PA, Luciano M, Wright MJ, Montgomery GW, Martin NG, Bates TC (2010): Dyslexia and DCDC2: normal variation in reading and spelling is associated with DCDC2 polymorphisms in an Australian population sample. *Eur J Hum Genet* 18:668–673.
27. Paracchini S, Ang QW, Stanley FJ, Monaco AP, Pennell CE, Whitehouse AJ (2011): Analysis of dyslexia candidate genes in the Raine cohort representing the general Australian population. *Genes Brain Behav* 10:158–165.
28. Scerri TS, Morris AP, Buckingham LL, Newbury DF, Miller LL, Monaco AP, *et al.* (2011): DCDC2, KIAA0319 and CMIP are associated with reading-related traits. *Biol Psychiatry* 70:237–245.
29. Pinel P, Fauchereau F, Moreno A, Barbot A, Lathrop M, Zelenika D, *et al.* (2012): Genetic variants of FOXP2 and KIAA0319/TTRAP/THEM2 locus are associated with altered brain activation in distinct language-related regions. *J Neurosci* 32:817–825.
30. Dumontheil I, Roggeman C, Ziermans T, Peyrard-Janvid M, Matsson H, Kere J, *et al.* (2011): Influence of the COMT genotype on working memory and brain activity changes during development. *Biol Psychiatry* 70:222–229.
31. Söderqvist S, McNab F, Peyrard-Janvid M, Matsson H, Kere J, Klingberg T (2010): The SNAP25 gene is linked to working memory capacity and maturation of the posterior cingulate cortex during childhood. *Biol Psychiatry* 68:1120–1125.
32. Woodcock RW (1987): *The Woodcock Reading Mastery Test—Revised.* Circle Pines, Minnesota: American Guidance Service.
33. Hayasaka S, Phan KL, Liberzon I, Worsley KJ, Nichols TE (2004): Nonstationary cluster-size inference with random field and permutation methods. *Neuroimage* 22:676–687.
34. McCandliss BD, Noble KG (2003): The development of reading impairment: A cognitive neuroscience model. *Ment Retard Dev Disabil Res Rev* 9:196–205.
35. Rumsey JM, Nace K, Donohue B, Wise D, Maisog JM, Andreason P (1997): A positron emission tomographic study of impaired word recognition and phonological processing in dyslexic men. *Arch Neurol* 54:562–573.
36. Turkeltaub PE, Gareau L, Flowers DL, Zeffiro TA, Eden GF (2003): Development of neural mechanisms for reading. *Nat Neurosci 6:*767–773.
37. Carreiras M, Seghier ML, Baquero S, Estévez, A, Lozano A, *et al.* (2009): An anatomical signature for literacy. *Nature* 461:983–896.
38. Yeatman JD, Feldman HM (2011): Neural plasticity after pre-linguistic injury to the arcuate and superior longitudinal fasciculi [published online ahead of print September 2]. *Cortex.*
39. Guttorm TK, Leppänen PH, Richardson U, Lyytinen H. Event-related potentials and consonant differentiation in newborns with familial risk for dyslexia. *J Learn Disabil* 2001;34:534–44.
40. Massinen S, Hokkanen ME, Matsson H, Tammimies K, Tapia-Paéz I, Dahlström-Heuser V, *et al.* (2011): Increased expression of the dyslexia candidate gene DCDC2 affects length and signaling of primary cilia in neurons. *PloS One* 6:e20580.
41. Peschansky VJ, Burbridge TJ, Volz AJ, Fiondella C, Wissner-Gross Z, Galaburda AM, *et al.* (2010): The effect of variation in expression of the candidate dyslexia susceptibility gene homolog Kiaa0319 on neuronal migration and dendritic morphology in the rat. *Cereb Cortex* 20:884–97.
42. Gabel LA, Gibson CJ, Gruen JR, Loturco JJ (2010): Progress towards a cellular neurobiology of reading disability. *Neurobiol Dis* 38:173–180.
43. Szalkowski CE, Fiondella CG, Galaburda AM, Rosen GD, Loturco JJ, Fitch RH. (2012): Neocortical disruption and behavioral impairments in rats following in utero RNAi of candidate dyslexia risk gene Kiaa0319. *Int J Dev Neurosci* 30:293–302.
44. Rosen GD, Bai J, Wang Y, Fiondella CG, Threlkeld SW, Loturco JJ, *et al.* (2007): Disruption of neuronal migration by RNAi of Dyx1c1 results in neocortical and hippocampal malformations. *Cereb Cortex* 17:2562–2572.
45. Luciano M, Lind PA, Duffy DL, Castles A, Wright MJ, Montgomery GW, *et al.* (2007): A haplotype spanning KIAA0319 and TTRAP is associated with normal variation in reading and spelling ability. *Biol Psychiatry* 62:811–817.

II

Behavioral/Cognitive

DCDC2 Polymorphism Is Associated with Left Temporoparietal Gray and White Matter Structures during Development

Fahimeh Darki,[1] Myriam Peyrard-Janvid,[2] Hans Matsson,[2] Juha Kere,[2,3,4] and Torkel Klingberg[1]
Departments of [1]Neuroscience, and [2]Biosciences and Nutrition, and [3]Science for Life Laboratory, Karolinska Institutet, 171 77 Solna, Sweden, and [4]Research Programs Unit, Haartman Institute, University of Helsinki, and Folkhälsan Institute of Genetics, 00014 Helsinki, Finland

Three genes, *DYX1C1*, *DCDC2*, and *KIAA0319*, have been previously associated with dyslexia, neuronal migration, and ciliary function. Three polymorphisms within these genes, rs3743204 (*DYX1C1*), rs793842 (*DCDC2*), and rs6935076 (*KIAA0319*) have also been linked to normal variability of left temporoparietal white matter volume connecting the middle temporal cortex to the angular and supramarginal gyri. Here, we assessed whether these polymorphisms are also related to the cortical thickness of the associated regions during childhood development using a longitudinal dataset of 76 randomly selected children and young adults who were scanned up to three times each, 2 years apart. rs793842 in *DCDC2* was significantly associated with the thickness of left angular and supramarginal gyri as well as the left lateral occipital cortex. The cortex was significantly thicker for T-allele carriers, who also had lower white matter volume and lower reading comprehension scores. There was a negative correlation between white matter volume and cortical thickness, but only white matter volume predicted reading comprehension 2 years after scanning. These results show how normal variability in reading comprehension is related to gene, white matter volume, and cortical thickness in the inferior parietal lobe. Possibly, the variability of gray and white matter structures could both be related to the role of *DCDC2* in ciliary function, which affects both neuronal migration and axonal outgrowth.

Key words: **Ciliary function; developmental dyslexia; neuroimaging; reading ability; single nucleotide polymorphism; SNP; supramarginal and angular gyrus**

Introduction

Developmental dyslexia, or reading disability, is one of the most common learning disorders among children (Shaywitz et al., 1990; Katusic et al., 2001). A different pattern of activation in the left temporoparietal, inferior parietal, and occipitotemporal cortical regions has been observed in impaired compared with normal readers (Shaywitz et al., 2002, 2004; Richlan et al., 2011; Richlan, 2012). Dyslexia has also been associated with structural deviations of gray and white matter in corresponding regions (Klingberg et al., 2000; Deutsch et al., 2005; Silani et al., 2005; Vinckenbosch et al., 2005; Niogi and McCandliss, 2006; Kronbichler et al., 2008; Altarelli et al., 2013). These differences could rather be seen as the end distribution of a continuum in the general population, without any diagnosis of dyslexia (Klingberg et al., 2000; Nagy et al., 2004; Beaulieu et al., 2005; Deutsch et al., 2005; Niogi and McCandliss, 2006; Darki et al., 2012).

A small number of candidate genes, such as *DYX1C1*, *DCDC2*, and *KIAA0319*, have been associated with increased risk for reading impairment (Taipale et al., 2003; Cope et al., 2005; Meng et al., 2005; Schumacher et al., 2006; Eicher et al., 2014) as well as with neuronal migration during cortical development (Wang et al., 2006; Gabel et al., 2010; Peschansky et al., 2010; Szalkowski et al., 2012). At the cellular level, *DYX1C1* and *DCDC2* have been implicated in regulating ciliary growth and function (Massinen et al., 2011; Chandrasekar et al., 2013). Impaired ciliary function may lead to misplacement of neurons in the cerebral cortex and may hinder the axonal outgrowth (Higginbotham et al., 2012). Thus, genetic polymorphisms associated with ciliar functioning may lead to disturbances in both white and gray matter in the brain.

Gray matter volume alterations in association with single nucleotide polymorphisms (SNPs) in or near the *DYX1C1*, *DCDC2*, and *KIAA0319* genes have been reported in some genetic imaging assessments (Meda et al., 2008; Jamadar et al., 2011). Functional MRI studies have also detected an association of genetic variants in *KIAA0319* and *DCDC2* with brain activation in superior temporal sulcus, as well as the left anterior inferior parietal and right

Received March 26, 2014; revised Aug. 26, 2014; accepted Sept. 16, 2014.

Author contributions: F.D., J.K., and T.K. designed research; F.D. performed research; F.D., M.P.-J., and H.M. analyzed data; F.D., M.P.-J., H.M., J.K., and T.K. wrote the paper.

This work was supported by the Knut and Alice Wallenberg Foundation, The Swedish Research Council, and a Swedish Royal Bank Tercentennial Foundation grant in the program "Learning and Memory in Children and Young Adults" to J.K. and T.K. We thank Jens Gisselgård, Ylva Samuelsson, Douglas Sjöwall, Iroise Dumontheil, Benjamin Garzon, Stina Söderqvist, and Sissela Bergman Nutley for help with the study administration; Kerstin Eriksson and Tomas Jonsson for the scanning of the participants; and Kristiina Tammimies, Ingegerd Fransson, and the Mutation Analysis Core Facility for genotyping.

The authors declare no competing financial interests.

Correspondence should be addressed to Torkel Klingberg, Karolinska Institutet, Retzius Väg 8, 171 77 Stockholm, Sweden. E-mail: torkel.klingberg@ki.se.

DOI:10.1523/JNEUROSCI.1216-14.2014

 0270-6474/14/340001-●$15.00/0

temporal gyrus and lateral occipital cortex (LOC; Cope et al., 2012; Pinel et al., 2012).

Three SNPs, rs3743204 (*DYX1C1*), rs793842 (*DCDC2*), and rs6935076 (*KIAA0319*), showed significant effects on the normal variability of white matter volume in left temporoparietal regions in which the white matter pathways connect the middle temporal gyrus (MTG) to the angular gyrus (AG) and the supramarginal gyrus (SMG; Darki et al., 2012). These cortical regions have been reported to be functionally and structurally different in individuals in whom dyslexia has been diagnosed compared with normal readers (Paulesu et al., 2001; McCandliss et al., 2003; Carreiras et al., 2009).

Knowing the involvement of the dyslexia susceptibility genes *DYX1C1*, *DCDC2*, and *KIAA0319* in neuronal migration and ciliary function, we aimed to assess whether the individual genotypes of the SNPs rs3743204, rs793842, and rs6935076 have any significant effect on the normal variability of cortical thickness in the temporal and parietal associated regions during development.

Materials and Methods

Participants

Seventy-six typically developing children and young adults, already included in our previous study (Darki et al., 2012), were scanned for the third time as a part of a longitudinal study (Söderqvist et al., 2010). The participants (41 males and 35 females) were in nine different age groups (6, 8, 10, 12, 14, 16, 18, 20, and 25 years of age) with no reports of any neurological or psychological disorders. This study was approved by the ethics committee of the Karolinska University Hospital. Informed consent was provided by the participants or the parents of children <18 years of age.

Genotyping

Thirteen SNPs located in or in close vicinity to three dyslexia susceptibility genes (*DYX1C1*: rs3743204, rs3743205, and rs17819126; *DCDC2*: rs793842, rs793862, rs807701, rs2328819 rs2792682, rs7751169, and rs9460974; *KIAA0319*: rs4504469, rs6935076, and rs2143340) were genotyped with matrix-assisted laser desorption/ionization–time-of-flight mass spectrometry with iPLEX Gold assays, as previously described (Darki et al., 2012).

We previously (Darki et al., 2012) reported that three of these SNPs, rs3743204 (*DYX1C1*), rs793842 (*DCDC2*), and rs6935076 (*KIAA0319*) showed significant effects on the normal variability of white matter volume for two imaging rounds (i.e., the first two time points of the longitudinal dataset). Here, we analyzed the structural MRI data from all three time points to investigate the association of these SNPs with white matter structure and the cortical thickness. The association between these SNPs and behavior measures was also assessed.

Behavioral assessment

All subjects were assessed with a reading comprehension task using narrative and expository texts from the Progress in International Reading literacy Trend Study (PIRLS 2001 T) and The International Association for the Evaluation of Educational Achievement Reading Literacy Study 1991. Reading comprehension tests included 77 items for four age groups including individuals ranging in age from 8 to 25 years and were administered either individually or in groups of 2–20 participants in a classroom (Söderqvist et al., 2010). Different age groups thus received different, but overlapping, sets of items. An item response theory analysis (Bond and Fox, 2003) was then used to achieve a reading ability *z*-score for each subject, which was used for further analysis.

Additionally, a word decoding task called "word chains" was tested. This is similar to the English Woodcock Johnson Word-ID test, in which the subjects had 72 sets of written words, each consisting of three words without spaces in between. The task was to read as many words as possible during 2 min and mark with a pencil where the spaces should occur. The score is based on the number of words that has been marked correctly (Woodcock, 1987).

Structural brain imaging and analysis

T1-weighted spin echo scans were collected with a 1.5 T Avanto scanner (Siemens Medical System) using a 3D magnetization-prepared rapid acquisition gradient echo sequence with TR = 2300 ms, TE = 2.92 ms, 256×256 matrix size, 176 sagittal slices, and 1 mm^3 isotropic voxel size.

Voxel-based morphometry, which segmented the brain into gray matter, white matter, and CSF, was performed on structural data collected across all three rounds of data collection using SPM5, Diffeomorphic Anatomical Registration Through Exponentiated (DARTEL) toolbox (Ashburner, 2007). The structural data of all individuals were first segmented into gray matter, white matter, and CSF using a mixture–model cluster analysis, which identifies the voxels by matching their intensities to the tissue types and combines this information with a priori knowledge from probability maps of these three tissues. Next, the tissue-segmented images were iteratively registered to each other to create a template. Then the images were subjected to a nonlinear modulation by multiplying the registered images with the Jacobian determinants. The modulation reflects the probability of being locally expanded or contracted to fit to the template. The modulated white matter segmented images were registered to Montreal Neurological Institute (MNI) space by affine transformation and then smoothed with an 8 mm Gaussian kernel for further statistical analysis.

SNP genotypes and white matter volume

All white matter segmented images were analyzed by second-level SPM analysis, using a flexible factorial design in SPM8, to assess the variation of white matter volume with respect to genotype variability. Flexible factorial design allowed specifying the participants and it considered the repeated measures for all individuals by including subjects and testing rounds as factors. The SNPs rs3743204 (*DYX1C1*), rs793842 (*DCDC2*), and rs6935076 (*KIAA0319*) were entered separately as a main factor in the model. The sample sizes by genotype are as follows: rs3743204 (GG, $n = 53$; GT/TT, $n = 23$); rs793842 (CC, $n = 21$; CT, $n = 41$; TT, $n = 14$); and rs6935076 (CC, $n = 30$; CT, $n = 39$; TT, $n = 7$). Age, sex, handedness, and total white matter volume were used as covariates, and the interaction of SNP, as the main factor, with age and sex was also added. This part of the analysis was repeated in the same way as the analysis previously published (Darki et al., 2012), but this time considering all three time points of the longitudinal data. We aimed to assess whether the effect of the previously published SNPs remains significant when adding the image data from the third time point. The exploratory analysis was performed on the cluster level with nonstationary cluster extent correction at $p = 0.05$ (Hayasaka et al., 2004) to find the main effect of SNPs. We then corrected for multiple comparisons of three SNPs and set the threshold of significance at $p = 0.016$ (Bonferroni correction of three tests). The significant regions were then saved as regions of interest (ROIs) and their overlapping area was used as a seed region for white matter tractography.

Diffusion tensor imaging and fiber tracking

Diffusion tensor imaging (DTI) with a field of view of 230×230 mm^2, a 128×128 matrix size, 40 slices, 2.5 mm slice thickness, and a b value of 1000 s/mm^2, and was performed in 64 gradient directions with one b0 image collected in the beginning. Eddy current and head motions were corrected with affine registration to the reference volume (b0 image) using FSL software. The diffusion tensor parameters were then estimated, and subsequently the DTI and fractional anisotropy (FA) data were constructed. Nonlinear registration was performed using Tract-Based Spatial Statistics (TBSS) version 1.2 (Smith et al., 2006), in FSL (Smith et al., 2004) to align all FA images to the mean FA image. TBSS back projection was used to map the significant ROI to the FA image of all individuals. Deterministic fiber tracking was then applied by ExploreDTI version 4.7.3 (Leemans et al., 2009), with 1 mm step size, considering an FA threshold of 0.15 and an angular difference of 30°, to find the white matter fibers passing through the significant ROI on individual DTI space. The traced white matter pathways of all individuals were then transformed to the mean FA template using the TBSS method for non-FA images in which the corresponding nonlinear transformation matrices for FA images was used to register the traced white matter

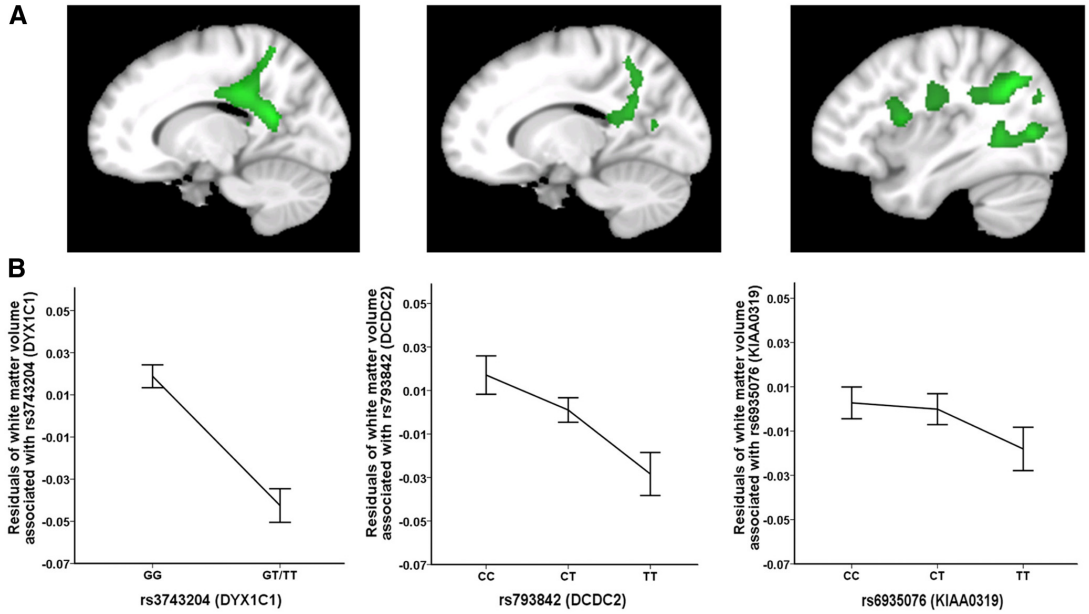

Figure 1. Main effect of three SNPs from the *DYX1C1*, *DCDC2*, and *KIAA0319* genes on white matter structure. ***A***, White matter clusters showing significant association between SNPs and white matter volume in sagittal sections. ***B***, Distribution of residuals of mean white matter volume in each significant region across different genotypes after correction for age, sex, and handedness. Error bars indicate ±1 SEM.

pathways to template. The aligned white matter pathways were then binarized and averaged across all subjects. The averaged map of white matter pathways was then overlapped with the Harvard-Oxford cortical structural atlas to find the cortical regions connected by white matter pathways.

Cortical thickness measurement

The cortical thickness of the structural images was estimated using an automatic longitudinal stream in Freesurfer (Reuter et al., 2012) by constructing models for the boundary between gray and white matter. First, a within-subject template was created for each subject using inverse consistent registration of the T1-weighted images (Reuter et al., 2010; Reuter and Fischl, 2011). Then, several processing steps (Dale et al., 1999; Fischl and Dale, 2000), including skull removal, template transformation, and atlas registration, were performed. Images were later segmented to white matter, gray matter, and pia, based on intensity and neighborhood voxel restrictions. The distance between the white matter and the pia was computed as the thickness at each location of cortex.

To investigate our main hypothesis regarding the effect of the SNPs on cortical thickness, we first identified the cortical regions connected by white matter pathways and then we extracted their cortical thickness using the workflow described in http://surfer.nmr.mgh.harvard.edu/fswiki/VolumeRoiCortical Thickness.

Statistical analyses

SNP genotypes and cortical thickness. To assess the effect of the SNPs on the cortical thickness of the corresponding regions, the cortical thickness of the particular ROIs was analyzed using a mixed linear model in SPSS version 21.0. The model was set for three repeated measures, and the "unstructured" type was chosen for repeated covariance. The measures of cortical thickness were entered separately as dependent variables, and the SNP genotypes were set as a factor. Age, sex, and their interactions by the SNPs, as well as handedness were entered as covariates. The main effect of the SNPs on the thickness of the cortex was tested for each ROI separately.

SNP genotypes and reading ability. The association of all three SNPs with reading scores was assessed using a mixed linear model considering three repeated measures of reading ability. The reading scores were entered as dependent variables, and the SNP genotypes were set as a factor. Age, sex, and handedness were considered as covariates. The main effect of the SNPs on the reading ability was assessed for each SNP separately. We later entered the SNP interaction by age and sex as covariates to assess for interaction possibility in the model.

Brain structure and behavior measures. The white matter volume in the SNP-associated regions as well as the thickness of the cortical areas were set separately as covariates of interest in the mixed linear model and were tested for a significant relationship to reading ability, including all three repeated measures (sex and handedness were covariates). Next, we entered age as a covariate to find the brain–behavior relationships after the effect of covariates were removed.

In another set of analyses, we assessed which brain measures can predict future reading ability. Round 1 and 2 brain measures were set as covariates, and they were analyzed to predict round 2 and 3 reading scores using a mixed linear model considering two repeated measures with sex and handedness as covariates. The model was then corrected for the effect of either age or reading at baseline to see which relationship would stay significant age independently.

Results

Genetic associations to white matter volume

In the assessment of the association of three dyslexia-related SNPs, rs793842 (*DCDC2*), rs6935076 (*KIAA0319*), and rs3743204 (*DYX1C1*), on white matter volume now including all three rounds of imaging of the longitudinal data, we found the same significant association with white matter volume for these SNPs, as already reported based on data from the first two time points (Darki et al., 2012). Figure 1*A* shows the clusters found to be significant for the association of each SNP. The clusters associated with these SNPs overlapped mainly with superior longitudinal fasciculus and the posterior part of corpus callosum based, on the Johns Hopkins probabilistic atlas. The rs6935076 and

Table 1. Coordinates for the effect of SNPs on white matter

SNP	Gene	FDR-corrected cluster-level *p* value	Cluster size	Peak voxel			
				z-score	MNI coordinates		
					x	*y*	*z*
rs3743204	*DYX1C1*	1.28×10^{-10}	9804	4.11	−16	−54	18
rs793842	*DCDC2*	8.19×10^{-5}	3353	4.24	−28	−70	33
rs6935076	*KIAA0319*	3.33×10^{-10}	8195	5.32	−34	−58	31
		3.32×10^{-10}	8285	4.01	36	−28	37

rs3743204 clusters were bilateral, while the significant region associated with rs793842 was located only in the left hemisphere. The peak MNI coordinates, the size of the clusters, and the false discovery rate (FDR)-corrected *p* values at cluster level are listed in Table 1. All three significant regions ($p < 8.19 \times 10^{-5}$) survived a more restricted significant threshold at multiple-comparison correction [e.g., correction for 13 SNPs (Darki et al., 2012), $p < 0.0038$] and were overlapped in left temporoparietal area (Fig. 2*A*) in the same location found earlier (Darki et al., 2012). Figure 1*B* illustrates the residual distribution of the mean white matter volume in each significant region for the related genotypes after correction for age, sex, and handedness.

Fiber tracking

An overlapping region of all three clusters was found in the left temporoparietal area (Fig. 2*A*) and was used as the seed region for fiber tracking. Using streamline fiber tracking, the tracts passed through this ROI were traced on all individuals DTI space separately, and then binarized and averaged across all subjects. Fiber tracking on one subject as well as the group-averaged map of the tracts across all individuals are shown in Figure 2, *B* and *C*, respectively. Figure 2*D* shows the white matter pathways reached to cortex after 10% thresholding. This was done to remove the uncertain voxels with the probability of having fibers in <10% of the subjects. The averaged map of white matter pathways was then overlapped with the Harvard-Oxford cortical structural atlas and subsequently labeled with different colors (Fig. 2*E*). We found the white matter pathways; passed through the SNP-associated region; and connected to the left MTG, SMG, and AG, as well as to the bilateral LOC, superior parietal lobules, precuneus, and cingulate gyrus.

rs793842 (*DCDC2*) associated with cortical thickness

The main effects of the three SNPs on the thickness of cortical areas were assessed for the left lateral regions identified by the tract tracing (Fig. 2*D*) as well as their homologous areas in right hemisphere. The only significant association was between rs793842 (*DCDC2*) and the left lateral cortical region ($F_{(2,83.99)} = 9.39$, $p = 2.09 \times 10^{-4}$, partial $\eta^2 = 0.140$). There was a trend for this SNP also for the right hemisphere ($p = 0.037$), but it did not survive the correction for multiple comparisons of six tests ($p_{\text{corrected}} < 0.008$). Next, to anatomically localize the associated regions in the left hemisphere, we tested the association of rs793842 with the thickness of each of the five segmented cortical areas (Fig. 2*E*). We found significant associations (Fig. 3*A*) between rs793842 (*DCDC2*) and the cortical thickness of left SMG ($F_{(2,86.96)} = 5.05$, $p = 2.68 \times 10^{-4}$, partial $\eta^2 = 0.152$), left AG ($F_{(2,88.78)} = 5.12$, $p = 7.87 \times 10^{-3}$, partial $\eta^2 = 0.112$), and left LOC ($F_{(2,84.21)} = 11.96$, $p = 2.70 \times 10^{-5}$, partial $\eta^2 = 0.165$). The cortex was significantly thicker for T-allele carriers, who also had lower white matter volume (Fig. 1*B*). There was also a significant interaction (Fig. 3*B*) between rs793842 and age on the thickness of left SMG ($F_{(2,114.78)} = 7.61$, $p = 7.88 \times 10^{-4}$) and left LOC ($F_{(2,110.38)} = 7.77$, $p = 6.94 \times 10^{-4}$). (The mixed linear model used here did not provide the effect size or the partial η squared. The partial η^2 values reported above are therefore the effect sizes from the analyses performed on time point 1 only.)

Rs793842 (*DCDC2*) associated with reading ability

Rs793842 (*DCDC2*) was the only SNP that showed significant association with reading comprehension scores ($F_{(2,50.02)} = 4.66$, $p = 0.014$) with lower reading scores for T-allele carriers who had significantly lower white matter volume in the left temporoparietal area, and thicker cortex in the left SMG, AG, and LOC. The SNP interaction by age was not significant. No genetic association was found for a test of single-word reading, the word chain test ($p = 0.608$).

Brain measures correlated with reading ability

The reading comprehension scores were positively correlated with white matter volume in all three white matter regions ($p < 5.00 \times 10^{-5}$), also after correction for age ($p < 0.001$). Reading comprehension scores were also associated with cortical thickness in parietal regions, including left SMG ($F_{(1,128.28)} = 8.45$, $p = 4.32 \times 10^{-3}$), right SMG ($F_{(1,152.68)} = 16.14$, $p = 9.2 \times 10^{-5}$), left AG ($F_{(1,137.73)} = 8.59$, $p = 3.95 \times 10^{-3}$), right AG ($F_{(1,144.97)} = 21.72$, $p = 7.0 \times 10^{-6}$), as well as the left and right LOC ($F_{(1,111.81)} = 7.51$, $p = 7.15 \times 10^{-3}$; and $F_{(1,130.28)} = 20.41$, $p = 1.4 \times 10^{-5}$, respectively). In contrast to the white matter associations, the gray matter correlations did not remain significant when age was included as a covariate.

The word chain scores were associated with the white matter volumes ($p < 10^{-6}$) as well as the cortical measures in all three bilateral regions ($p < 0.036$ for MTG, $p < 0.001$ for SMG, $p < 1.64 \times 10^{-4}$ for AG, and $p < 1.0 \times 10^{-5}$ for LOC). The cortical measures did not remain significant after entering age as a covariate, but the relationships between white matter volumes and word chain scores did remain significant ($p < 0.010$).

White matter volume predicted reading ability 2 years later

The white matter volumes in the SNP-associated regions were the only brain measures that significantly predicted future reading comprehension ($p < 4.60 \times 10^{-5}$) and word chain scores ($p < 0.003$). The volumes of white matter remained a significant predictor for reading comprehension 2 years later, even after correcting for age ($p < 0.001$) or reading ($p < 0.041$) at baseline.

To quantify the amount of information gained from genetic markers and brain measures compared with information gained from knowing the baseline reading comprehension score in predicting future reading ability, we compared the following two models: Model 1: $\text{Reading2} = \beta_1 \times \text{age} + \beta_2 \times \text{sex} + \beta_3 \times \text{handedness} + \beta_4 \times \text{Reading1}$, $r^2 = 0.617$ ($r = 0.785$); Model 2: $\text{Reading2} = \beta_1 \times \text{age} + \beta_2 \times \text{sex} + \beta_3 \times \text{handedness} + \beta_4 \times \text{gene} + \beta_5 \times \text{white matter} + \beta_6 \times \text{cortical thickness}$, $r^2 = 0.613$ ($r = 0.783$). The results show that genetic information and brain measures at baseline ($r^2 = 0.613$) are approximately as informative as knowing the baseline reading ability ($r^2 = 0.617$) in predicting future reading comprehension.

In another analysis, we aimed to assess how much of the variance in reading scores can be explained by the brain measures. Using three different models, we showed that reading at baseline explained 8.4% more variance than the model predicted by age, sex, and handedness ($r^2 = 0.533$). Adding genetic and structural information explained another 5.9% of unique variance about future reading comprehension.

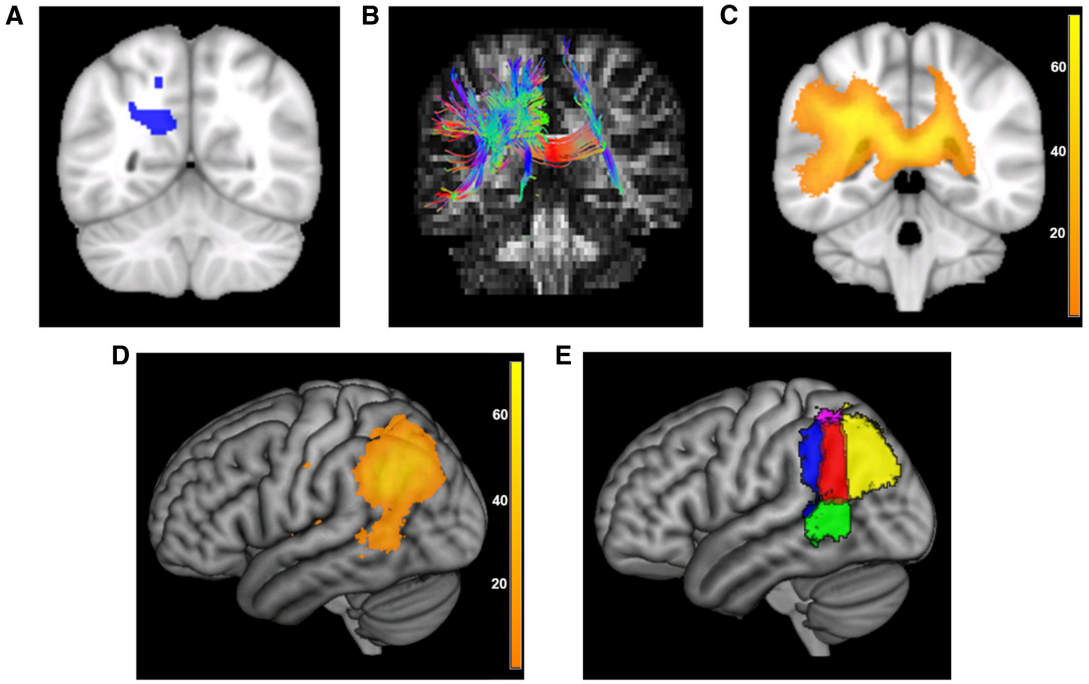

Figure 2. ***A***, Overlap region between the significant white matter areas associated with the three dyslexia-related SNPs: rs3743204 (*DYX1C1*), rs793842 (*DCDC2*), and rs6935076 (*KIAA0319*). ***B***, Example of fiber tracking of one individual (red, green, and blue fibers show left–right, anterior–posterior, and inferior–superior directions, respectively). ***C***, Probability map of traced fibers across all individuals. ***D***, The cortical regions most consistently connected are the middle temporal gyrus, supramarginal and angular gyri, as well as the lateral occipital cortex. The color bars correspond to the number of subjects with available white matter pathways. ***E***, Overlapped white matter pathways with Harvard-Oxford cortical structural atlas are labeled with different colors; red for left angular gyrus, blue for left supramarginal gyrus, green for left middle temporal cortex, yellow for lateral occipital parietal cortex, and purple for superior parietal cortex.

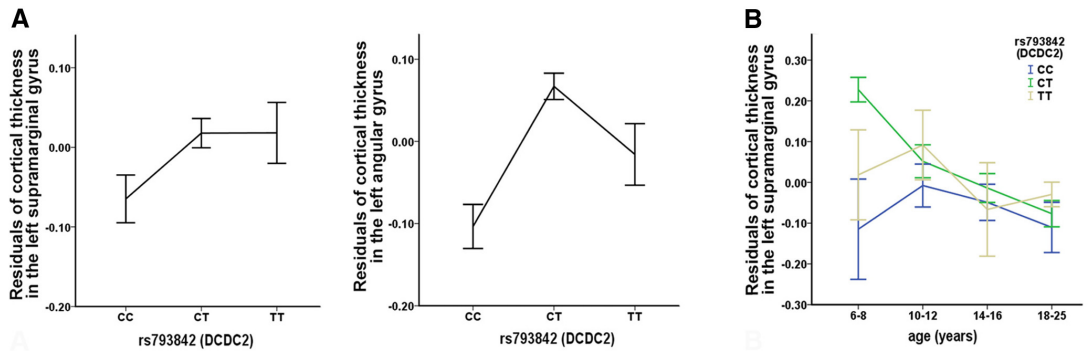

Figure 3. ***A***, Cortical thickness of left supramarginal and angular gyri across rs793842 (*DCDC2*) genotypes, after correction for age, sex, and handedness. All three time points are collapsed together. ***B***, rs793842 interaction by age for the residuals from the mean cortical thickness of left supramarginal gyrus across four different age groups after correction for sex and handedness. Error bars indicate ±1 SEM.

White matter volume and cortical thickness

The white matter volume of left temporoparietal pathways negatively correlated with the cortical thickness of left AG ($p = 0.004$), SMG ($p = 0.048$), and MTG ($p = 0.039$) after correcting for the effect of sex and handedness. We did not correct for the effect of age to keep the developmental aspect of brain maturation. In another analysis, we corrected for the effect of age to see whether the link between white matter and gray matter structures are age dependent. After correcting for age, the correlation was not significant. The associations of *DCDC2* polymorphism with white matter volume and cortical thickness were also significant after the effect of age was removed. This suggests that the genetic associations are not dependent on the developmental relationship between brain white and gray matter measures, and that they are related to the interindividual differences.

Discussion

Here we expanded our previous analysis of the associations of three dyslexia candidate genes with brain structural measures and found that variation in *DCDC2* (rs793842) affected the cortical thickness in left SMG and AG. By including three rounds of the longitudinal imaging data, we replicated our previous findings of the effect of all three SNPs (rs3743204 of *DYX1C1*, rs793842 of *DCDC2*, and rs6935076 of *KIAA0319*) on white matter volume in left temporoparietal region (Darki et al., 2012). Both white and gray matter structures were associated with reading ability.

The white matter pathways passing through the overlapping area of the SNP-associated regions connected to the left SMG, AG, posterior MTG, and the bilateral LOC. The parietal and temporal cortical areas have been reported to be hypoactive in dyslexic subjects (Paulesu et al., 2001; McCandliss et al., 2003; Richlan et al., 2011; Richlan, 2012). Moreover, these regions showed volumetric differences in late literates relative to illiterates (Carreiras et al., 2009). The role of these cortical regions in language comprehension and semantic processing has also been established in several functional neuroimaging studies (Chertkow et al., 1997; Binder et al., 2009; Turken and Dronkers, 2011; Noonan et al., 2013).

Based on the temporoparietal white matter region, our fiber tracking was restricted to temporoparietal pathways, and they did not terminate at occipitotemporal cortical regions, which were reported to be structurally different in dyslexic individuals compared with normal control subjects (Kronbichler et al., 2008; Altarelli et al., 2013). We found connections to the LOC with the fibers extending from the posterior part of corpus callosum. LOC has been previously associated with functional and structural abnormalities in dyslexia (Pernet et al., 2009; Danelli et al., 2013). The white matter volume in the posterior part of the corpus callosum and cingulum, with the connection to the parietal, occipital, and temporal lobes, has also been associated with the other dyslexia candidate locus, MRPL19/C2ORF3 (Scerri et al., 2012), suggesting that this locus is associated with visual perception and possibly general cognitive abilities such as recognition and imagination (Danelli et al., 2013).

In the present study, the white matter volume in the SNP-associated regions as well as the cortical thickness of the parietal ROIs were significantly correlated with reading comprehension and word chain scores. This is consistent with previously published studies, which have assessed the associations between reading and white and gray matter structures (Klingberg et al., 2000; Nagy et al., 2004; Deutsch et al., 2005; Ben-Shachar et al., 2007; Blackmon et al., 2010; Welcome et al., 2011; Vandermosten et al., 2012; Wandell and Yeatman, 2013). Here, we also showed that white matter volume in the left temporoparietal tract predicted future reading ability. This emphasizes the role of white matter in driving cognitive development in children, as was previously shown for working memory (Darki and Klingberg, 2014; Ullman et al., 2014).

rs793842 within the *DCDC2* gene was also significantly associated with reading ability, with lower reading scores for T-allele carriers. We did not find this association in our previous study (Darki et al., 2012) where we had two rounds of the longitudinal data. T-allele carriers had significantly lower white matter volume in left temporoparietal area, and thicker cortex in left SMG, AG, and LOC. Previously, the genetic markers of *DCDC2*, *KIAA0319*, and *DYX1C1* genes have been associated with variations in general reading ability (Luciano et al., 2007; Bates et al., 2010; Lind et al., 2010). To our knowledge, rs793842 from DCDC2 has not previously been associated with dyslexia, but it is in linkage disequilibrium with previously associated markers.

The genomic distance between *DCDC2* and *KIAA0319* is only ~130 kb; however, this interval is relatively rich in recombinations, and thus there is no linkage disequilibrium between the markers for both genes (Schumacher et al., 2006). Thus, any associations detected are likely to be specific for the gene implicated and not reflect a genetic effect of the other gene. The *DCDC2* SNP rs793842, which showed association with cortical thickness, happens to be highly informative, with a minor allele frequency of 0.47, which may yield optimal power for detecting associations, given that the functional haplotype covaries with this marker. Because of the more limited power for the other polymorphisms with lower frequencies, we cannot exclude the effects that the other gene might have on cortical thickness.

All three dyslexia susceptibility genes studied in this article have been associated with dyslexia (Paracchini et al., 2008; Couto et al., 2010; Newbury et al., 2011; Scerri et al., 2011; Venkatesh et al., 2013), neuronal migration (Wang et al., 2006; Gabel et al., 2010; Peschansky et al., 2010; Szalkowski et al., 2012), and ciliary function (Massinen et al., 2011; Chandrasekar et al., 2013) in developing neocortex. Another study (Rosen et al., 2007) reported neocortical and hippocampal malformations in *Dyx1c1* knock-down rat brains. Similar to *Dyx1c1* and *Kiaa0319*, the knock-down expression of *Dcdc2* in rats disturbed the migration of neuronal precursors (Meng et al., 2005; Adler et al., 2013). Furthermore, it has been shown that the expression of *DCDC2* regulates the cilia length and signaling in primary rat hippocampal neurons, suggesting that *DCDC2* affects the structure and function of primary cilia (Massinen et al., 2011). The essential role of the other dyslexia candidate gene, *DYX1C1*, for cilia growth and motility in zebrafish has also been reported (Chandrasekar et al., 2013). Interestingly, the proteins produced by *DYX1C1* and *DCDC2* form protein–protein complexes in a neuroblastoma cell line, suggesting that they relate to interactions at the cellular level, perhaps in cilia function (Tammimies et al., 2013).

Besides the animal models, neuroimaging studies have tried to find the link between genetic markers in dyslexia susceptibility genes and structural and functional phenotypes in human brain. Alteration in gray matter distribution has been related to a 2.4 kb deletion within *DCDC2* with higher gray matter volume in the superior and middle temporal gyri, the occipitoparietal and intraparietal areas, and the inferior and middle frontal gyri for the heterozygous healthy subjects (Meda et al., 2008). *DCDC2* has also been associated with brain activation during phonological processing tasks in the superior anterior and posterior cingulate gyrus, and the left inferior frontal gyrus (Pinel et al., 2012). These studies suggest a wider cortical association with *DCDC2*, not only a link to parietal and temporal cortex as in the present study.

While the white matter pathways studied here were correlated with the thickness of the anatomically connected cortical areas during development, they did not reveal any significant correlation between each other after the effect of age was removed. This suggests that *DCDC2* has an independent effect on white matter structure and cortical thickness, and that the relationship between these brain measures has not driven the genetic associations.

In summary, we attempted to find the link between dyslexia genes, gray matter structure, and reading ability. Knowing the role of these genes (*DCDC2*, *KIAA0319*, and *DYX1C1*) in neuronal migration and ciliary function as well as considering the association of these genes with variations in general reading ability

(Luciano et al., 2007; Bates et al., 2010; Lind et al., 2010), we assessed whether these genetically coded molecular and neuronal mechanisms influence the brain changes, and subsequently behavior. The findings also suggest that neuroimaging can provide intermediate phenotypes as a bridge between genetic markers and behavior outcome.

References

Adler WT, Platt MP, Mehlhorn AJ, Haight JL, Currier TA, Etchegaray MA, Galaburda AM, Rosen GD (2013) Position of neocortical neurons transfected at different gestational ages with shRNA targeted against candidate dyslexia susceptibility genes. PloS One 8:e65179. CrossRef Medline

Altarelli I, Monzalvo K, Iannuzzi S, Fluss J, Billard C, Ramus F, Dehaene-Lambertz G (2013) A functionally guided approach to the morphometry of occipitotemporal regions in developmental dyslexia: evidence for differential effects in boys and girls. J Neurosci 33:11296–11301. CrossRef Medline

Ashburner J (2007) A fast diffeomorphic image registration algorithm. Neuroimage 38:95–113. CrossRef Medline

Bates TC, Lind PA, Luciano M, Montgomery GW, Martin NG, Wright MJ (2010) Dyslexia and DYX1C1: deficits in reading and spelling associated with a missense mutation. Mol Psychiatry 15:1190–1196. CrossRef Medline

Beaulieu C, Plewes C, Paulson LA, Roy D, Snook L, Concha L, Phillips L (2005) Imaging brain connectivity in children with diverse reading ability. Neuroimage 25:1266–1271. CrossRef Medline

Ben-Shachar M, Dougherty RF, Wandell BA (2007) White matter pathways in reading. Curr Opin Neurobiol 17:258–270. CrossRef Medline

Binder JR, Desai RH, Graves WW, Conant LL (2009) Where is the semantic system? A critical review and meta-analysis of 120 functional neuroimaging studies. Cereb Cortex 19:2767–2796. CrossRef Medline

Blackmon K, Barr WB, Kuzniecky R, Dubois J, Carlson C, Quinn BT, Blumberg M, Halgren E, Hagler DJ, Mikhly M, Devinsky O, McDonald CR, Dale AM, Thesen T (2010) Phonetically irregular word pronunciation and cortical thickness in the adult brain. Neuroimage 51:1453–1458. CrossRef Medline

Bond TG, Fox CM (2003) Applying the Rasch model: fundamental measurement in the human sciences, Ed 2. Toledo, OH: University of Toledo.

Carreiras M, Seghier ML, Baquero S, Estévez A, Lozano A, Devlin JT, Price CJ (2009) An anatomical signature for literacy. Nature 461:983–986. CrossRef Medline

Chandrasekar G, Vesterlund L, Hultenby K, Tapia-Páez I, Kere J (2013) The zebrafish orthologue of the dyslexia candidate gene DYX1C1 is essential for cilia growth and function. PLoS One 8:e63123. CrossRef Medline

Chertkow H, Bub D, Deaudon C, Whitehead V (1997) On the status of object concepts in aphasia. Brain Lang 58:203–232. CrossRef Medline

Cope N, Harold D, Hill G, Moskvina V, Stevenson J, Holmans P, Owen MJ, O'Donovan MC, Williams J (2005) Strong evidence that KIAA0319 on chromosome 6p is a susceptibility gene for developmental dyslexia. Am J Hum Genet 76:581–591. CrossRef Medline

Cope N, Eicher JD, Meng H, Gibson CJ, Hager K, Lacadie C, Fulbright RK, Constable RT, Page GP, Gruen JR (2012) Variants in the DYX2 locus are associated with altered brain activation in reading-related brain regions in subjects with reading disability. Neuroimage 63:148–156. CrossRef Medline

Couto JM, Livne-Bar I, Huang K, Xu Z, Cate-Carter T, Feng Y, Wigg K, Humphries T, Tannock R, Kerr EN (2010) Association of reading disabilities with regions marked by acetylated H3 histones in KIAA0319. Am J Med Genet B Neuropsychiatr Genet 153:447–462. CrossRef Medline

Dale AM, Fischl B, Sereno MI (1999) Cortical surface-based analysis: I. Segmentation and surface reconstruction. Neuroimage 9:179–194. CrossRef Medline

Danelli L, Berlingeri M, Bottini G, Ferri F, Vacchi L, Sberna M, Paulesu E (2013) Neural intersections of the phonological, visual magnocellular and motor/cerebellar systems in normal readers: implications for imaging studies on dyslexia. Hum Brain Mapp 34:2669–2687. CrossRef Medline

Darki F, Klingberg T (2014) The role of fronto-parietal and fronto-striatal networks in the development of working memory: a longitudinal study. Cereb Cortex. Advance online publication. Retrieved September 22, 2014. doi:10.1093/cercor/bht352. CrossRef Medline

Darki F, Peyrard-Janvid M, Matsson H, Kere J, Klingberg T (2012) Three dyslexia susceptibility genes, DYX1C1, DCDC2, and KIAA0319, affect temporo-parietal white matter structure. Biol Psychiatry 72:671–676. CrossRef Medline

Deutsch GK, Dougherty RF, Bammer R, Siok WT, Gabrieli JD, Wandell B (2005) Children's reading performance is correlated with white matter structure measured by diffusion tensor imaging. Cortex 41:354–363. CrossRef Medline

Eicher JD, Powers NR, Miller LL, Mueller KL, Mascheretti S, Marino C, Willcutt EG, DeFries JC, Olson RK, Smith SD, Pennington BF, Tomblin JB, Ring SM, Gruen JR (2014) Characterization of the DYX2 locus on chromosome 6p22 with reading disability, language impairment, and IQ. Hum Genet 133:869–881. CrossRef Medline

Fischl B, Dale AM (2000) Measuring the thickness of the human cerebral cortex from magnetic resonance images. Proc Natl Acad Sci U S A 97:11050–11055. CrossRef Medline

Gabel LA, Gibson CJ, Gruen JR, LoTurco JJ (2010) Progress towards a cellular neurobiology of reading disability. Neurobiol Dis 38:173–180. CrossRef Medline

Hayasaka S, Phan KL, Liberzon I, Worsley KJ, Nichols TE (2004) Nonstationary cluster-size inference with random field and permutation methods. Neuroimage 22:676–687. CrossRef Medline

Higginbotham H, Eom TY, Mariani LE, Bachleda A, Hirt J, Gukassyan V, Cusack CL, Lai C, Caspary T, Anton ES (2012) Arl13b in primary cilia regulates the migration and placement of interneurons in the developing cerebral cortex. Dev Cell 23:925–938. CrossRef Medline

Jamadar S, Powers NR, Meda SA, Gelernter J, Gruen JR, Pearlson GD (2011) Genetic influences of cortical gray matter in language-related regions in healthy controls and schizophrenia. Schizophr Res 129:141–148. CrossRef Medline

Katusic SK, Colligan RC, Barbaresi WJ, Schaid DJ, Jacobsen SJ (2001) Incidence of reading disability in a population-based birth cohort, 1976–1982, Rochester, Minn. Mayo Clin Proc 76:1081–1092. CrossRef Medline

Klingberg T, Hedehus M, Temple E, Salz T, Gabrieli JD, Moseley ME, Poldrack RA (2000) Microstructure of temporo-parietal white matter as a basis for reading ability: evidence from diffusion tensor magnetic resonance imaging. Neuron 25:493–500. CrossRef Medline

Kronbichler M, Wimmer H, Staffen W, Hutzler F, Mair A, Ladurner G (2008) Developmental dyslexia: gray matter abnormalities in the occipitotemporal cortex. Hum Brain Mapp 29:613–625. CrossRef Medline

Leemans A, Jeurissen B, Sijbers J, Jones D (2009) ExploreDTI: a graphical toolbox for processing, analyzing, and visualizing diffusion MR data. Paper presented at ISRM 17th Annual Scientific Meeting and Exhibition, Honolulu, HI, April.

Lind PA, Luciano M, Wright MJ, Montgomery GW, Martin NG, Bates TC (2010) Dyslexia and DCDC2: normal variation in reading and spelling is associated with DCDC2 polymorphisms in an Australian population sample. Eur J Hum Genet 18:668–673. CrossRef Medline

Luciano M, Lind PA, Duffy DL, Castles A, Wright MJ, Montgomery GW, Martin NG, Bates TC (2007) A haplotype spanning KIAA0319 and TTRAP is associated with normal variation in reading and spelling ability. Biol Psychiatry 62:811–817. CrossRef Medline

Massinen S, Hokkanen ME, Matsson H, Tammimies K, Tapia-Páez I, Dahlström-Heuser V, Kuja-Panula J, Burghoorn J, Jeppsson KE, Swoboda P, Peyrard-Janvid M, Toftgård R, Castrén E, Kere J (2011) Increased expression of the dyslexia candidate gene DCDC2 affects length and signaling of primary cilia in neurons. PLoS One 6:e20580. CrossRef Medline

McCandliss BD, Cohen L, Dehaene S (2003) The visual word form area: expertise for reading in the fusiform gyrus. Trends Cogn Sci 7:293–299. CrossRef Medline

Meda SA, Gelernter J, Gruen JR, Calhoun VD, Meng H, Cope NA, Pearlson GD (2008) Polymorphism of DCDC2 reveals differences in cortical morphology of healthy individuals—a preliminary voxel based morphometry study. Brain Imaging Behav 2:21–26. CrossRef Medline

Meng H, Smith SD, Hager K, Held M, Liu J, Olson RK, Pennington BF, DeFries JC, Gelernter J, O'Reilly-Pol T, Somlo S, Skudlarski P, Shaywitz SE, Shaywitz BA, Marchione K, Wang Y, Paramasivam M, LoTurco JJ, Page GP, Gruen JR (2005) DCDC2 is associated with reading disability and modulates neuronal development in the brain. Proc Natl Acad Sci U S A 102:17053–17058. CrossRef Medline

Nagy Z, Westerberg H, Klingberg T (2004) Maturation of white matter is

associated with the development of cognitive functions during childhood. J Cogn Neurosci 16:1227–1233. CrossRef Medline

Newbury DF, Paracchini S, Scerri TS, Winchester L, Addis L, Richardson AJ, Walter J, Stein JF, Talcott JB, Monaco AP (2011) Investigation of dyslexia and SLI risk variants in reading-and language-impaired subjects. Behav Genet 41:90–104. CrossRef Medline

Niogi SN, McCandliss BD (2006) Left lateralized white matter microstructure accounts for individual differences in reading ability and disability. Neuropsychologia 44:2178–2188. CrossRef Medline

Noonan KA, Jefferies E, Visser M, Lambon Ralph MA (2013) Going beyond inferior prefrontal involvement in semantic control: evidence for the additional contribution of dorsal angular gyrus and posterior middle temporal cortex. J Cogn Neurosci 25:1824–1850. CrossRef Medline

Paracchini S, Steer CD, Buckingham LL, Morris AP, Ring S, Scerri T, Stein J, Pembrey ME, Ragoussis J, Golding J, Monaco AP (2008) Association of the KIAA0319 dyslexia susceptibility gene with reading skills in the general population. Am J Psychiatry 165:1576–1584. CrossRef Medline

Paulesu E, Démonet JF, Fazio F, McCrory E, Chanoine V, Brunswick N, Cappa SF, Cossu G, Habib M, Frith CD, Frith U (2001) Dyslexia: cultural diversity and biological unity. Science 291:2165–2167. CrossRef Medline

Pernet C, Andersson J, Paulesu E, Demonet JF (2009) When all hypotheses are right: a multifocal account of dyslexia. Hum Brain Mapp 30:2278–2292. CrossRef Medline

Peschansky VJ, Burbridge TJ, Volz AJ, Fiondella C, Wissner-Gross Z, Galaburda AM, Lo Turco JJ, Rosen GD (2010) The effect of variation in expression of the candidate dyslexia susceptibility gene homolog Kiaa0319 on neuronal migration and dendritic morphology in the rat. Cereb Cortex 20:884–897. CrossRef Medline

Pinel P, Fauchereau F, Moreno A, Barbot A, Lathrop M, Zelenika D, Le Bihan D, Poline JB, Bourgeron T, Dehaene S (2012) Genetic variants of FOXP2 and KIAA0319/TTRAP/THEM2 locus are associated with altered brain activation in distinct language-related regions. J Neurosci 32:817–825. CrossRef Medline

Reuter M, Fischl B (2011) Avoiding asymmetry-induced bias in longitudinal image processing. Neuroimage 57:19–21. CrossRef Medline

Reuter M, Rosas HD, Fischl B (2010) Highly accurate inverse consistent registration: a robust approach. Neuroimage 53:1181–1196. CrossRef Medline

Reuter M, Schmansky NJ, Rosas HD, Fischl B (2012) Within-subject template estimation for unbiased longitudinal image analysis. Neuroimage 61:1402–1418. CrossRef Medline

Richlan F (2012) Developmental dyslexia: dysfunction of a left hemisphere reading network. Front Hum Neurosci 6:120. CrossRef Medline

Richlan F, Kronbichler M, Wimmer H (2011) Meta-analyzing brain dysfunctions in dyslexic children and adults. Neuroimage 56:1735–1742. CrossRef Medline

Rosen GD, Bai J, Wang Y, Fiondella CG, Threlkeld SW, LoTurco JJ, Galaburda AM (2007) Disruption of neuronal migration by RNAi of Dyx1c1 results in neocortical and hippocampal malformations. Cereb Cortex 17:2562–2572. CrossRef Medline

Scerri TS, Morris AP, Buckingham LL, Newbury DF, Miller LL, Monaco AP, Bishop DV, Paracchini S (2011) DCDC2, KIAA0319 and CMIP are associated with reading-related traits. Biol Psychiatry 70:237–245. CrossRef Medline

Scerri TS, Darki F, Newbury DF, Whitehouse AJ, Peyrard-Janvid M, Matsson H, Ang QW, Pennell CE, Ring S, Stein J, Morris AP, Monaco AP, Kere J, Talcott JB, Klingberg T, Paracchini S. (2012) The dyslexia candidate locus on 2p12 is associated with general cognitive ability and white matter structure. PLoS One 7:e50321. CrossRef Medline

Schumacher J, Anthoni H, Dahdouh F, König IR, Hillmer AM, Kluck N, Manthey M, Plume E, Warnke A, Remschmidt H (2006) Strong genetic evidence of DCDC2 as a susceptibility gene for dyslexia. Am J Hum Genet 78:52–62. CrossRef Medline

Shaywitz BA, Shaywitz SE, Pugh KR, Mencl WE, Fulbright RK, Skudlarski P, Constable RT, Marchione KE, Fletcher JM, Lyon GR, Gore JC (2002) Disruption of posterior brain systems for reading in children with developmental dyslexia. Biol Psychiatry 52:101–110. CrossRef Medline

Shaywitz BA, Shaywitz SE, Blachman BA, Pugh KR, Fulbright RK, Skudlarski P, Mencl WE, Constable RT, Holahan JM, Marchione KE, Fletcher JM, Lyon GR, Gore JC (2004) Development of left occipitotemporal systems for skilled reading in children after a phonologically-based intervention. Biol Psychiatry 55:926–933. CrossRef Medline

Shaywitz SE, Shaywitz BA, Fletcher JM, Escobar MD (1990) Prevalence of reading disability in boys and girls. JAMA 264:998–1002. CrossRef Medline

Silani G, Frith U, Demonet JF, Fazio F, Perani D, Price C, Frith CD, Paulesu E (2005) Brain abnormalities underlying altered activation in dyslexia: a voxel based morphometry study. Brain 128:2453–2461. CrossRef Medline

Smith SM, Jenkinson M, Woolrich MW, Beckmann CF, Behrens TE, Johansen-Berg H, Bannister PR, De Luca M, Drobnjak I, Flitney DE, Niazy RK, Saunders J, Vickers J, Zhang Y, De Stefano N, Brady JM, Matthews PM (2004) Advances in functional and structural MR image analysis and implementation as FSL. Neuroimage 23:S208–S219. CrossRef Medline

Smith SM, Jenkinson M, Johansen-Berg H, Rueckert D, Nichols TE, Mackay CE, Watkins KE, Ciccarelli O, Cader MZ, Matthews PM, Behrens TE (2006) Tract-based spatial statistics: voxelwise analysis of multi-subject diffusion data. Neuroimage 31:1487–1505. CrossRef Medline

Söderqvist S, McNab F, Peyrard-Janvid M, Matsson H, Humphreys K, Kere J, Klingberg T (2010) The SNAP25 gene is linked to working memory capacity and maturation of the posterior cingulate cortex during childhood. Biol Psychiatry 68:1120–1125. CrossRef Medline

Szalkowski CE, Fiondella CG, Galaburda AM, Rosen GD, Loturco JJ, Fitch RH (2012) Neocortical disruption and behavioral impairments in rats following in utero RNAi of candidate dyslexia risk gene Kiaa0319. Int J Dev Neurosci 30:293–302. CrossRef Medline

Taipale M, Kaminen N, Nopola-Hemmi J, Haltia T, Myllyluoma B, Lyytinen H, Muller K, Kaaranen M, Lindsberg PJ, Hannula-Jouppi K, Kere J (2003) A candidate gene for developmental dyslexia encodes a nuclear tetratricopeptide repeat domain protein dynamically regulated in brain. Proc Natl Acad Sci U S A 100:11553–11558. CrossRef Medline

Tammimies K, Vitezic M, Matsson H, Le Guyader S, Bürglin TR, Ohman T, Strömblad S, Daub CO, Nyman TA, Kere J, Tapia-Páez I (2013) Molecular networks of DYX1C1 gene show connection to neuronal migration genes and cytoskeletal proteins. Biol Psychiatry 73:583–590. CrossRef Medline

Turken AU, Dronkers NF (2011) The neural architecture of the language comprehension network: converging evidence from lesion and connectivity analyses. Front Syst Neurosci 5:1. CrossRef Medline

Ullman H, Almeida R, Klingberg T (2014) Structural maturation and brain activity predict future working memory capacity during childhood development. J Neurosci 34:1592–1598. CrossRef Medline

Vandermosten M, Boets B, Wouters J, Ghesquière P (2012) A qualitative and quantitative review of diffusion tensor imaging studies in reading and dyslexia. Neurosci Biobehav Rev 36:1532–1552. CrossRef Medline

Venkatesh SK, Siddaiah A, Padakannaya P, Ramachandra NB (2013) Lack of association between genetic polymorphisms in ROBO1, MRPL19/C2ORF3 and THEM2 with developmental dyslexia. Gene 529:215–219. CrossRef Medline

Vinckenbosch E, Robichon F, Eliez S (2005) Gray matter alteration in dyslexia: converging evidence from volumetric and voxel-by-voxel MRI analyses. Neuropsychologia 43:324–331. CrossRef Medline

Wandell BA, Yeatman JD (2013) Biological development of reading circuits. Curr Opin Neurobiol 23:261–268. CrossRef Medline

Wang Y, Paramasivam M, Thomas A, Bai J, Kaminen-Ahola N, Kere J, Voskuil J, Rosen GD, Galaburda AM, Loturco JJ (2006) DYX1C1 functions in neuronal migration in developing neocortex. Neuroscience 143:515–522. CrossRef Medline

Welcome SE, Chiarello C, Thompson PM, Sowell ER (2011) Reading skill is related to individual differences in brain structure in college students. Hum Brain Mapp 32:1194–1205. CrossRef Medline

Woodcock RW (1987) Woodcock reading mastery tests, revised. Circle Pines, MN: American Guidance Service.

III

OPEN ACCESS Freely available online

PLOS ONE

The Dyslexia Candidate Locus on 2p12 Is Associated with General Cognitive Ability and White Matter Structure

Thomas S. Scerri[1¤], Fahimeh Darki[2], Dianne F. Newbury[1], Andrew J. O. Whitehouse[3], Myriam Peyrard-Janvid[4], Hans Matsson[4], Qi W. Ang[5], Craig E. Pennell[5], Susan Ring[6], John Stein[7], Andrew P. Morris[1], Anthony P. Monaco[1], Juha Kere[4,8,9], Joel B. Talcott[10], Torkel Klingberg[2], Silvia Paracchini[1,11]*

1 Wellcome Trust Centre for Human Genetics, University of Oxford, Oxford, United Kingdom, **2** Department of Neuroscience, Karolinska Institutet, Stockholm, Sweden, **3** Telethon Institute for Child Health Research, Centre for Child Health Research, University of Western Australia, West Perth, Australia, **4** Department of Biosciences and Nutrition at Novum, Karolinska Institutet, Stockholm, Sweden, **5** School of Women's and Infants' Health, University of Western Australia, Crawley, Australia, **6** School of Social and Community Medicine, University of Bristol, Bristol, United Kingdom, **7** Department of Physiology, University of Oxford, Oxford, United Kingdom, **8** Molecular Medicine Research Programme, University of Helsinki, and Folkhälsan Institute of Genetics, Helsinki, Finland, **9** Science for Life Laboratory, Karolinska Institutet, Stockholm, Sweden, **10** Aston Brain Centre, School of Life and Health Sciences, Aston University, Birmingham, United Kingdom, **11** School of Medicine, University of St Andrews, St Andrews, United Kingdom

Abstract

Independent studies have shown that candidate genes for dyslexia and specific language impairment (SLI) impact upon reading/language-specific traits in the general population. To further explore the effect of disorder-associated genes on cognitive functions, we investigated whether they play a role in broader cognitive traits. We tested a panel of dyslexia and SLI genetic risk factors for association with two measures of general cognitive abilities, or IQ, (verbal and non-verbal) in the Avon Longitudinal Study of Parents and Children (ALSPAC) cohort (N>5,000). Only the *MRPL19/C2ORF3* locus showed statistically significant association (minimum P = 0.00009) which was further supported by independent replications following analysis in four other cohorts. In addition, a fifth independent sample showed association between the *MRPL19/C2ORF3* locus and white matter structure in the posterior part of the corpus callosum and cingulum, connecting large parts of the cortex in the parietal, occipital and temporal lobes. These findings suggest that this locus, originally identified as being associated with dyslexia, is likely to harbour genetic variants associated with general cognitive abilities by influencing white matter structure in localised neuronal regions.

Citation: Scerri TS, Darki F, Newbury DF, Whitehouse AJO, Peyrard-Janvid M, et al. (2012) The Dyslexia Candidate Locus on 2p12 Is Associated with General Cognitive Ability and White Matter Structure. PLoS ONE 7(11): e50321. doi:10.1371/journal.pone.0050321

Editor: Jean-Claude Baron, University of Cambridge, United Kingdom

Received June 29, 2012; **Accepted** October 17, 2012; **Published** November 28, 2012

Funding: This work was funded by the UK Medical Research Council (G0800523/86473 to SP) and was supported by a Wellcome Trust core grant (075491/Z/04, 090532/Z/09/Z). The UK Medical Research Council (74882) the Wellcome Trust (076467) and the University of Bristol provided core support for ALSPAC. The RAINE study is supported by the National Health and Medical Research Council (NHMRC) the University of Western Australia (UWA), the UWA Faculty of Medicine, Dentistry and Health Sciences, the Raine Medical Research Foundation, Curtin University, the Telethon Institute for Child Health Research, and the Women and Infants Research Foundation. The imaging study was supported by Knut and Alice Wallenberg Foundation, The Swedish Research Council and a Swedish Royal Bank Tercentennial Foundation grant in the program "Learning and Memory in Children and Young Adults" (KAW 2005.0179, 2010.0105, K2010-61X-21441-01-3 and PDOKJ028/2006:12 to TK and JK). All laboratory work and the collection of Guy's and Manchester's families of the SLIC collection were funded by The Wellcome Trust. The collection of families from Cambridge (CLASP) was funded by The Wellcome Trust, British Telecom, The Isaac Newton Trust, a National Health Service (NHS) Anglia & Oxford Regional R&D Strategic Investment Award, and an NHS Eastern Region R&D Training Fellowship Award. The funders had no role in study design, data collection and analysis, decision to publish, or preparation of the manuscript.

Competing Interests: The authors have declared that no competing interests exist.

* E-mail: sp58@st-andrews.ac.uk

¤ Current address: The Walter and Eliza Hall Institute for Medical Research, Melbourne, Australia

Introduction

Dyslexia (or reading disability, RD) and specific language impairment (SLI) are common neurodevelopmental disorders, reflecting specific deficits in the acquisition of literacy skills and oral language, respectively [1]. For both disorders, a diagnosis is achieved by excluding known causes of the deficits, such as co-occurring sensory or neurological impairment or lack of educational opportunity. RD and SLI are complex traits resulting from the interaction of multiple factors of both genetic and environmental origin, yet the biological underpinnings and cascading cognitive deficits remain poorly understood. Several genes have been proposed as susceptibility candidates for both RD and SLI. The RD candidates include the *ROBO1*, *KIAA0319*, *DCDC2* and *DYX1C1* genes and the *MRPL19/C2ORF3* locus [2]. The SLI candidates include the *CMIP*, *ATP2C2* and *CNTNAP2* genes [3]. It has been shown that most of the dyslexia risk genes (*KIAA0319*, *DCDC2*, *DYX1C1* and *ROBO1*) are involved in cortical development and specifically in neuronal migration [4]. An important unanswered research question is how genes involved in such a general process as cortical development contribute to the risk for specific neurodevelopmental disorders. Several studies have addressed this research question by investigating whether candidate genes implicated in a specific disorder show pleiotropic effects, which could, for example, help explain the high comorbidity observed between SLI, RD and ADHD [5,6,7]. To date only modest associations have been reported for shared genetic factors across these separate conditions [8,9,10]. Recently

Table 1. Details of phenotypic measures.

	ALSPAC	SLI families	Dyslexia families	Dyslexia cases	Raine
VIQ (mean± SD)	WISC (109.1±16.3)	WISC (100.1±15.4)	BAS/WAIS (60.8±8)	BAS/WAIS (56.9±8)	PPVT (104.9±11.5)
PIQ (mean ± SD)	WISC (101.3±16.7)	WISC (95.4±16.7)	BAS (55±9)	BAS (55.5±7.4)	RCPM (61.8±25.8)
Age at test in years	8	6–16	6–25	8–18	10
Male:female (ratio)	2,946:2,959 (1.00)	319:186 (1.70)	384:254 (1.51)	196:87 (2.25)	708:683 (1.03)
VIQ:READ correlation	0.57	0.62	0.40	0.44	0.40
PIQ:READ correlation	0.35	0.37	0.32	0.41	0.20

VIQ (verbal IQ); PIQ (performance (non-verbal) IQ); SD (standard deviation); WISC (Wechsler Intelligence Scale for Children); BAS (British Abilities Scales); WAIS (Wechsler Adult Intelligence Scale); PPVT (Peabody Picture Vocabulary Test); RCPM (Raven's Coloured Progressive Matrices).

doi:10.1371/journal.pone.0050321.t001

we conducted an association study in the Avon Longitudinal Study of Parents and Children (ALSPAC) cohort to explore potential genetic overlaps between SLI and RD [11]. We analysed a panel of single nucleotide polymorphisms (SNPs), previously reported to be associated with either RD or SLI, and tested them for association with literacy and language related phenotypes. We reported highly specific effects for *DCDC2*, *KIAA0319* and *CMIP* with measures of single-word reading and spelling [11]. These data suggested genetic effects on specific and independent aspects of cognitive function rather than on multiple or more generalised phenotypes.

A direct genetic effect of the impact on broader cognitive abilities for RD and SLI candidate genes has never been tested. General cognitive ability, assessed with standardised intelligence tests, is a highly heritable trait [12,13], yet very few genes have been identified that impact upon these trait [14]. Most of the reported candidate genes have lacked adequate sample size and replications [15]. A recent genome-wide association study (GWAS) supports the strong heritability of cognitive abilities, but with effects that are spread across a large number of genetic factors and therefore not easily detectable in isolation [16]. In the present study, we used a candidate gene approach to investigate a precise question, namely whether genetic risk factors for RD and SLI have a broader impact on general cognitive function. This hypothesis is supported by the consistent observation of significant correlation between reading abilities and general cognition. We analysed RD and SLI candidate genes for association with general cognitive ability in the ALSPAC cohort and detected a statistically significant association at the chromosome 2p12 dyslexia-associated locus. The effect size was small but reproducible in independent samples. Given previous associations between white matter structure and both language-related phenotypes [17] and IQ [18], we looked for any correlations between genotypes at the *MRPL19/C2ORF3* locus and white matter structure. We found associations in the posterior corpus callosum and cingulum, connecting large sections of the parietal, occipital and temporal cortices. The widespread connectivity of this white matter region is consistent with a more general effect on both language and intellectual function.

Results

We analysed 19 SNPs for association with verbal IQ (VIQ) and non-verbal IQ (performance IQ; PIQ) in the ALSPAC child cohort (**Table 1**) across the *MRPL19/C2ORF3*, *KIAA0319*, *DCDC2*, *ATP2C2* and *CMIP* genes (**Table 2**). These markers were selected for previously reported associations with reading- and language-related phenotypes [11]. We detected significant associations (p-values$<$0.001) with VIQ and the SNPs rs714939 (*MRPL12/C2ORF3* locus) and rs6935076 (*KIAA0319*). The rs714939 SNP was also the only marker that showed a trend for association with PIQ (P = 0.006). A marker in *CMIP*, rs6564903, also showed a trend of association for VIQ (P = 0.004). Our previous study [11] showed that *KIAA0319* and *CMIP* are associated with a measure of single word reading (READ) [19] in a subset of the ALSPAC sample. Given the high correlation between VIQ and READ (r = 0.571; Table 1) [11], it is plausible that the association we observed here was driven by reading ability. Therefore, we included READ as covariate when analysing the association with VIQ (**Table 2**). This analysis showed that the associations with rs6935076 (*KIAA0319*) and rs6564903 (*CMIP*) became attenuated, whereas rs714939 remained significantly associated with VIQ. Therefore, while the association with the *KIAA0319* and *CMIP* markers may have been driven by the correlation with reading, the associations at the 2p12 locus appeared to be specific to IQ.

Another SNP at the *MRPL19/C2ORF3* locus, rs917235, also showed a trend of association with VIQ (**Table 2**). For both rs917235 and rs714939, the G alleles are associated with lower performance. These were the same alleles associated with dyslexia in the original report [20]. The most robust association in this previous study was reported for two haplotypes, in different populations, that overlapped for rs917235 and rs714939; specifically, the "GG" haplotype formed by these two markers increased susceptibility to dyslexia. Accordingly, we also tested the rs917235/rs714939 haplotypes for association with VIQ (**Table 3**) in the ALSPAC cohort. The "GG" haplotype gave the strongest association with lower VIQ scores (P = 0.00009). When READ was used as a covariate, the association became weaker but remained significant (P = 0.00024). Furthermore, the "AA" haplotype showed significant association with higher VIQ scores and with an effect size of similar magnitude.

To replicate these results, we tested the *MRPL19/C2ORF3* markers for association with VIQ and PIQ in four independent samples (**Table 4**). We consistently found a trend of association across the four collections, where either of the two originally associated markers had the G allele associated with lower performance. Associations were particularly evident in the SLI families (rs714939; P = 0.009; PIQ) and in the unrelated cases with dyslexia (rs917235; P = 0.0004; VIQ). The same SNPs did not show association with single word reading measures in previous studies using the same samples [9,11,21] excluding the possibility that these associations are driven by the high correlation between VIQ and reading ability. We also re-analysed all of the samples for association with reading using IQ as covariate, but again none of the samples including the ALSPAC cohort showed any associa-

Table 2. Single-SNP analyses in the ALSPAC cohort.

			Verbal IQ			Performance IQ			Verbal IQ with READ as a covariate		
Chr	**Gene (locus)**	**SNP**	**N**	**Beta**	**P**	**N**	**Beta**	**P**	**N**	**Beta**	**P**
2	*MRPL19/C2ORF3*	rs1000585	5565	−0.038	0.06859	5560	0.005	0.8475	5159	−0.037	0.03911
2	*MRPL19/C2ORF3*	rs917235	5796	−0.043	0.03136	5789	−0.01	0.6773	5330	−0.044	0.0102
2	*MRPL19/C2ORF3*	rs714939	5555	0.069	**0.00099**	5550	0.068	0.00631	5149	0.061	**0.00066**
6	*DCDC2*	rs793862	5636	−0.034	0.148	5627	−0.018	0.5077	5182	−0.017	0.3908
6	*DCDC2*	rs807701	5837	−0.009	0.6705	5831	0.02	0.4176	5369	−0.003	0.8591
6	*DCDC2*	rs807724	5671	−0.026	0.2885	5664	−0.024	0.4166	5210	−0.013	0.5418
6	*DCDC2*	rs1087266	5850	−0.006	0.7773	5843	0.003	0.8914	5380	−0.001	0.9315
6	*KIAA0319*	rs761100	5825	−0.046	0.02341	5816	0.004	0.8837	5362	−0.045	0.00871
6	*KIAA0319*	rs6935076	5468	0.083	**0.00011**	5463	0.026	0.3026	5071	0.048	0.00862
6	*KIAA0319*	rs2038137	5569	−0.052	0.01319	5564	−0.015	0.5587	5161	−0.045	0.01142
6	*KIAA0319*	rs9461045	5641	−0.044	0.09869	5634	−0.013	0.6763	5190	0.002	0.9172
6	*KIAA0319*	rs2143340	5554	−0.053	0.06262	5549	−0.011	0.7384	5148	0.001	0.9517
16	*CMIP*	rs12927866	5570	−0.053	0.01085	5565	−0.017	0.4918	5163	−0.038	0.02997
16	*CMIP*	rs6564903	5750	−0.058	0.00385	5743	−0.024	0.3224	5289	−0.036	0.03382
16	*CMIP*	rs4265801	5565	0.028	0.1667	5560	0.013	0.5895	5159	0.02	0.2499
16	*CMIP*	rs16955705	5563	−0.035	0.0867	5558	0.001	0.9578	5158	−0.022	0.2104
16	*ATP2C2*	rs16973771	5503	0	0.985	5499	0.016	0.5133	5100	0	0.995
16	*ATP2C2*	rs2875891	5569	−0.007	0.728	5564	0.014	0.593	5161	−0.005	0.7846
16	*ATP2C2*	rs8045507	5560	−0.009	0.6748	5555	0.018	0.4787	5153	−0.003	0.8716

p-values<0.001 are emboldened.
BETA are relative to the minor allele.
doi:10.1371/journal.pone.0050321.t002

tions (data not shown). The unrelated cases with dyslexia was the only sample that showed stronger association with VIQ, while the other samples showed associations mainly with PIQ. The dyslexia families and Raine samples only showed a modest trend of association, but it was in the same allelic direction (rs917235; P = 0.064 and rs714939; P = 0.059, respectively). Haplotype analysis in all replication sets revealed a similar trend, with the "GG" haplotype associated with lower performance, but did not show associations stronger than single SNP analyses (data not shown).

We assessed the effect of genetic variants at the *MRPL19/C2ORF3* locus on white matter structure in the Swedish cohort. Among seven genotyped markers, only rs917235 showed significant association with variation in white matter volume ($P_{corrected} = 1.27 \times 10^{-3}$ at cluster level with the threshold of P<0.01). Specifically, the G allele, already shown to be associated with lower IQ, was associated with lower white matter volume. This white matter cluster was located bilaterally and confined mainly to the posterior part of the corpus callosum and the cingulum (**Figure 1A**).

The significant cluster in the posterior corpus callosum (**Figure 1A**) was then used as a seed region for fiber tracking (see **Figure 1B** for tracking in one individual) performed in 30 randomly selected subjects. The pathways from each subject were then overlaid on a common template to identify the most consistent localization of pathways (**Figure 1C**). Next, we identified the parts of cortex that were closest to the end-points of the white matter tracts. This analysis showed that the pathways

Table 3. Summary results for rs917235/rs714939 haplotype associations with VIQ in the ALSPAC cohort.

	N = 5428	Haplotype		Haplotype analysis with READ as a covariate	
		N = 5428		N = 5030	
HAPLOTYPE	**%**	**BETA**	**P**	**BETA**	**P**
GG	0.317	−0.093	**0.00009**	−0.074	**0.00024**
AG	0.299	0.004	0.857	−0.005	0.821
AA	0.236	0.063	0.0175	0.072	**0.00116**
GA	0.148	0.076	0.0231	0.038	0.176

p-values statistically significant are in bold.
doi:10.1371/journal.pone.0050321.t003

Table 4. P-values from single-SNP analyses for VIQ and PIQ in replication samples.

	ALSPAC			SLI families			Dyslexic families			Dyslexic cases			Raine		
SNP	**N**	**VIQ**	**PIQ**	**N**	**VIQ**	**PIQ**	**N**	**VIQ**	**PIQ**	**N**	**VIQ**	**PIQ**	**N**	**VIQ**	**PIQ**
rs1000585	5565	0.069	0.848	411 sib	0.393	0.272	604 sib	0.796	0.397	279	0.011	0.745	NT		
rs917235	5795	0.031	0.677	418 sib	0.574	0.304	599 sib	0.416	0.064	282	**0.0004**	0.464	1094	0.335	0.955
rs714939	5555	**0.001**	0.006	413 sib	0.034	0.009	592 sib	0.928	0.567	277	0.639	0.079	1080	0.846	0.059

p-values statistically significant are in bold.
RA = Risk alleles are given only for results showing trend of association ($p<0.1$); NT = not tested.
Risk allele was G for all SNPs in all samples.
doi:10.1371/journal.pone.0050321.t004

passing through the region connected the right postcentral gyrus, superior parietal lobule, precuneous, lateral occipital cortex and fusiform gyrus to analogous areas in the left hemisphere (**Figure 1D**).

Discussion

We evaluated the effect of candidate genes for RD and SLI on measures of general cognitive ability in the ALSPAC cohort. The *MRPL19/C2ORF3* locus showed a statistically significant association with general cognitive abilities (VIQ and PIQ). *KIAA0319* and *CMIP* variants also showed associations, but these genes have previously been found associated with reading ability in the ALSPAC sample [11], hence the associations detected here could be an artefact due to the correlation between VIQ and measures of single word-reading. Indeed, the associations between the *KIAA0319* and *CMIP* markers and VIQ were attenuated when a reading measure was used as a covariate. Conversely, *MRPL19/C2ORF3* markers did not show any association with single-word reading in the ALSPAC cohort [11]. Furthermore, this association remained significant when reading ability was used as a covariate and is supported by a consistent trend of association with IQ in four independent samples. The association would not stand a genome-wide correction for significance level, but this would be consistent with a recent GWAS that predicts multiple and small-size factors contributing to IQ [16]. Our candidate gene approach

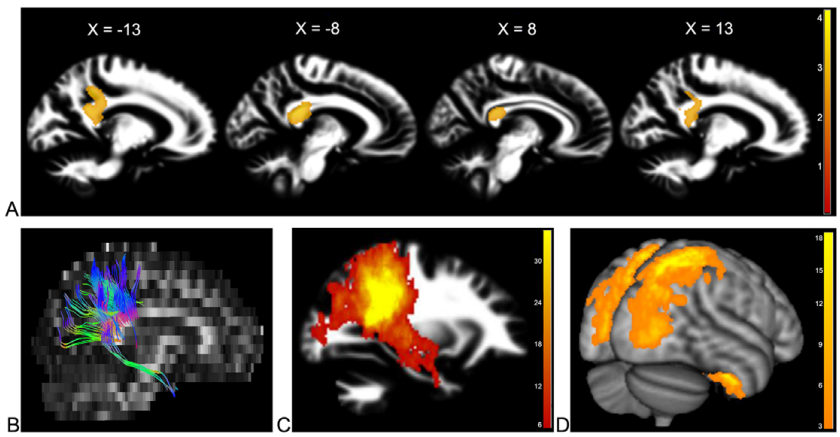

Figure 1. Imaging results. (A) Main association of rs917235 with white matter volume. Sagittal view of the significant cluster associated with rs917235 at the MNI coordinates of X = −13, −8, 8, and 13 mm relative to the midline. The background image is the average of all individuals' white matter segmented images. The colour-bar shows the z-scores of the statistical analysis. (B–D) Structural connectivity. (B) A sample of fiber tracking from one individual passing through the region associated with rs917235. Different colours show the direction of pathways (red for left-right, blue for superior-inferior, and green for anterior-posterior). (C) Overlay of tract tracing from 30 randomly selected individuals. The colour-bar is a count for the number of subjects; yellow shows the most probable pathways. (D) Cortical end-points of the white matter pathways showing that the fibers connect right postcentral gyrus, superior parietal lobule, precuneous, occipital cortex and temporal fusiform gyrus to the analogous left regions.
doi:10.1371/journal.pone.0050321.g001

was based on the selection of previously reported disorder-associated genotypes, suggesting a more generalised effect across multiple cognitive traits. Our interpretation is that the chromosome 2 locus has an effect on cognition by influencing neurodevelopment. The effect on specific endophenotypes will depend on ascertainment criteria, methodology for phenotypic assessment and differences in genetic background. All these elements will have a significant role in the outcome of association analyses when sample sizes are relatively small.

To date, only a few common genetic variants have been associated with measures of verbal and nonverbal reasoning. These include variants in the *CHRM2, COMT* and *BDNF* genes [14]. GWASs, which have recently had an enormous success in identifying genetic variants contributing to complex traits, had little success in mapping variants associated with cognitive abilities, with no indication of major genetic contributing loci [16,22,23]. The generally accepted model proposes that cognitive abilities are influenced by many genes of small effect [24] and are therefore difficult to map in the relatively small-sized samples currently available. Gene group-base analysis might be more effective by testing biological functions determined by multiple genes [25].

Both rs714939 and rs917235 are within an intergenic region between the *FAM176A* and *MRPL19/C2ORF3* loci. The original study associating this locus with dyslexia showed an effect on gene expression of the co-regulated genes *MRPL19* and *C2ORF3*, and differential expression across a set of brain regions [20]. These genes are transcribed in a head-to-head orientation on chromosome 2p12. Visualisation of *MRPL19* and *C2ORF3* in the Allen Brain Atlas (a resource of human gene expression data derived from 3 post-mortem males aged 24 to 57 years old at time of death; http://www.brain-map.org/), show that these two genes are most highly expressed in white matter of the corpus callosum and the cingulum when compared to all other regions. This is in contrast to *KIAA0319*, *CMIP* and *ATP2C2* which show very low expression in white matter, and *FAM176A* which shows moderate expression. There is no direct evidence that these two SNPs are the causative variants and it is likely that together they tag the effect of a nearby functional factor. The *FAM176A* gene, also expressed in fetal brain, cannot be ruled out as being influenced by these two SNPs. Interestingly, rs714939 is located in a region of high H3K4Me1 marks (ENCODE ChIP-Seq data, GRCh37/hg19 assembly visualised in the UCSC Genome Browser (http://genome.ucsc.edu/cgi-bin/hgGateway)). H3K4Me1 is a monomethylation of lysin 4 of the H3 histone protein and this modification is often found near regulatory elements. This region of high H3K4Me1 spans 9–10 kb and could be involved in the cis-regulation of any of the three neighbouring genes.

The imaging results provide a neural correlate to the genetic polymorphism. Our interpretation is that the genetic variants contribute to structural variation in a relatively large area of white matter which affects both reasoning and reading. It should be pointed out, however, that this is an association study that does not provide any direction of causality. It cannot be excluded that genes affect behavior, which in turn affect the white matter. Our neuroimaging analysis revealed a significant association between rs917235 and white matter volume of the posterior part of the corpus callosum and cingulum. The G allele, associated with lower IQ in the behavioural analysis, was specifically associated with lower white matter volume in this region. Previous studies have reported correlations between white matter structure and measures of IQ [26,27,28,29], supporting the idea that neural connectivity of the brain is an endophenotype underpinning general intellectual ability [18]. Tract tracing of fibers passing through the correlated white matter region showed that they establish long-range connections with large regions of the parietal and occipital cortices, and a smaller region within temporo-occipital cortex. Intra- and superior parietal have been associated with performance on reasoning tasks [30] and the inferior parietal cortex is important for language-related functions [31]. The thickness of the splenium of the corpus callosum, which connects large parts of the occipital, parietal and temporal lobes, has been previously associated with intelligence [32]. Based on parieto-frontal integration theory of intelligence (P-FIT) [30], the lateral cortex and fusiform gyrus from the temporal lobe are involved in cognitive ability since they participate in visual perception, recognition and imagination. The superior parietal, supramarginal and angular gyri are involved in structural symbolism and abstraction. These regions are also important for language-related functions. The posterior part of the corpus callosum has been previously reported as a white matter region with structural differences between normal and dyslexic readers. [33,34,35,36]. It has been also shown that the posterior part of the corpus callosum is bigger in children with dyslexia rather than in typically developing children [37] The widespread connectivity of the white matter region associated with rs917235 is thus consistent with the previous neuroimaging associations to both language and general cognitive abilities. However, substantially more cortical regions and associated brain functions are likely to underlie general cognitive abilities. The integration of genetics with structural and functional imaging approaches holds potential for further elucidating the effects of genes on the normal and atypical development of cognitive function. With a similar approach we showed that three dyslexia susceptibility genes *DYX1C1, DCDC2* and *KIAA0319* are associated with white matter volume in distinct but overlapping regions of the left temporo-parietal hemisphere, and that the white matter volume in these regions also correlated with reading ability [38]. A recent study found association between candidate genes for language and reading impairment (*FOXP2* and *KIAA0319*, respectively) and regionally specific brain activations assessed with fMRI [39]. Another study reported two independent SNP associations, both on chromosome 12, with brain volume measures as well as suggestive evidence of an effect on cognitive abilities [40]. Most recently, a study has found a genome-wide significant association between a SNP (rs2298948) within *C2ORF3* (called *GCFC2* in that study) and hippocampal volume [41]. The hippocampus plays an important role in learning and spatial memory, and this is correlated with hippocampus volume.

The association of cognitive abilities with a genetic locus, originally identified as a candidate for dyslexia susceptibility, is independent from a clinical diagnosis of dyslexia and SLI. The association was statistically significant in the ALSPAC sample, which represents the general population, and we did not observe any associations with reading-related measures in either ALSPAC or the other replication samples, including the ones selected for dyslexia or SLI. It is possible that the original association with developmental dyslexia at the *MRPL19/C2ORF3* locus [20] was due to a sampling effect and the high correlation between the verbal component of cognitive abilities and reading. Alternatively, the same genetic variants may have different phenotypic effects when combined with alternative genetic or environmental factors and would become apparent in separate sample subgroups. Multivariate genetic analysis have consistently suggested a correlation of about 0.6 between general cognitive ability and learning [42] but there is less agreement in estimating the effects across the range of the entire phenotypic distribution [43]. This would imply that some factors may have specific effects only at the extremes of the phenotype where disorder diagnosis would apply.

In summary, we report an association of measures of general cognitive abilities with the chromosome 2p12 locus implicated in dyslexia. We show, for the first time, that the same genetic locus is associated with white matter volume in the posterior corpus callosum. Furthermore, fibers throughout this region connected cortical regions involved in both language and general cognitive abilities. Follow-up studies might identify the functional genetic variant(s) and the gene(s) implicated. Such findings will contribute to our understanding of the biological pathways underlying normal and atypical cognition and the possible shared factor(s) mediating general cognitive functions and highly prevalent developmental disorders such as dyslexia.

Materials and Methods

Ethics Statement

Informed written consent was obtained from the parents, with the option for them or their children to withdraw at any time. Ethical approval for the ALSPAC cohort was obtained from the ALSPAC Law and Ethics Committee and the Local Research Ethics Committees. Ethical approval for the SLIC cohort was granted by local ethics committees. Ethical approval for the Oxford/Reading and Aston studies was acquired from the Oxfordshire Psychiatric Research Ethics Committee (OPREC O01.02). For the Raine Study, participant recruitment and all follow-ups of the study families were approved by the Human Ethics Committee at King Edward Memorial Hospital and/or Princess Margaret Hospital for Children in Perth. For the Swedish sample, the study was approved by the Ethics Board of the Karolinska University Hospital (Stockholm).

Initial Sample

The ALSPAC cohort consists of over 14,000 children from the southwest of England that had expected dates of delivery between 1st April 1991 and 31st December 1992 [44]. From age 7 years, all children were annually assessed for a wide range of physical, behavioural, and neuropsychological traits, including reading and language-related measures. DNA is available for approximately 11,000 children. For this study, individuals with a non-white ancestry were excluded and after filtering for missing genotypic or phenotypic data we conducted the analysis in a sample of 5905 children. Cognitive ability was assessed using the Wechsler Intelligence Scales for Children (WISC-III) [45] for both verbal and performance IQ (VIQ and PIQ, respectively; **Table 1**). The VIQ scale included the subtests for Information, Similarities, Arithmetic, Vocabulary, Comprehension and Digit span. The PIQ scale included the subtests for Picture completion, Coding, Picture arrangement, Block design and Object assembly.

Replication Samples

The SLI Consortium (SLIC) cohort has been described in detail previously [46,47,48]. This family-based sample includes approximately 400 individuals from 181 families. The samples were assessed at one of five separate centres across the UK: The Newcomen Centre at Guy's Hospital, London, the Cambridge Language and Speech Project (CLASP [49]), the Child Life and Health Department at the University of Edinburgh [50], the Department of Child Health at the University of Aberdeen and the Manchester Language Study [51,52]. Cognitive ability of all children in the SLIC sample was assessed using the WISC-III [45] applying the same VIQ and PIQ subtests listed for ALSPAC. In the SLIC sample, the PIQ score (cut-off at PIQ>80) was used to exclude children whose language problems were accompanied by deficits in non-verbal skills.

The dyslexia-based sample has been described previously [53,54]. It includes 684 siblings from 288 unrelated nuclear families and 282 unrelated cases with dyslexia, recruited through the Dyslexia Research Centre clinics in Oxford and Reading, and the Aston Dyslexia and Development Assessment Centre in Birmingham. VIQ and PIQ were obtained from the BAS similarities and BAS matrices subtests respectively [55]. The similarities sub-scale of the Wechsler Adult Intelligence Scales (WAIS), a measure analogous to the BAS similarities test, was used when age was >17.5 years [45].

The Western Australian Pregnancy Cohort (Raine) study is a longitudinal investigation of 2900 pregnant women and their offspring recruited between 1989 and 1991 [56]. From the original cohort, 2868 children have been followed over two decades. The Raine sample is representative of the larger Australian population (88% Caucasian); only those children with both biological parents of white European origin were included in the current analyses. Verbal and non-verbal ability was assessed at 10 years of age using the Peabody Picture Vocabulary Test–Revised (PPVT-R) [57] and the Raven's Coloured Progressive Matrices (RCPM) [58], respectively. The PPVT-R provides a measure of receptive vocabulary, requiring children to select which of four pictures corresponds to an aurally presented word. Raw scores are converted to a Verbal IQ, standardized for age 2 years and above (based around a mean of 100 and a SD of 15). RCPM is a 36 item multiple choice test that presents a matrix-like arrangement of figural symbols and requires the child to select the missing symbols from a set of six alternatives. Raw scores are converted to percentiles, which provide an indication of performance relative to other children of a similar age. This assessment is standardized for children between 4.9 and 12.0 years of age.

The Swedish sample used for neuroimaging consists of 76 Swedish speaking children and young adults (age range 6 to 25 years) randomly selected from the "Brainchild" study, a longitudinal study of typical development [59,60]. The participants were from the population register in the town of Nynäshamn, Sweden, and showed no evidence of neurological or psychological disorders. DNA was available for all subjects.

Genotyping and statistical analysis

We analysed 19 SNPs across the *MRPL19/C2ORF3, KIAA0319, DCDC2, ATP2C2* and *CMIP* loci that were recently genotyped in the ALSPAC child cohort [11]. The sample size in the present study is larger because we did not apply an IQ filter as described in the previous analysis. SNPs were genotyped using either Sequenom iPLEX assays according to the manufacturer's instructions or the KBiosciences service using their in-house technology (http://www.kbioscience.co.uk/). The genotyping in the samples selected for dyslexia and SLI was conducted with Sequenom iPLEX assays as part of previous studies [9].

For the Raine study, DNA samples were genotyped on an Illumina 660 Quad Array [61].

For the Swedish sample, seven SNPs (rs3088180, rs4853169, rs917235, rs6732511, rs714939, rs17689640 and rs17689863) located at the *MRPL19/C2ORF3* locus were genotyped using the Sequenom iPLEX system as previously described [59].

Quantitative analyses were performed within PLINK (1.07) [62] using additive tests of association. We included two additional phenotypes (VIQ and PIQ) to the multiple testing correction applied in our previous study of the ALSPAC sample [11] which corrected for the analysis of 11 clusters of SNPs showing significant linkage disequilibrium (LD; r^2>0.6) and 2 phenotypes. Therefore we corrected here the significance level of P = 0.05 for 44 independent tests (11 SNP clusters analysed for four phenotypes)

resulting in P = 0.001. The ALSPAC cohort has been tested previously for other SNPs and phenotypes, therefore these tests should be considered in calculating a significant threshold p-value, or the genome-significant threshold of 5×10^{-8} should be applied. However, this would be too conservative for the scope of this study which analyses previously reported genetic markers and tests a specific hypothesis rather than conducting an explorative exercise. Family-based cohorts were analysed using QTDT [63].

Image analysis

For the Swedish sample, three-dimensional structural T1-weighted imaging with magnetization-prepared rapid gradient echo sequence (TR = 2300 ms, TE = 2.92 ms, 256×256 mm, 176 sagittal slices and 1 mm^3 voxel size) with the field of view of 256×256 mm, 256 slices, and 1 mm^3 voxel size was carried out on all the participants and repeated two years later for 69 subjects. White matter segmentation, followed by an alignment technique, was performed on the structural data using the Diffeomorphic Anatomical Registration using Exponentiated Lie algebra (DARTEL) toolbox in SPM (www.fil.ion.ucl.ac.uk/spm/software/spm5). Images were then spatially smoothed with an 8 mm Gaussian kernel. The DARTEL outputs are white matter segmented images which reflect the signal intensity modulated by volume transformations applied to individual images to register them into the MNI template.

Diffusion tensor imaging (DTI) was also acquired using a field of view 230×230 mm, matrix size 128×128 mm, 19 slices with 6.5 mm thickness b-max 1000 s/mm^2 in 20 directions. Eddy current and head motion were corrected using affine registration to a reference volume using FSL (www.fmrib.ox.ac.uk/fsl/). The diffusion tensors were then computed for each voxel and the DTI and fractional anisotropy (FA) data were then constructed.

The seven SNPs were entered separately as a main factor in a flexible factorial design second-level SPM analysis. This included both the individual images with and without repeated measures, to assess the variation of white matter with respect to the genetic markers and was corrected for the effect of age, sex, handedness and total white matter volume. Age X gene and gender X gene interaction effects were also included in the model. As a part of this exploratory analysis, the significance level was corrected at the cluster level using non-stationary cluster extent correction [64] for multiple comparisons resulting from searching the entire white matter volume as well as for the seven SNPs (Bonferroni correction, $P_{corrected}<0.0014$ for comparison of searching the entire brain with a threshold of $P<0.01$, as implemented in the SPM software).

The region showing the significant effect was saved as a binary region of interest (ROI). This ROI was then transformed to each individual's DTI space, to be used as a seed ROI for white matter fiber tracking. Deterministic fiber tracking was applied on 30 randomly selected subjects by starting tractography from the ROI following the principal eigenvector direction using 1 mm steps, considering thresholds of 0.15 for FA values and 30 for angular degree using ExploreDTI v4.7.3. (www.exploredti.com). Computed tracts from all individuals were then averaged across all 30 participants to derive a probabilistic map of the white matter pathways passing through the overlapping areas.

Acknowledgments

We are grateful to all the families and sample donors who took part in this study. We are grateful to Dorothy Bishop for her guidance in handling cognitive phenotypes and useful discussion. SP is a Royal Society University Research Fellow. DFN is an MRC Career Development Fellow and a Junior Research Fellow of St John's College, Oxford. AW is a NHMRC Career Development Fellow. This publication is the work of the authors and SP will serve as guarantor for the contents of this paper.

Author Contributions

Conceived and designed the experiments: CEP SR JS A.P. Monaco JK JBT TK SP. Performed the experiments: TSS FD DN AJOW MP HM SP. Analyzed the data: TSS FD DN AJOW MP HM QWA A.P. Morris JBT SP. Wrote the paper: TSS FD DN AJOW MP HM JK JBT SP.

References

1. Pennington BF, Bishop DV (2009) Relations among speech, language, and reading disorders. Annu Rev Psychol 60: 283–306.
2. Scerri TS, Schulte-Korne G (2010) Genetics of developmental dyslexia. Eur Child Adolesc Psychiatry 19: 179–197.
3. Newbury DF, Monaco AP (2010) Genetic advances in the study of speech and language disorders. Neuron 68: 309–320.
4. Galaburda AM, LoTurco J, Ramus F, Fitch RH, Rosen GD (2006) From genes to behavior in developmental dyslexia. Nat Neurosci 9: 1213–1217.
5. Snowling M, Bishop DV, Stothard SE (2000) Is preschool language impairment a risk factor for dyslexia in adolescence? J Child Psychol Psychiatry 41: 587–600.
6. McArthur GM, Hogben JH, Edwards VT, Heath SM, Mengler ED (2000) On the "specifics" of specific reading disability and specific language impairment. J Child Psychol Psychiatry 41: 869–874.
7. Pennington BF (2006) From single to multiple deficit models of developmental disorders. Cognition 101: 385–413.
8. Rice ML, Smith SD, Gayan J (2009) Convergent genetic linkage and associations to language, speech and reading measures in families of probands with Specific Language Impairment. J Neurodev Disord 1: 264–282.
9. Newbury DF, Paracchini S, Scerri TS, Winchester L, Addis L, et al. (2011) Investigation of dyslexia and SLI risk variants in reading and language-impaired subjects. Behav Genet 41: 90–104.
10. Bates TC, Luciano M, Medland SE, Montgomery GW, Wright MJ, et al. (2011) Genetic Variance in a Component of the Language Acquisition Device: ROBO1 Polymorphisms Associated with Phonological Buffer Deficits. Behav Genet 41: 50–57.
11. Scerri TS, Morris AP, Buckingham LL, Newbury DF, Miller LL, et al. (2011) DCDC2, KIAA0319 and CMIP are associated with reading-related traits. Biol Psychiatry 70: 237–245.
12. Bouchard TJ, Jr., McGue M (1981) Familial studies of intelligence: a review. Science 212: 1055–1059.
13. Plomin R, Spinath FM (2002) Genetics and general cognitive ability (g). Trends Cogn Sci 6: 169–176.
14. Deary IJ, Johnson W, Houlihan LM (2009) Genetic foundations of human intelligence. Hum Genet 126: 215–232.
15. Chabris CF, Hebert BM, Benjamin DJ, Beauchamp JP, Cesarini D, et al. (2012) Most reported genetic associations with general intelligence are probably false positives. Psychological Science In press.
16. Davies G, Tenesa A, Payton A, Yang J, Harris SE, et al. (2011) Genome-wide association studies establish that human intelligence is highly heritable and polygenic. Mol Psychiatry 16: 996–1005.
17. Klingberg T, Hedehus M, Temple E, Salz T, Gabrieli JD, et al. (2000) Microstructure of temporo-parietal white matter as a basis for reading ability: evidence from diffusion tensor magnetic resonance imaging. Neuron 25: 493–500.
18. Deary IJ, Penke L, Johnson W (2010) The neuroscience of human intelligence differences. Nat Rev Neurosci 11: 201–211.
19. Rust J, Golombok S, Trickey G (1993) WORD: Wechsler Objective Reading Dimensional Manual. Sidcup, UK: Psychological Corporation.
20. Anthoni H, Zucchelli M, Matsson H, Muller-Myhsok B, Fransson I, et al. (2007) A locus on 2p12 containing the co-regulated MRPL19 and C2ORF3 genes is associated to dyslexia. Hum Mol Genet 16: 667–677.
21. Paracchini S, Ang QW, Stanley FJ, Monaco AP, Pennell CE, et al. (2010) Analysis of dyslexia candidate genes in the Raine cohort representing the general Australian population. Genes Brain Behav 10: 158–165.
22. Davis OS, Butcher LM, Docherty SJ, Meaburn EL, Curtis CJ, et al. (2010) A three-stage genome-wide association study of general cognitive ability: hunting the small effects. Behav Genet 40: 759–767.
23. Pan Y, Wang KS, Aragam N (2011) NTM and NR3C2 polymorphisms influencing intelligence: family-based association studies. Prog Neuropsychopharmacol Biol Psychiatry 35: 154–160.
24. Plomin R (1999) Genetics and general cognitive ability. Nature 402: C25–29.
25. Ruano D, Abecasis GR, Glaser B, Lips ES, Cornelisse LN, et al. (2010) Functional gene group analysis reveals a role of synaptic heterotrimeric G proteins in cognitive ability. Am J Hum Genet 86: 113–125.

26. Deary IJ, Bastin ME, Pattie A, Clayden JD, Whalley LJ, et al. (2006) White matter integrity and cognition in childhood and old age. Neurology 66: 505–512.
27. Schmithorst VJ, Wilke M, Dardzinski BJ, Holland SK (2005) Cognitive functions correlate with white matter architecture in a normal pediatric population: a diffusion tensor MRI study. Hum Brain Mapp 26: 139–147.
28. Chiang MC, Barysheva M, Shattuck DW, Lee AD, Madsen SK, et al. (2009) Genetics of brain fiber architecture and intellectual performance. J Neurosci 29: 2212–2224.
29. Fjell AM, Westlye LT, Amlien IK, Walhovd KB (2011) Reduced white matter integrity is related to cognitive instability. J Neurosci 31: 18060–18072.
30. Jung RE, Haier RJ (2007) The Parieto-Frontal Integration Theory (P-FIT) of intelligence: converging neuroimaging evidence. Behav Brain Sci 30: 135–154; discussion 154–187.
31. Richlan F, Kronbichler M, Wimmer H (2011) Meta-analyzing brain dysfunctions in dyslexic children and adults. Neuroimage 56: 1735–1742.
32. Luders E, Thompson PM, Narr KL, Zamanyan A, Chou YY, et al. (2011) The link between callosal thickness and intelligence in healthy children and adolescents. Neuroimage 54: 1823–1830.
33. Vandermosten M, Boets B, Poelmans H, Sunaert S, Wouters J, et al. (2012) A tractography study in dyslexia: neuroanatomic correlates of orthographic, phonological and speech processing. Brain 135: 935–948.
34. Frye RE, Hasan K, Xue L, Strickland D, Malmberg B, et al. (2008) Splenium microstructure is related to two dimensions of reading skill. Neuroreport 19: 1627–1631.
35. Dougherty RF, Ben-Shachar M, Deutsch GK, Hernandez A, Fox GR, et al. (2007) Temporal-callosal pathway diffusivity predicts phonological skills in children. Proc Natl Acad Sci U S A 104: 8556–8561.
36. Odegard TN, Farris EA, Ring J, McColl R, Black J (2009) Brain connectivity in non-reading impaired children and children diagnosed with developmental dyslexia. Neuropsychologia 47: 1972–1977.
37. Hasan KM, Molfese DL, Walimuni IS, Stuebing KK, Papanicolaou AC, et al. (2012) Diffusion tensor quantification and cognitive correlates of the macrostructure and microstructure of the corpus callosum in typically developing and dyslexic children. NMR Biomed.
38. Darki F, Peyrard-Janvid M, Matsson H, Kere J, Klingberg T (2012) Three Dyslexia Susceptibility Genes, DYX1C1, DCDC2, and KIAA0319, Affect Temporo-Parietal White Matter Structure. Biol Psychiatry.
39. Pinel P, Fauchereau F, Moreno A, Barbot A, Lathrop M, et al. (2012) Genetic Variants of FOXP2 and KIAA0319/TTRAP/THEM2 Locus Are Associated with Altered Brain Activation in Distinct Language-Related Regions. J Neurosci 32: 817–825.
40. Stein JL, Medland SE, Vasquez AA, Hibar DP, Senstad RE, et al. (2012) Identification of common variants associated with human hippocampal and intracranial volumes. Nat Genet.
41. Melville SA, Buros J, Parrado AR, Vardarajan B, Logue MW, et al. (2012) Multiple loci influencing hippocampal degeneration identified by genome scan. Ann Neurol 72: 65–75.
42. Plomin R, Kovas Y (2005) Generalist genes and learning disabilities. Psychol Bull 131: 592–617.
43. Haworth CM, Dale PS, Plomin R (2009) Generalist genes and high cognitive abilities. Behav Genet 39: 437–445.
44. Golding J, Pembrey M, Jones R (2001) ALSPAC–the Avon Longitudinal Study of Parents and Children. I. Study methodology. Paediatr Perinat Epidemiol 15: 74–87.
45. Wechsler D, Golombok S, Rust J (1992) WISC-IIIUK: Wechsler Intelligence Scale for Children. Sidcup, UK: The Psycological Corporation.
46. SLIC (2002) A genomewide scan identifies two novel loci involved in specific language impairment. Am J Hum Genet 70: 384–398.
47. SLIC (2004) Highly significant linkage to the SLI1 locus in an expanded sample of individuals affected by specific language impairment. Am J Hum Genet 74: 1225–1238.
48. Falcaro M, Pickles A, Newbury DF, Addis L, Banfield E, et al. (2008) Genetic and phenotypic effects of phonological short-term memory and grammatical morphology in specific language impairment. Genes Brain Behav 7: 393–402.
49. Burden V, Stott CM, Forge J, Goodyer I (1996) The Cambridge Language and Speech Project (CLASP). I. Detection of language difficulties at 36 to 39 months. Dev Med Child Neurol 38: 613–631.
50. Clark A, O'Hare A, Watson J, Cohen W, Cowie H, et al. (2007) Severe receptive language disorder in childhood–familial aspects and long-term outcomes: results from a Scottish study. Arch Dis Child 92: 614–619.
51. Conti-Ramsden G, Botting N (1999) Characteristics of children attending language units in England: a national study of 7-year-olds. Int J Lang Commun Disord 34: 359–366.
52. Conti-Ramsden G, Crutchley A, Botting N (1997) The extent to which psychometric tests differentiate subgroups of children with SLI. J Speech Lang Hear Res 40: 765–777.
53. Francks C, Paracchini S, Smith SD, Richardson AJ, Scerri TS, et al. (2004) A 77-kilobase region of chromosome 6p22.2 is associated with dyslexia in families from the United Kingdom and from the United States. Am J Hum Genet 75: 1046–1058.
54. Scerri TS, Paracchini S, Morris A, MacPhie IL, Talcott J, et al. (2010) Identification of candidate genes for dyslexia susceptibility on chromosome 18. PLoS One 5: e13712.
55. Elliot C, Murray D, Pearson L (1983) British Abilities Scales Windsor, UK: NFER-Nelson.
56. Newnham JP, Evans SF, Michael CA, Stanley FJ, Landau LI (1993) Effects of frequent ultrasound during pregnancy: a randomised controlled trial. Lancet 342: 887–891.
57. Dunn L, Dunn L (1981) Peabody Picture Vocabulary Test-Revised: Manual. Circle Pines, MN: American Guidance Services.
58. Raven JC (1976) Ravens Coloured Progressive Matrices. London: Oxford Psychologists Press.
59. Dumontheil I, Roggeman C, Ziermans T, Peyrard-Janvid M, Matsson H, et al. (2011) Influence of the COMT genotype on working memory and brain activity changes during development. Biol Psychiatry 70: 222–229.
60. Soderqvist S, McNab F, Peyrard-Janvid M, Matsson H, Humphreys K, et al. (2010) The SNAP25 gene is linked to working memory capacity and maturation of the posterior cingulate cortex during childhood. Biol Psychiatry 68: 1120–1125.
61. Whitehouse AJ, Bishop DV, Ang QW, Pennell CE, Fisher SE (2011) CNTNAP2 variants affect early language development in the general population. Genes Brain Behav.
62. Purcell S, Neale B, Todd-Brown K, Thomas L, Ferreira MA, et al. (2007) PLINK: a tool set for whole-genome association and population-based linkage analyses. Am J Hum Genet 81: 559–575.
63. Abecasis GR, Cardon LR, Cookson WO (2000) A general test of association for quantitative traits in nuclear families. Am J Hum Genet 66: 279–292.
64. Hayasaka S, Phan KL, Liberzon I, Worsley KJ, Nichols TE (2004) Nonstationary cluster-size inference with random field and permutation methods. Neuroimage 22: 676–687.

IV

The Journal of Neuroscience

http://jneurosci.msubmit.net

JN-RM-2843-14

Human ROBO1 regulates white matter structure in corpus callosum

Juha Kere, Karolinska Institutet
Fahimeh Darki, Karolinska Institutet
Satu Massinen, University of Helsinki
Elina Salmela, University of Helsinki
Hans Matsson, Karolinska Institutet
Myriam Peyrard-Janvid, Karolinska Institutet
Torkel Klingberg, Karolinska Institute

Commercial Interest: No

ABSTRACT:

The axon guidance receptor, Robo1, controls the pathfinding of callosal axons in mice. In order to determine whether the orthologous *ROBO1* gene is involved in callosal development also in humans, we studied polymorphisms in the *ROBO1* gene and variation in the white matter structure in the corpus callosum using both structural and diffusion tensor magnetic resonance imaging. We found that five polymorphisms in the regulatory region of *ROBO1* were associated with white matter volume in the posterior part of the corpus callosum pathways. One of the polymorphisms, rs7631357, was also significantly associated with the probability of connections to the parietal cortical regions. Our results demonstrate that human *ROBO1* may be involved in the regulation of the structure and connectivity of posterior part of corpus callosum.

Keywords: structural MRI; DTI; single nucleotide polymorphism; SNP; roundabout; axon guidance receptor homolog 1; midline crossing; axonal pathfinding

INTRODUCTION

The corpus callosum (CC), a white matter structure found only in placental mammals, is the largest axon tract in the brain. Within the CC, the axons from callosal projection neurons cross the cortical midline, connect the two cerebral hemispheres and are involved in many higher cognitive functions by transferring information between the hemispheres (Fame et al., 2011).

The extension and pathfinding of the callosal axons is crucial for the establishment of correct circuitry in the brain. These processes are tightly regulated by a variety of receptors and their repulsive or attracting ligands, each with their specific spatiotemporal role. One of the key molecules involved in callosal development in mice is the roundabout homolog 1 (*Robo1*) receptor, binding the chemorepulsive Slit ligands, especially Slit2 (Andrews et al., 2006; López-Bendito et al., 2007; Unni et al., 2012).

Homozygous *Robo1* knock-out mice ($Robo1^{-/-}$) die at birth and display defects in the development of the CC ranging from severe dysgenesis to only minor defects in the pathfinding of callosal axons (Andrews et al., 2006; López-Bendito et al., 2007; Unni et al., 2012). In the $Robo1^{-/-}$ mice, the misrouted callosal axons terminate in the septum without crossing the midline (Andrews et al., 2006; Unni et al., 2012) whereas those that crossed the midline form normal homotopic connections in the contralateral hemisphere (Unni et al., 2012).

Besides the role of *Robo1* in axon guidance, the inhibition of Robo1-mediated signaling has been reported for its role in proliferation and migration of neocortical

interneurons (Andrews et al., 2006; Andrews et al., 2008; Hernández-Miranda et al., 2011). Robo1 has also been found to regulate the proliferation and generation of pyramidal neurons (Yeh et al., 2014) and their migration to layers II/III in the neocortex (Gonda et al., 2013). In mice, there are four homologous genes in the Roundabout receptor family, of which *Robo1*, *Robo2* and *Robo3* are expressed in the central nervous system and also in other tissues, such as the adrenal gland, limbs and eye, respectively, whereas *Robo4* expression is limited mostly to endothelial cells (The FANTOM Consortium, 2014).

The precise role of *ROBO1* in the development of CC is unknown. *ROBO1* has been suggested to play a role in dyslexia (Hannula-Jouppi et al., 2005; Tran et al., 2014) and general language ability (Bates et al., 2011) which require efficient communication between the hemispheres.

Within the normal population, the expression of *ROBO1* is known to vary (Spielman et al., 2007), most probably reflecting genetic variation in the *ROBO1* locus. Numerous studies have reported inter-individual variability in the CC structure (Luders et al., 2010; Paul, 2011; Hasan et al., 2012; Vandermosten et al., 2012; Vandermosten et al., 2013). We hypothesized that if *ROBO1* controls midline crossing of callosal axons in humans, we might see the association of *ROBO1* single nucleotide polymorphisms (SNPs) with CC structure. Moreover, since *ROBO1* has been found to regulate the migration and laminar distribution of pyramidal neurons in mice, we tested the effect of *ROBO1* SNPs on the thickness of cortex.

MATERIALS & METHODS

Participants

Structural magnetic resonance imaging and diffusion weighted imaging were carried out on 76 typically developing children and young adults, aged between 6 to 25 years. The participants were randomly selected from a longitudinal study (three time-points, each two years apart) and they were all from the population registry in Nynäshamn, Sweden (Söderqvist et al., 2010). The study was approved by the local ethics committee of the Karolinska University Hospital, Stockholm, Sweden. Informed consent was provided by the participants or the parents of children aged below 18 years old.

Genotyping and quality control steps

Genotyping was performed on the Affymetrix Genome-wide Human SNP array 6.0, including more than 906600 SNPs and more than 946000 probes for detecting copy number variation. The genotyping was done on one batch with DNA extracted from blood (n = 63) and two batches with DNA extracted from saliva (n = 19 and n = 8) using standard methods and commercial kits.

Two individuals were removed from the blood batch in initial quality control. DNA from these individuals was re-extracted from saliva, and genotyping was re-done using saliva DNA.

The genotypes were called using Birdsuite version 1.5.5 (Korn et al. 2008) separately on each batch. Conversion of the output files to PLINK-compatible format was done using the Birdsuite to PLINK pipeline version 1.6.6.

(https://www.broadinstitute.org/ftp/pub/mpg/birdsuite/Birdsuite_Pipeline.pdf). The reference genome assembly used was hg18.

Quality control was done using PLINK version 1.07. (Purcell et al., 2007) and conducted on two levels: exclusion of individuals and exclusion of SNPs. No individuals were removed due to low genotype call rates. The average genotype call rate of individuals was over 98% in all of the batches. In total 13 individuals were removed from the analysis based on either gender discordance detected using heterozygosity rates of X-chromosomal SNPs (one individual), excessive heterozygosity detected by calculating inbreeding coefficients (three individuals), possible cryptic relatedness estimated by pairwise identity-by-state analysis (two individuals) or known relatedness (seven individuals). Out of the known and suspected sib-pairs, the sibling with a larger proportion of missing genotypes was removed from the analysis.

Before quality control, 909622 SNPs were available for analysis. SNPs with a proportion of missing genotypes > 0.05 or with a missing genotype for more than one individual in any batch were removed from all batches (48451 SNPs in total). In addition, the following SNPs were removed: 137753 SNPs with minor allele frequency (MAF) <0.01, 26 SNPs showing deviation from Hardy-Weinberg equilibrium ($p < 1e^{-05}$), 39 SNPs showing non-random missingness with respect to neighboring genotype and 37 SNPs showing association with batch membership. Overall, 79.5% (723316/909622) of the markers passed all quality control filters.

After filtering, 76 individuals (41 males and 35 females) and 723316 diploid SNPs remained. The average individual call rate was 99.7%, and the lowest individual call rate was 97.4%.

Selection of *ROBO1* SNPs

From the quality-controlled genotype data, we first selected all SNPs from the genomic interval chr3:78,720,000-80,000,000 (hg18); in total 201 SNPs. This area encompasses all of the annotated transcript variants of the *ROBO1* gene (NM_002941.3, NM_133631.3 and NM_001145845.1) as well as roughly 300 kb and 10kb upstream of the longest variant (NM_002941.3).

A subset of these SNPs was chosen for a two-phase association study. For the first phase, we selected tagging SNPs in order to efficiently capture the common genetic variation in the area while keeping the multiple testing burden to a minimum: Haploview (Barrett et al., 2005) was used to construct a haplotype map using the 201 SNPs. Pairwise comparisons of markers > 1000 kb apart were ignored. The resulting 19 haplotype blocks were subjected to Haploview's Tagger algorithm in order to find best tagging SNPs for them, with settings of the minor allele frequency (MAF) > 0.1 and a maximum number of tags to pick of = 20. The selected 20 tagging SNPs (rs3773216, rs9875094, rs3773232, rs1457659, rs416551, rs7629522, rs162870, rs162871, rs162262, rs162429, rs7631406, rs12497294, rs6770483, rs9835692, rs9876238, rs4856291, rs4856447, rs12488868, rs6768880, rs9830013) captured 98 alleles (58% of the 169 alleles with MAF > 0.1) at $r^2 >= 0.8$ and 57% of alleles with mean r^2 of 0.937.

In the second phase, we refined the association analysis by selecting additional SNPs within and between the two haplotype blocks whose tagging SNPs (rs17396958 and rs1393375) had shown association in the first phase. We chose MAF > 10% as cutoff. The SNPs that did not show association in the first phase and the SNPs tagged by them were excluded. Of those SNPs that were in perfect LD with each other, only one SNP was selected. Between rs17396958 and rs1393375 we also dropped out all but one SNP per group from groups of SNPs that were in strong LD with each other ($r^2 > 0.8$). In total there were 28 SNPs used in the second phase: rs6770755, rs7651370, rs7631357, rs4564923, rs6548621, rs9832405, rs7637338, rs6548628, rs9853895, rs9820160, rs7432676, rs9309825, rs13071586, rs13072324, rs6771681, rs7618126, rs7432306, rs6548650, rs7644521, rs1995402, rs17380584, rs11917376, rs11706346, rs1393360, rs1502298, rs10511118, rs1502305, and rs10511119.

Structural Brain Imaging and Voxel-Based Morphometry

We applied three-dimensional magnetization prepared rapid gradient echo (MP-RAGE) sequence with TR = 2300 msec and TE = 2.92 msec to collect structural MRI data with 256 × 256 mm^2 field of view (FOV), 256 × 256 matrix size, 176 sagittal slices, and 1 mm^3 isotropic voxel size. The structural images were then processed using voxel-based morphometry (VBM) method, which segmented the brain into gray matter, white matter and cerebral spinal fluid.

Diffeomorphic Anatomical Registration Through Exponentiated Lie Algebra (DARTEL), as a part of SPM5 software, was performed on structural data collected at all three time-points and white matter was segmented after all images were registered to the template. The modulated white matter segmented images were then smoothed

with an 8 mm Gaussian kernel and fed into a higher-level statistical analysis for detecting any SNPs associations with white matter volume.

Diffusion Tensor Imaging (DTI)

Diffusion tensor imaging, with the scanning parameters of 230 × 230 mm^2 FOV, 128 × 128 matrix size, 40 slices with thickness of 2.5 mm, and b-value of 1000 sec/mm^2 in 64 gradient directions, was collected at the third round of longitudinal data collection (Söderqvist et al., 2010). Eddy current and head motions were corrected with affine registration for all diffusion-weighted images to a reference volume using FSL software (http://fsl.fmrib.ox.ac.uk/fsl/fslwiki/). The diffusion tensor parameters were then estimated for each voxel, and subsequently the DTI and fractional anisotropy (FA) data were constructed. Nonlinear registration was carried out using Tract-Based Spatial Statistics, TBSS v1.2, (http://fsl.fmrib.ox.ac.uk/fsl/fslwiki/TBSS) to align all FA images to the mean FA skeleton.

Probabilistic fiber tracking of CC

To find the CC white matter fibers, the body of CC was selected as seed region and probabilistic tractography was performed on all individuals' DTI data, initiating from all voxels within the seed masks using probtrackx tool of FDT v2.0, FSL (http://fsl.fmrib.ox.ac.uk/fsl/fsl-4.1.9/fdt/fdt_probtrackx.html). The fiber tracking parameters were set as default, 5000 streamline samples, step length of 0.5 mm, and curvature threshold of 0.2. At the individual level, the tracts were thresholded by 5% of the samples to remove the voxels with low probability of connection (Leh et al., 2006). In the next step, all of the traced white matter pathways were aligned using the TBSS method for non-FA images and then binarized and averaged across all subjects.

In order to define a mask of CC fibers, the group probability map of the tracts was finally thresholded at the group level by keeping the pathways that were present in 90% of the cases. This mask was later used as a region of interest for small volume correction in higher level statistical analysis of the white matter volume in association with *ROBO1* SNPs.

Probabilistic fiber tracking for segmenting CC

Five different cortical regions of interest including anterior frontal, superior frontal, parietal, temporal and occipital cortex were selected bilaterally as target regions for probabilistic fiber tracking of CC to segment this large white matter tract to smaller segments. These cortical regions were defined based on the Harvard-Oxford cortical atlas and the body of CC was considered as the seed region for initiating the fiber tracking.

In the next step, the white matter fibers found from all five regions of interest were thresholded by 5% of the maximum values to exclude the tracts with the probability of connections lower than the threshold. After segmenting the CC pathways based on the probabilistic fiber tracking of the CC, the averages of two different indices were computed in these five segmented white matter tracts. The first index was the probability of connection to each cortical region which indicates the structure of white matter pathways (such as number, thickness, size and the myelination of axons). The second one was FA which reflects the organization and packing of the axons as well as myelination.

Cortical thickness measurements

To assess the association of *ROBO1* SNPs with thickness of cortex, the cortical thickness of the structural MRI data was computed using automatic longitudinal stream in FreeSurfer (Reuter et al., 2012). All structural data were first registered to a within-subject template (Reuter et al., 2010; Reuter and Fischl, 2011). After applying several processing steps (Dale et al., 1999; Fischl and Dale, 2000) including skull removing, template transformation and atlas registration, the images were later segmented to white matter, gray matter, and pial, based on intensity and neighborhood voxel restrictions. Thickness of cortex was computed as the distance between the white matter and the pial. The cortical thickness of the cortical regions of interst (including left and right anterior frontal, superior frontal, parietal, temporal and occipital) were then calculated using the workflow described in http://surfer.nmr.mgh.harvard.edu/fswiki/VolumeRoiCortical Thickness.

Statistical Analyses

The white matter segmented images were analyzed by higher-level SPM analysis, using a flexible factorial design (www.fil.ion.ucl.ac.uk/spm/software/spm8), to assess the association of *ROBO1* SNPs with white matter volume. In the first phase of assessment, all 20 SNPs were entered separately as a main factor in the model. Subjects and testing time-points were also considered as factors in the flexible factorial model to take into account the repeated measures. Age, gender, handedness and total white matter volume were used as covariates and the interactions of SNP, as the main factor, with age and gender were also added. Two of the SNPs (rs17396958 and rs1393375) were significantly associated with white matter volume in the posterior part of the corpus callosum. In the second phase, we tagged 28 SNPs within

and between the two haplotype blocks of these two SNPs. Then the exploratory analysis was done within the white matter masked by the group probability map of the CC tracts, with non-stationary cluster extent correction, at FDR-corrected cluster level (p-value of 0.05). We corrected for multiple comparisons (Bonferroni correction) of the number of SNPs (28 SNPs) and accordingly set the threshold of significant p-values at 0.0018.

After fiber tracking and segmenting the CC into five parts, the mean value of two indices (probability of connection and FA) were computed in these five segments. These measures were then analyzed for associations between these brain measures and the SNPs significantly associated with white matter volume within CC in the second phase of the analysis using linear regression in IBM SPSS statistics 21.0 software. For each test, brain meaures were included as dependent variable and age, gender, handedness and genotypes were included as independent variables.

The same linear regression analysis were also performed for the measures of cortical thickness in all five cortical regions of interest using the thickness measures as the dependent variable and similar independent variables as mentioned above.

RESULTS

Five *ROBO1* SNPs associated with white matter volume in the CC

On the initial round designed to test the hypothesis whether common SNPs anywhere within the *ROBO1* gene associated with morphological variation of CC, 20 SNPs in the genomic region of the *ROBO1* gene were chosen for voxel based analysis on

white matter segmented images. Two of the SNPs (rs17396958 and rs1393375) were significantly associated with white matter volume in posterior part of CC ($p = 5.4\times10^{-6}$ and $p = 2.02\times10^{-5}$, respectively, at FDR-corrected cluster level of p-value < 0.05). The associated SNPs are both situated upstream of the *ROBO1* transcription start site, possibly in regulatory regions.

Because the 20 SNPs covered less than 50% of single nucleotide variation in the *ROBO1* locus, we then attempted to refine the genetic association by selecting more SNPs between and within the haplotype blocks that associated with CC structure in the initial round, and then repeated the analysis with the new SNPs. In this phase of the analysis, five of the 28 SNPs (Fig. 1) showed significant effect on white matter volume in the right posterior part of CC, connecting the parietal and occipital cortical regions. All significant clusters overlapped with each other (p-value at the FDR level, correcting for multiple comparison of 28 SNPs, $p < 0.0018$). Table 1 lists the peak coordinates, the cluster size and the p-value of the clusters significantly associated with each of those five SNPs.

The five associated SNPs are situated in the second intron of the longest transcript variant (NM_002941.3) of *ROBO1*, and are therefore pontential sites for the regulation of *ROBO1* expression. The SNPs appear to belong to an extended haplotype block, although Haploview software has further divided it into three smaller blocks (Fig. 2).

The BrainCloud database contains information on the temporal dynamics and genetic control of transcription in human prefrontal cortex (Colantuoni et al.,

2011). In this database, only one SNP (rs331142) in the *ROBO1* gene showed association to ROBO1 expression ($P = 4.6 \times 10^{-5}$) but it did not reach genome-wide statistical significance (Tran et al., 2014). Rs33114 is not found on the Affymetrix Genome-wide Human SNP array 6.0 that was used in the genotyping in our study and is situated roughly 600 kb from the haplotype block containing the five SNPs associated with white matter volume from our study.

Rs7631357 correlates with the probability of connection to parietal areas

Two different indices (probability of connection and FA) computed in the five segmented white matter tracts (shown in Fig. 3A) were analyzed for associations between these measures and the five SNPs significantly associated with white matter volume within CC. After correction for multiple comparisons ($p < 0.002$, Bonferroni correction for 25 tests), the probability of connection of the body of the CC to the parietal areas significantly correlated with one of the SNPs, rs7631357 ($p = 1.09 \times 10^{-5}$). The FA values did not correlate with the genotype variations in any of these regions. The logarithmic graph shows the significant level of the association of each SNP and the probabilities of connections to different regions of interest (Fig. 3B).

In another analysis, we tested the association of the rs7631357 SNP with the probability of connection of callosal pathways within the segment of CC which connected to parietal cortical areas. We found that the probability indices in the posterior part of CC significantly correlated with this SNP genotypes (shown in red, Fig. 4). The significant associated region partially overlaps with the region previously

found for the association of the same SNP with white matter volume (shown in blue, Fig. 4).

In the assessment of the association of *ROBO1* SNPs to cortical regions of interest in both left and right hemispheres, three SNPs (rs6770755, p = 0.015; rs6761657, p = 0.026; rs7651370, p = 0.009) showed significant association with cortical thickness of left parietal region. Although none remained significant after correction for multiple comparisons of 50 tests, the trend speaks in agreement with white matter associations in posterior part of CC with connections to parietal cortex.

DISCUSSION

The association of *ROBO1* SNPs with white matter structure was assessed using two white matter structural measures (white matter volume and probability of connections). We found that five SNPs in the presumed regulatory region of *ROBO1* were associated with white matter volume in the posterior part of the CC.

Robo1 has been implicated in axonal pathfinding in mice: in *Robo1*$^{-/-}$ knockout mice a variable amount of callosal axons were misrouted. In our study the participants are from the normal population of typically developing children and young adults. We had no RNA samples from them for measuring *ROBO1* expression. In this study, we were able to correlate the variations in *ROBO1* SNPs with white matter structure in the CC. SNP rs7631357 significantly correlated with both the white matter volume in the posterior part of CC and the probability of connections from the body of CC to parietal regions. These findings fit well with previous observations of the role of Robo1 in axonal path finding in mice (Andrews et al., 2006), although it should be

mentioned that the white matter indices do not directly explain the biophysical factors such as size, diameter, membranes, myelin thickness or packing of axons.

The posterior part of CC interconnects the temporal, parietal and occipital cortices with large and heavily myelinated axons (Aboitiz et al., 1992). Although morphological and shape analysis studies have reported some inconsistent findings, the posterior CC has been reported larger in dyslexic subjects compared to normal readers in some CC shape analysis studies (Duara et al., 1991; Rumsey et al., 1997; Duta, 2000; Hasan et al., 2012). The microstructure of posterior CC, such as FA, has also been associated with reading skills and has been found higher in dyslexic compared with typically developing readers (Frye et al., 2008).

Previously, SNPs within three dyslexia candidate susceptibility genes (*DYX1C1*, *DCDC2*, and *KIAA0319*) have been shown to be associated with white matter volume in the left temporo-parietal region. Moreover, the white volume was positively correlated with reading ability (Darki et al., 2012). The white matter regions associated with the *ROBO1* SNPs partially overlapped with the white matter area found in association with rs6935076 in *KIAA0319* (Darki et al., 2012).

ROBO1 has previously been shown to functionally affect midline crossing of auditory pathways in humans (Lamminmäki et al., 2012). In a rare Finnish family there was a deficit in interaural interaction that correlated with the expression levels of *ROBO1*. Interaural interaction is dependent on axonal midline crossing present at some stage of the afferent central auditory pathway passing through the brainstem, the midbrain and the thalamus, ending up at the auditory cortex. Our results are the first to suggest

that *ROBO1* may also regulate the midline crossing of callosal axons in humans. In contrast to previous studies of *ROBO1* in a single Finnish family, our results link for the first time the *ROBO1* gene to a specific structural feature of the human brain in the general population.

We also studied whether the *ROBO1* SNPs would be associated with cortical thickness. Three SNPs showed a trend towards association, which fits well with previous observations of *Robo1* controlling neocortical lamination in mice (Gonda et al., 2013). Taken together, our results suggest that similarly to *Robo1* in mice, the human *ROBO1* is likely to have various roles in axonal pathfinding and neuronal migration during brain development.

Interestingly, the *ROBO1* SNPs associating with the structural measures in CC and cortex are localized to the most proximal third of the gene, i.e., the region that harbors several correlated minor transcription start sites for *ROBO1*. These promoters (annotated by the FANTOM5 study as p4, p6, p9, p11 and p27) are associated with *ROBO1* expression especially in the fetal temporal, parietal and occipital lobes (The FANTOM Consortium, 2014). This expression pattern agrees overall with a role of the genomic region harboring the associated SNPs in regulating axon growth during the fetal period and thus structural correlates even after birth.

The sample size used in our study is relatively small and consequently their replication in larger data sets may further refine the observed genetic regulatory effect. Overall, the results demonstrate that variability in the human *ROBO1* locus may contribute to the variability in the structure and connectivity of posterior part of

CC, and is likely to have functional relevance in the transfer of information between the hemispheres.

REFERENCES

Aboitiz F, Scheibel AB, Fisher RS, Zaidel E (1992) Fiber composition of the human corpus callosum. Brain research 598:143-153.

Andrews W, Liapi A, Plachez C, Camurri L, Zhang J, Mori S, Murakami F, Parnavelas JG, Sundaresan V, Richards LJ (2006) Robo1 regulates the development of major axon tracts and interneuron migration in the forebrain. Development 133:2243-2252.

Andrews W, Barber M, Hernadez-Miranda LR, Xian J, Rakic S, Sundaresan V, Rabbitts TH, Pannell R, Rabbitts P, Thompson H (2008) The role of Slit-Robo signaling in the generation, migration and morphological differentiation of cortical interneurons. Developmental biology 313:648-658.

Barrett JC, Fry B, Maller J, Daly MJ (2005) Haploview: analysis and visualization of LD and haplotype maps. Bioinformatics 21:263-265.

Bates TC, Luciano M, Medland SE, Montgomery GW, Wright MJ, Martin NG (2011) Genetic variance in a component of the language acquisition device: ROBO1 polymorphisms associated with phonological buffer deficits. Behavior genetics 41:50-57.

Colantuoni C, Lipska BK, Ye T, Hyde TM, Tao R, Leek JT, Colantuoni EA, Elkahloun AG, Herman MM, Weinberger DR (2011) Temporal dynamics and genetic

control of transcription in the human prefrontal cortex. Nature 478:519-523.

Dale AM, Fischl B, Sereno MI (1999) Cortical surface-based analysis: I. Segmentation and surface reconstruction. Neuroimage 9:179-194.

Darki F, Peyrard-Janvid M, Matsson H, Kere J, Klingberg T (2012) Three Dyslexia Susceptibility Genes, DYX1C1, DCDC2, and KIAA0319, Affect Temporo-Parietal White Matter Structure. Biological psychiatry 72:671-676.

Duara R, Kushch A, Gross-Glenn K, Barker WW, Jallad B, Pascal S, Loewenstein DA, Sheldon J, Rabin M, Levin B (1991) Neuroanatomic differences between dyslexic and normal readers on magnetic resonance imaging scans. Archives of neurology 48:410-416.

Duta N (2000) Corpus callosum shape analysis: a comparative study of group differences associated with dyslexia, gender and handedness.

Fame RM, MacDonald JL, Macklis JD (2011) Development, specification, and diversity of callosal projection neurons. Trends in neurosciences 34:41-50.

Fischl B, Dale AM (2000) Measuring the thickness of the human cerebral cortex from magnetic resonance images. Proceedings of the National Academy of Sciences 97:11050-11055.

Frye RE, Hasan K, Xue L, Strickland D, Malmberg B, Liederman J, Papanicolaou A (2008) Splenium microstructure is related to two dimensions of reading skill. Neuroreport 19:1627.

Gonda Y, Andrews WD, Tabata H, Namba T, Parnavelas JG, Nakajima K, Kohsaka S, Hanashima C, Uchino S (2013) Robo1 regulates the migration and

laminar distribution of upper-layer pyramidal neurons of the cerebral cortex. Cerebral Cortex 23:1495-1508.

Hannula-Jouppi K, Kaminen-Ahola N, Taipale M, Eklund R, Nopola-Hemmi J, Kääriäinen H, Kere J (2005) The axon guidance receptor gene ROBO1 is a candidate gene for developmental dyslexia. PLoS Genetics 1:e50.

Hasan KM, Molfese DL, Walimuni IS, Stuebing KK, Papanicolaou AC, Narayana PA, Fletcher JM (2012) Diffusion tensor quantification and cognitive correlates of the macrostructure and microstructure of the corpus callosum in typically developing and dyslexic children. NMR in Biomedicine 25:1263-1270.

Hernández-Miranda LR, Cariboni A, Faux C, Ruhrberg C, Cho JH, Cloutier J-F, Eickholt BJ, Parnavelas JG, Andrews WD (2011) Robo1 regulates semaphorin signaling to guide the migration of cortical interneurons through the ventral forebrain. The Journal of neuroscience 31:6174-6187.

Lamminmäki S, Massinen S, Nopola-Hemmi J, Kere J, Hari R (2012) Human ROBO1 regulates interaural interaction in auditory pathways. The Journal of neuroscience 32:966-971.

Leh SE, Johansen-Berg H, Ptito A (2006) Unconscious vision: new insights into the neuronal correlate of blindsight using diffusion tractography. Brain 129:1822-1832.

López-Bendito G, Flames N, Ma L, Fouquet C, Di Meglio T, Chedotal A, Tessier-Lavigne M, Marín O (2007) Robo1 and Robo2 cooperate to control the guidance of major axonal tracts in the mammalian forebrain. The Journal of neuroscience 27:3395-3407.

Luders E, Thompson PM, Toga AW (2010) The development of the corpus callosum in the healthy human brain. The Journal of neuroscience 30:10985-10990.

Paul LK (2011) Developmental malformation of the corpus callosum: a review of typical callosal development and examples of developmental disorders with callosal involvement. Journal of neurodevelopmental disorders 3:3-27.

Purcell S, Neale B, Todd-Brown K, Thomas L, Ferreira MA, Bender D, Maller J, Sklar P, De Bakker PI, Daly MJ (2007) PLINK: a tool set for whole-genome association and population-based linkage analyses. The American Journal of Human Genetics 81:559-575.

Reuter M, Fischl B (2011) Avoiding asymmetry-induced bias in longitudinal image processing. Neuroimage 57:19-21.

Reuter M, Rosas HD, Fischl B (2010) Highly accurate inverse consistent registration: a robust approach. Neuroimage 53:1181-1196.

Reuter M, Schmansky NJ, Rosas HD, Fischl B (2012) Within-subject template estimation for unbiased longitudinal image analysis. Neuroimage 61:1402-1418.

Rumsey JM, Nace K, Donohue B, Wise D, Maisog JM, Andreason P (1997) A positron emission tomographic study of impaired word recognition and phonological processing in dyslexic men. Archives of neurology 54:562-573.

Spielman RS, Bastone LA, Burdick JT, Morley M, Ewens WJ, Cheung VG (2007) Common genetic variants account for differences in gene expression among ethnic groups. Nature genetics 39:226-231.

Söderqvist S, McNab F, Peyrard-Janvid M, Matsson H, Humphreys K, Kere J, Klingberg T (2010) The SNAP25 Gene Is Linked to Working Memory Capacity and Maturation of the Posterior Cingulate Cortex During Childhood. Biological psychiatry 68:1120-1125.

Tran C, Wigg KG, Zhang K, Cate‐Carter TD, Kerr E, Field LL, Kaplan BJ, Lovett MW, Barr CL (2014) Association of the ROBO1 gene with reading disabilities in a family‐based analysis. Genes, Brain and Behavior 13:430-438.

Unni DK, Piper M, Moldrich RX, Gobius I, Liu S, Fothergill T, Donahoo A-LS, Baisden JM, Cooper HM, Richards LJ (2012) Multiple Slits regulate the development of midline glial populations and the corpus callosum. Developmental biology 365:36-49.

Vandermosten M, Boets B, Wouters J, Ghesquière P (2012) A qualitative and quantitative review of diffusion tensor imaging studies in reading and dyslexia. Neuroscience & Biobehavioral Reviews 36:1532-1552.

Vandermosten M, Poelmans H, Sunaert S, Ghesquière P, Wouters J (2013) White matter lateralization and interhemispheric coherence to auditory modulations in normal reading and dyslexic adults. Neuropsychologia 51:2087-2099.

Yeh ML, Gonda Y, Mommersteeg MT, Barber M, Ypsilanti AR, Hanashima C, Parnavelas JG, Andrews WD (2014) Robo1 Modulates Proliferation and Neurogenesis in the Developing Neocortex. The Journal of neuroscience 34:5717-5731.

Figure 1: Five SNPs showed significant effect on white matter volume in the right posterior part of the CC.

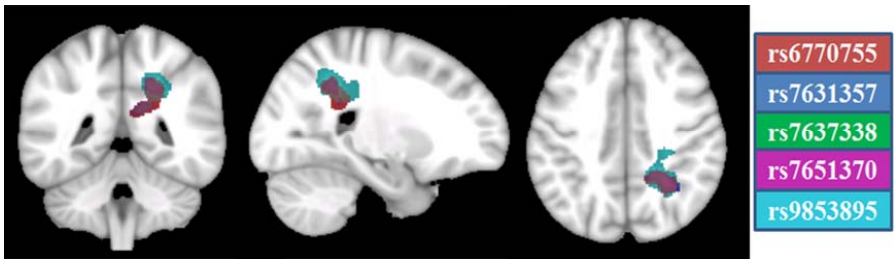

Figure 2: Genomic extend of *ROBO1* on the minus strand of chromosome 3 (top) and magnified most 5' one-third of the gene (bottom), focus of the second round of genotyping. The SNPs found in the quality controlled genotype data set are marked in black. The tagging SNPs selected in round one are marked in red, and the round 2 SNPs are marked in green. The SNPs that were associated with white matter volume in the CC are marked with an asterisk. The 19 haplotype blocks are displayed as black triangles and the LD plot constructed using Haploview, as well as the three ROBO1 transcript variants (NM_002941.3, NM_133631.3 and NM_001145845.1) extracted from UCSC genomic browser. Genomic coordinates are marked according to GRCh37/hg19.

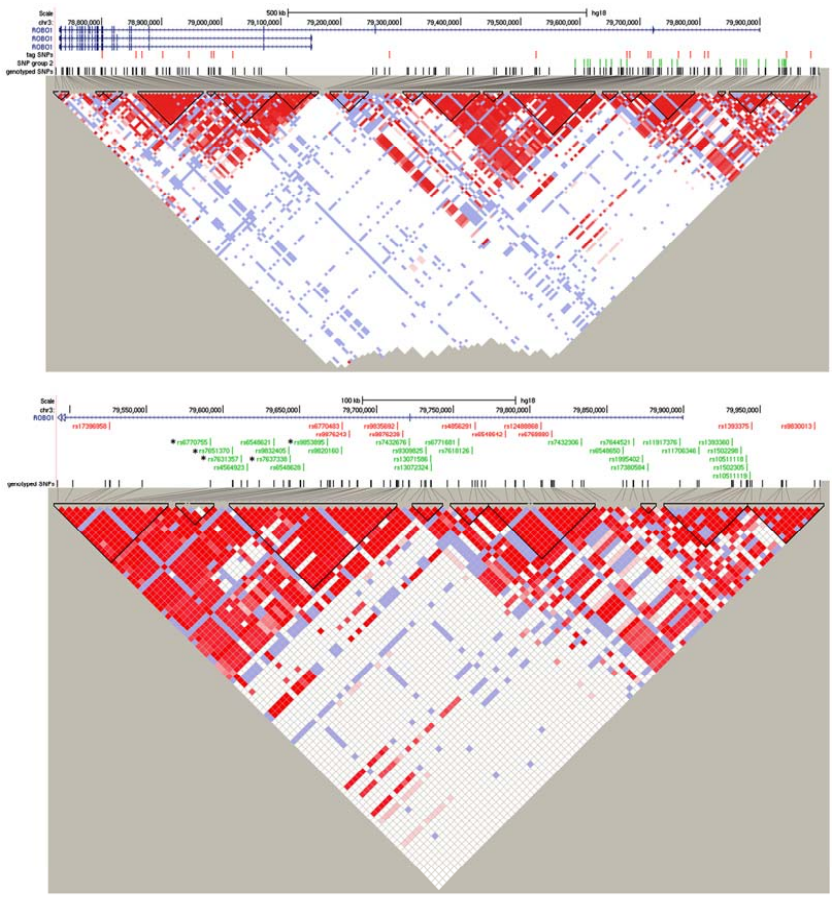

Figure 3: (A) Five different segments of CC segmented by the probabilistic fiber tracking of the body of CC with connections to the anterior frontal, superior frontal, parietal, temporal and occipital cortex, bilaterally. (B) Logarithmic scale of the p-values for the associations between five significant SNPs and the probability of connection in five different segments of the CC (shown by different colors in a sagittal section of the brain).

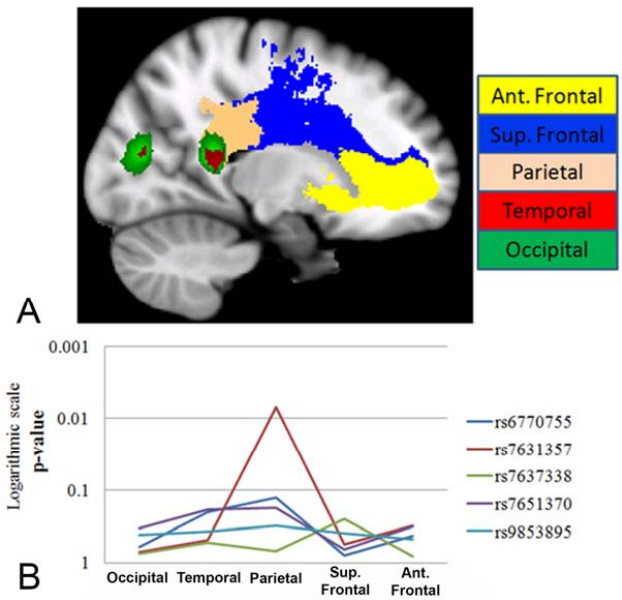

Figure 4: The SNP rs7631357 significantly associated with white matter volume (the cluster is shown in blue) and with probability indices as shown in red. Both regions overlapped in the right posterior part of the CC.

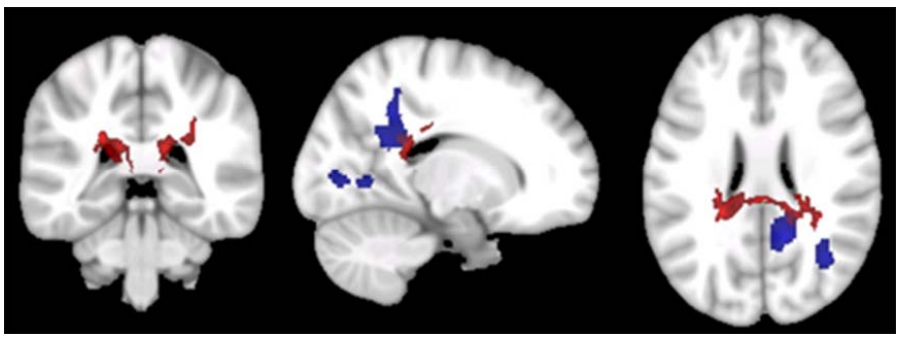

Table 1: Coordinates of the peak voxels for each cluster associated with each SNP.

SNP	$P_{FDR\text{-}corrected}$ Cluster-level	Cluster size	Peak Voxel	
			Z	x, y, z (MNI)
rs6770755	5.49×10^{-5}	1701	6.43	37, -66, 30
rs7631357	1.40×10^{-3}	130	5.13	41, -65, 30
rs7637338	3.89×10^{-4}	78	4.58	42, -65, 25
rs7651370	6.40×10^{-5}	1326	6.03	37, -66, 30
rs9853895	4.89×10^{-5}	2182	5.79	29, -52, 38

V

Cerebral Cortex Advance Access published January 9, 2014

Cerebral Cortex
doi:10.1093/cercor/bht352

The Role of Fronto-Parietal and Fronto-Striatal Networks in the Development of Working Memory: A Longitudinal Study

Fahimeh Darki and Torkel Klingberg

Department of Neuroscience, Karolinska Institutet, Stockholm, Sweden

Address correspondence to Torkel Klingberg, Department of Neuroscience, Karolinska Institutet, Developmental Cognitive Neuroscience Lab, Retzius Väg 8, Room A3-312, 17 177 Stockholm, Sweden. Email: torkel.klingberg@ki.se

The increase in working memory (WM) capacity is an important part of cognitive development during childhood and adolescence. Cross-sectional analyses have associated this development with higher activity, thinner cortex, and white matter maturation in fronto-parietal networks. However, there is still a lack of longitudinal data showing the dynamics of this development and the role of subcortical structures. We included 89 individuals, aged 6–25 years, who were scanned 1–3 times at 2-year intervals. Functional magnetic resonance imaging (fMRI) was used to identify activated areas in superior frontal, intraparietal cortices, and caudate nucleus during performance on a visuo-spatial WM task. Probabilistic tractography determined the anatomical pathways between these regions. In the cross-sectional analysis, WM capacity correlated with activity in frontal and parietal regions, cortical thickness in parietal cortex, and white matter structure [both fractional anisotropy (FA) and white matter volume] of fronto-parietal and fronto-striatal tracts. However, in the longitudinal analysis, FA in white matter tracts and activity in caudate predicted future WM capacity. The results show a dynamic of neural networks underlying WM development in which cortical activity and structure relate to current capacity, while white matter tracts and caudate activity predict future WM capacity.

Keywords: caudate nucleus, cortical thickness, development, DTI, fMRI, working memory

Introduction

Working memory (WM) capacity increases during childhood and adolescence, which is important for academic performance and cognition (Gathercole et al. 2003; Dumontheil and Klingberg 2012). Impaired WM capacity is associated with several developmental neuropsychiatric and learning disorders, including attention-deficit/hyperactivity disorder (ADHD; Nigg 2001; Westerberg et al. 2004; Martinussen et al. 2005) and dyscalculia (McLean and Hitch 1999; Camos 2008; Szucs et al. 2013). It is therefore important to characterize the neural basis of this development.

WM capacity in children and adolescents is positively correlated with brain activity, most consistently localized to the intraparietal cortex, superior frontal sulcus, and dorsolateral prefrontal cortex (Klingberg et al. 2002; Kwon et al. 2002; Crone et al. 2006; Scherf et al. 2006; Olesen et al. 2007). Measures of cortical thinning in the frontal and parietal cortex are also correlated with WM capacity (Tamnes et al. 2010; Østby et al. 2011; Tamnes et al. 2013) and also with reasoning ability, which is an ability highly correlated with WM (Sowell et al. 2004; Shaw et al. 2006; Tamnes et al. 2011; Wendelken et al. 2011). Furthermore, white matter maturation of the pathways between the parietal and frontal cortex, including the superior longitudinal fasciculus, correlate with WM capacity during childhood and adolescence (Olesen, Nagy, et al. 2003; Nagy et al. 2004; Østby et al. 2011; Vestergaard et al. 2011).

These studies thus suggest that improvements in WM capacity are associated with a gradual maturation of white and gray matter in a fronto-parietal network. It is not clear, however, how these changes are related to each other, and if certain changes cause the later changes in WM performance. The role of the striatum for development is also unclear. The caudate nucleus is activated during performance of WM tasks in nonhuman primates (Levy et al. 1997), children (Klingberg et al. 2002; Ziermans et al. 2012), and adults (Postle et al. 2000), but its role in development is unclear.

One reason why the dynamics of WM development has not been clarified is that most of these studies have been cross-sectional, correlating the current cognitive ability with current structure or activity. An exception here is the study by Ullman et al. (2014), who used a longitudinal design and a multivariate analysis to show that there were differences between multivariate models correlating with current cognitive capacity and the models predicting the change of capacity over the next 2 years. Since this study was multivariate, it was not designed to specify the role of anatomically defined regions or networks.

In the current study, we first identified the regions of interest (ROIs) based on the main effect of WM during development (Dumontheil et al. 2011; Ziermans et al. 2012) for a group of 89 individuals, aged 6–25 years, who were scanned 1–3 times at 2-year intervals. Using diffusion tensor imaging (DTI), we then traced the white matter tracts connecting these regions. Measures of blood-oxygen-level dependent (BOLD) contrast and cortical thickness were extracted from functionally defined ROIs. White matter volume and fractional anisotropy (FA) were also measured along the fronto-parietal and front-striatal white matter pathways. The brain measures together with visuo-spatial WM capacity were assessed for 3 time points with 2-year intervals and used to characterize the relationship between brain and WM during development.

Methods

Participants

Eighty-nine typically developing children and young adults (6–25 years old) were selected randomly from participants in a larger, behavioral longitudinal study (Söderqvist et al. 2010). The subjects in the larger longitudinal study were randomly selected from the population registry in Nynäshamn. The data collection was conducted 3 times, each 2 years apart. The study was approved by the local ethics committee of the Karolinska University Hospital, Stockholm, Sweden. Informed consent was provided by the participants or the parents of children aged below 18 years old. Figure 1 shows the distribution of the included participants in all the behavioral and imaging assessments.

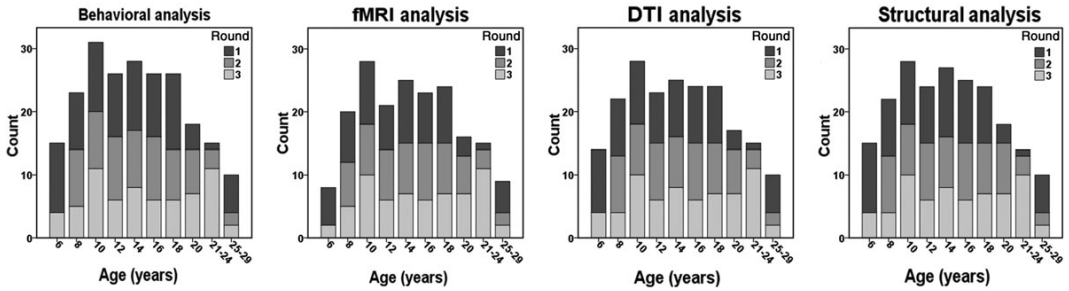

Figure 1. Distribution of the data for the different analyses across rounds 1, 2, and 3 of data collection, based on different age groups.

Assessment of Visuo-Spatial Working Memory

Visuo-spatial WM was assessed individually using a computerized Dot Matrix task from the Automated Working Memory Assessment (AWMA) battery (Alloway 2007). A number of dots in a four-by-four grid were displayed sequentially for 1000 ms, with a 500-ms interval. The task was to remember the location and the order of the dots. After few practice trials, the test started from the first level including one dot with 6 trials. By giving 4 correct responses, it continued to the next level where one more dot was added to the test. Three incorrect answers were the criteria for terminating the test on one level. The total number of correct trials was computed as a visuo-spatial WM score.

Brain Imaging and Analysis

Multimodal brain imaging and analyses were applied longitudinally to find the relationship between brain structure and function in WM-related networks. First, the functional magnetic resonance imaging (fMRI) ROIs were identified based on the main effect of WM during development. Then, the white matter pathways connecting these ROIs were traced using DTI data. Mean white matter volume and FA were computed along the white matter pathways. The BOLD contrast and cortical thickness were also extracted from functionally defined ROIs. Figure 2 illustrates the pipeline used for the multimodal image analyses, transformations between different modalities and the extraction of measures of interest.

Functional Brain Imaging and Processing

T_2*-weighted functional images were acquired on a 1.5-T Siemens scanner (Siemens, Erlangen, Germany) with a gradient-echo-planar imaging (EPI) sequence: time repetition (TR) = 3000 ms, time echo (TE) = 50 ms, field of view (FOV) of 220×220 mm^2, 64×64 matrix size, and 4.5 mm slice thickness. The same imaging sequence was applied for the second and third rounds of the study data collection, respectively, 2 and 4 years later. Participants performed 10 min of visuo-spatial WM task (Dumontheil et al. 2011) in the scanner. Dots were presented sequentially in a four-by-four grid, and the task was to remember the order and the position of a dot.

Preprocessing, first- and second-level analyses of the fMRI data were performed with SPM5 (www.fil.ion.ucl.ac.uk/spm/software/spm5) (Dumontheil et al. 2011; Ziermans et al. 2012). Functional images were first preprocessed by slice timing and motion correction. Then, the images were aligned and normalized to the Montreal Neurological Institute template and finally were high-pass (140 s) filtered and smoothed with a 12-mm Gaussian kernel.

Second-level analysis was performed using SPM5 for the group analysis of the WM contrast images using the flexible factorial design by considering subject and round of the scans as factors. After correcting for the effect of age and sex, the main WM contrast was performed at a false discovery rate (FDR) threshold of $P < 0.05$, to identify regions that were recruited during task performance. The activation map of main WM contrast, thresholded at FDR < 0.000001, was then split into smaller ROIs, so that each region was centered around a single local maximum. ROIs were defined so that individual regions did not overlap, and together covered the majority of the WM activation.

To implement the ROI-based functional and structural analyses on the fronto-parietal and fronto-striatal networks, 3 different functional ROIs, including the superior frontal, intraparietal (superior and inferior), and also the caudate nucleus were selected. Mean of the parameters estimated in the first-level analysis was computed for these significant clusters using MarsBar (Brett et al. 2002). The computed mean contrast values were then analyzed using a mixed linear model in an IBM SPSS statistics 21.0 software for the correlation and prediction assessments.

DTI and Probabilistic Fiber Tracking

DTI, with the scanning parameters of: FOV = 230×230 mm^2, matrix size = 128×128, 40 slices, 2.5 mm of slice thickness, and *b*-value of 1000 s/mm^2 in 64 gradient directions, was carried out at the third round of data collection of the longitudinal study. This was an additional sequence which was added to increase the resolution of the DT images and consequently to improve the tractography results. For the longitudinal assessment of white matter pathways, we used another sequence for which the data were available for all 3 rounds of data collection. This dataset was collected with a FOV of 230×230 mm^2, matrix size of 128×128, 19 slices with 6.5 mm thickness, and *b*-value of 1000 s/mm^2 in 20 gradient directions.

Eddy current and head motions were corrected with affine registration for all diffusion-weighted images to a reference volume using an FSL software (http://fsl.fmrib.ox.ac.uk/fsl/fslwiki/). The diffusion tensor parameters were then estimated for each voxel, and subsequently the DTI and FA data were constructed. Nonlinear registration was carried out using Tract-Based Spatial Statistics, TBSS v1.2, (http://fsl.fmrib.ox.ac.uk/fsl/fslwiki/TBSS) to align all FA images to the mean FA skeleton. To find the white matter pathways within the fronto-parietal and fronto-striatal networks, the functional ROIs (superior frontal, intraparietal, and caudate) were registered first to the mean FA image. In the next step, the back projection of the TBSS method was used to transform back the functional ROIs (Fig. 2*A*) to the DTI space of all individuals.

Probabilistic tractography was performed on all individuals' high-resolution DTI data (collected at the third round), initiating from all voxels within the seed masks using the probtrackx tool of FDT v2.0, FSL (http://fsl.fmrib.ox.ac.uk/fsl/fsl-4.1.9/fdt/fdt_probtrackx.html). For the fronto-striatal pathways, it began separately from the left and right caudate functionally defined regions by considering superior frontal as inclusion masks; whereas for fronto-parietal connections, the tractography initiated from the superior frontal and the inclusion masks were the intraparietal regions. The default parameters (5000 streamline samples, step length of 0.5 mm, and curvature threshold of 0.2) were used for the probabilistic fiber tracking. At the individual level, the tracts were thresholded by 5% of the samples to remove the voxels with low probability of connection (Leh et al. 2006). In the next step, all the traced white matter pathways were aligned using the TBSS

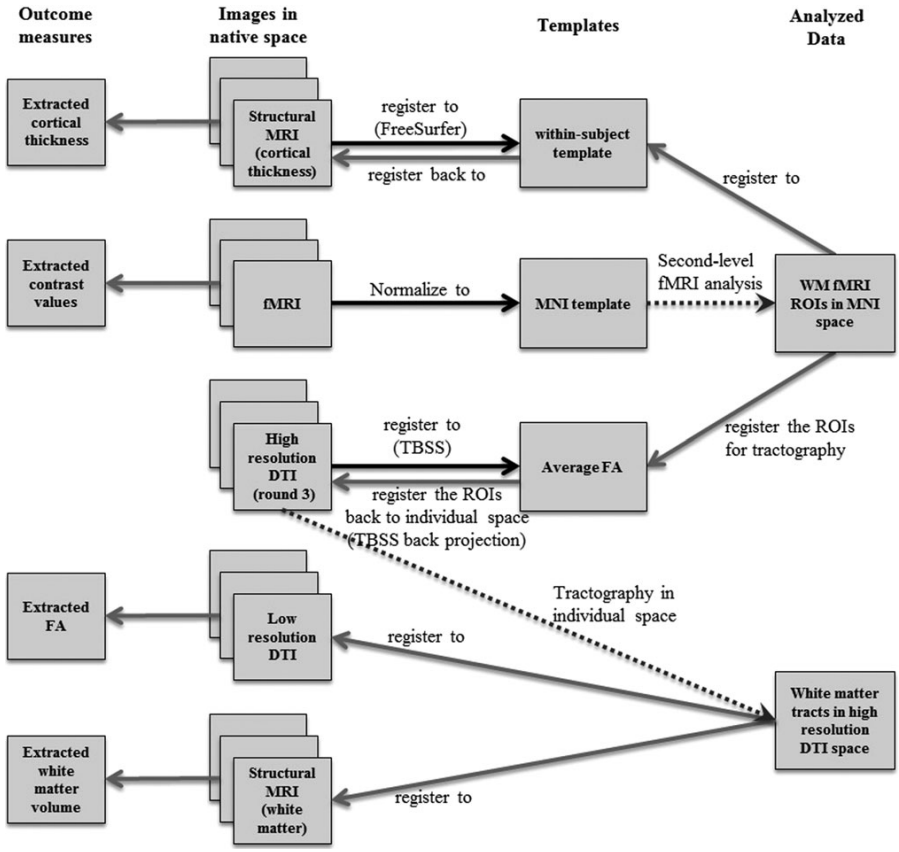

Figure 2. Image analysis and registration pipeline showing the registration between the native space and the template within each modality as well as the transformations between different modalities. Black and gray arrows show the registration and back projection transformations, respectively. The dotted arrows show the steps for fMRI second-level analysis as well as DTI tractography.

method for non-FA images and then binarized and averaged across all subjects. For visualization, the tractography results were finally thresholded at the group level by keeping the pathways that were present in 90% of the cases. The group-averaged maps of both the fronto-parietal and fronto-striatal networks are shown in Figure 2*B*, *C*.

To find the white matter pathways in each individual space, the white matter pathways traced by probabilistic tracking on high-resolution data were registered to the low-resolution longitudinal FA images. We then thresholded the tracts by 5% of the maximum number of samples and subsequently measured the mean FA values within this individual space, for all 3 rounds.

Structural Brain Imaging

T_1-weighted spin echo scans were collected using a 3-dimensional magnetization-prepared rapid gradient-echo sequence with TR = 2300 ms, TE = 2.92 ms, FOV of 256 × 256 mm^2, 256 × 256 matrix size, 176 sagittal slices, and 1 mm^3 isotropic voxel size. To speed up the acquisition, the GRAPPA parallel imaging (acceleration factor of 2) was also performed. The structural images were then processed with 2 different methods. The first technique was voxel-based morphometry (VBM), which segmented the brain into gray matter, white matter, and cerebral spinal fluid. The volume of white matter in the pathways of interest (the fronto-striatal and fronto-parietal) was computed using the white matter segmented images. The second technique was cortical thickness measurement using the freesurfer software (https://surfer.nmr.mgh.harvard.edu). This method was used for measuring the cortical thickness of the gray matter in the mentioned cortical ROIs.

Structural Brain Analysis: Voxel-Based Morphometry

VBM was performed on structural data collected across all 3 rounds of data collection using the SPM5, Diffeomorphic Anatomical Registration Through Exponentiated (DARTEL) toolbox. The modulated white matter segmented images were then smoothed with an 8-mm Gaussian kernel. The traced fronto-parietal and fronto-striatal tracts were first thresholded by 5% of their maximum value and then registered to the segmented white matter images, individually for all 3 time points. The averaged white matter volume in these 2 pathways was then computed to be used in the subsequent statistical analyses.

Structural Brain Analysis: Cortical Thickness Measurement

Cortical thickness of the structural dataset was estimated using automatic longitudinal stream in FreeSurfer (Reuter et al. 2012). This tool measures the thickness of the cortex by constructing models for the boundary between gray and white matter. First, a within-subject template was created for each subject using inverse consistent registration

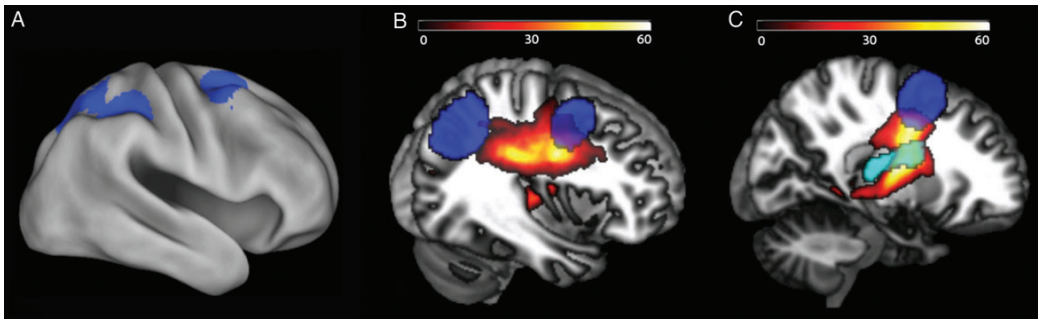

Figure 3. (*A*) Functionally active cortical regions (superior frontal, superior, and inferior parietal) during the performance on a visuo-spatial WM task. (*B*) Population map of the probabilistic fiber tracking of fronto-parietal pathways connecting superior frontal to intraparietal cortex. (*C*) Population map of fronto-striatal pathways, connecting caudate (shown by light blue) to the superior frontal ROI. The color bars correspond to the number of subjects with available white mater pathways.

(Reuter et al. 2010; Reuter and Fischl 2011). Then, several processing steps (Dale et al. 1999; Fischl and Dale 2000) including skull removing, template transformation, and atlas registration were performed. Images were later segmented to white matter, gray matter, and pial, based on intensity and neighborhood voxel restrictions. The distance between the white and the pial was computed as the thickness at each location of the cortex. The cortical thickness of the 2 particular cortical regions (superior frontal and intraparietal ROIs) was then calculated using the workflow described in http://surfer.nmr.mgh.harvard.edu/fswiki/VolumeRoiCortical Thickness.

ROI-Based Statistical Analyses

As the main aim of this research, the functional and structural ROI-based measures in the fronto-striatal and fronto-parietal networks were assessed for concurrent- and prediction-based correlations between brain–brain and brain–WM measures. The mean values of the WM functional contrast and cortical thickness were extracted from functionally active cortical regions during visuo-spatial WM task performance inside the scanner. Since the structural and functional measures in analogous areas were highly correlated (all $r > 0.84$), we averaged them in both the left and right hemispheres. The white matter volume and FA were also computed from the white matter pathways traced by probabilistic fiber tracking of fronto-parietal and fronto-striatal tracts. Visuo-spatial WM was the only behavioral measure in this study.

Cross-Sectional Analysis

To assess the concurrent correlations between brain and behavior measures, the ROI-based mean scores were analyzed using a mixed linear model in the IBM SPSS statistics 21.0 software with a restricted maximum likelihood (REML) method, considering 3 repeated measures and the "unstructured" type for repeated covariance. For brain–WM cross-sectional analysis, WM scores and brain measures were set as dependent variables and covariates of interest, respectively. Sex was also considered as a covariate. We did not control for the effect of age in the first set of analyses to keep the variations relating to the effects of age and related brain maturation. Later, in a separate analysis, we controlled for age to find the age-independent relationships.

Longitudinal Analysis

For the prediction analyses, the correlations between current to future measures were tested by the same model, mixed linear model; however the "compound symmetry" type was selected for the repeated covariance which assumes that the variance is constant across occasions (Fitzmaurice et al. 2012). In this case, we considered 2 repeated measures. For the first measures, the round 1 and 2 values were observed as current to future, respectively. And for the second measures, the round 2 and 3 were considered current to future values. Then, in a separate analysis, the model was corrected for the effect of sex as well as age at the current time point. The interaction with age was also assessed in the prediction analyses.

Results

The superior frontal and intraparietal cortical regions (Fig. 3*A*), as well as the caudate nucleus (shown with light blue in Fig. 3*C*), which were previously found active during performance on a visuo-spatial WM task (Dumontheil et al. 2011), were selected as seed ROI for fiber tracking of the fronto-parietal and fronto-striatal pathways. The averaged group map of the fronto-parietal tract is displayed sagittally in Figure 3*B* for the right hemisphere. The population map of the white matter pathways traced by probabilistic tractography of the voxels within caudate nucleus with the inclusion of superior frontal ROI is also shown in Figure 3*C*.

Cross-Sectional Analysis

The concurrent correlations between brain–WM and brain–brain measures were tested by the mixed linear model, including 3 repeated measures. The model was first tested without age correction. Then, in the further analysis, we corrected for the effect of age to see which of the concurrent relationships were age-independent.

Brain–WM Cross-Sectional Correlations

The estimated parameters, *F*, degrees of freedom (df), and *P*-values for the concurrent brain–WM relationships, are listed in Table 1 and are illustrated in Figure 4. BOLD contrast in both frontal and parietal areas correlated with current WM capacity ($P < 4.2 \times 10^{-4}$), whereas the correlation between the contrast values and the WM score was not significant for caudate nucleus. The volume of white matter and FA values in both fronto-parietal and fronto-striatal tracts correlated with the current WM score ($P < 1.7 \times 10^{-5}$ and $P < 7.4 \times 10^{-4}$, respectively). The cortical thickness of the functional ROIs in the parietal region negatively correlated with the current WM capacity ($P = 2.7 \times 10^{-3}$), whereas the thickness in superior frontal and the volume of the caudate nucleus did not correlate with the WM score. All the significant correlations survived the multiple comparisons correction for 10 tested correlations as listed in Table 1.

Out of the relationships that survived the multiple comparison corrections, FA values of the both fronto-parietal and fronto-striatal pathways ($P < 0.013$) as well as BOLD in cortical ROIs ($P < 0.027$) and the cortical thickness in superior frontal ($P = 0.020$) remained significant after the linear effect of age was removed. This shows that the correlations between these brain measures and WM capacity were not only related to brain maturation, but also to age-independent interindividual variations. We also tested removing the quadratic effect of age. The associations that survived this correction were the same as those marked by ** in Table 1.

Table 1
Correlation of brain measures with concurrent WM performance (cross-sectional analysis)

Imaging measures	Regions	Estimated parameters	*F* (df)	*P*-value
BOLD contrast values	Superior frontal*	3.55	13.02 (146.34)	**4.22×10^{-4}**
	Parietal**	3.25	30.16 (134.72)	**$< 10^{-6}$**
	Caudate	2.55	2.91 (142.46)	0.09
Cortical thickness volume	Superior frontal*	5.36	2.65 (150.83)	0.11
	Parietal	−9.20	9.28 (108.89)	**2.66×10^{-3}**
White matter volume	Caudate	0.01	0.03 (113.85)	0.863
	Fronto-parietal	41.56	21.35 (68.99)	**1.70×10^{-5}**
	Fronto-striatal	46.51	24.14 (69.28)	**6.00×10^{-6}**
Fractional anisotropy	Fronto-parietal*	79.91	11.98 (120.93)	**7.41×10^{-4}**
	Fronto-striatal*	92.49	13.27 (119.68)	**4.00×10^{-4}**

P-values in bold indicate the significant relationships after correction for multiple comparisons of 10 tests ($P < 0.005$).
*, **Significant after the effect of age was removed.
*$P < 0.05$, not corrected for multiple comparisons.
**$P < 0.05$, corrected for multiple comparisons.

Brain–Brain Cross-Sectional Correlations

The estimated parameters, *F*, (df), and *P*-values, for the correlations between the concurrent brain–brain measures are listed in Table 2. Regarding the fronto-parietal network, cortical thickness of the parietal ROIs correlated with BOLD contrast values in the corresponding regions ($P = 4.6 \times 10^{-4}$, significant after multiple comparisons of 18 tests as listed in Table 2), though this relationship was not significant for the superior frontal ROI. In the assessment of the relationship between fMRI activity and white matter structure, the correlation between the volume of fronto-parietal pathways and contrast values in parietal area was significant, $P = 1.4 \times 10^{-3}$ (significant after multiple comparisons). Furthermore, the volume of caudate correlated significantly with both white matter volume and FA of the fronto-striatal pathway ($P = 0.039$ and 0.003, respectively).

In separate analyses, we corrected for the linear effect of age in order to assess which of the brain–brain relationships were due to age. The significant correlations between white matter volume and BOLD contrast as well as the cortical thickness remained significant for both networks, after removing the effect of age. We also tested removing the quadratic effect of age. The associations that survived this correction were the same as those marked by ** in Table 2. Relationships between FA and cortical measures were only significant for cortical thickness. BOLD to cortical thickness correlations were not significant after the effect of age was removed, which indicated an influence of age.

Longitudinal Analysis of Working Memory Capacity

Table 3 lists the estimated parameters of the correlations between current brain measures to future WM scores, including no covariates. We found that future WM capacity could be

Table 2
Concurrent correlations of brain–brain measures in fronto-parietal and fronto-striatal networks (cross-sectional analysis)

		BOLD contrast values					
		Superior frontal			Parietal		
		Estimated parameters	*F* (df)	*P*-value	Estimated parameters	*F* (df)	*P*-value
Cortical thickness	Superior frontal	−0.26	1.32 (143.16)	0.25	—	—	—
	Parietal	—	—	—	−0.98	12.99 (113.03)	**4.65×10^{-4}**
		White matter volume					
		Fronto-parietal			Fronto-striatal		
		Estimated parameters	*F* (df)	*P*-value	Estimated parameters	*F* (df)	*P*-value
BOLD contrast values	Superior frontal*	0.01	3.12 (33.68)	0.09	0.02	3.47 (34.24)	0.07
	Parietal*	0.01	11.88 (35.52)	**1.47×10^{-3}**	—	—	—
	Caudate*	—	—	—	0.01	3.22 (38.51)	0.08
Cortical thickness volume	Superior frontal*	0.04	5.99 (43.02)	**0.02**	0.04	6.16 (42.86)	**0.02**
	Parietal*	−0.01	0.18 (43.46)	0.65	—	—	—
	Caudate**	—	—	—	0.01	4.37 (91.87)	**0.04**
		Fractional anisotropy					
		Fronto-parietal			Fronto-striatal		
		Estimated parameters	*F* (df)	*P*-value	Estimated parameters	*F* (df)	*P*-value
BOLD contrast values	Superior frontal	0.01	2.78 (93.62)	0.09	0.02	4.38 (65.48)	0.04
	Parietal	0.02	0.54 (84.55)	0.46	—	—	—
	Caudate*	—	—	—	0.01	4.55 (58.20)	**0.04**
Cortical thickness volume	Superior frontal*	0.03	7.51 (98.25)	**7.31×10^{-3}**	0.02	3.66 (148.53)	0.06
	Parietal	0.02	2.14 (100.07)	0.146	—	—	—
	Caudate*	—	—	—	0.01	9.23 (62.23)	**3.48×10^{-3}**

P-values in bold indicate the significant relationships after correction for multiple comparisons of 18 tests ($P < 0.0027$).
*, **Significant after the effect of age was removed.
*$P < 0.05$, not corrected for multiple comparisons.
**$P < 0.05$, corrected for multiple comparisons.

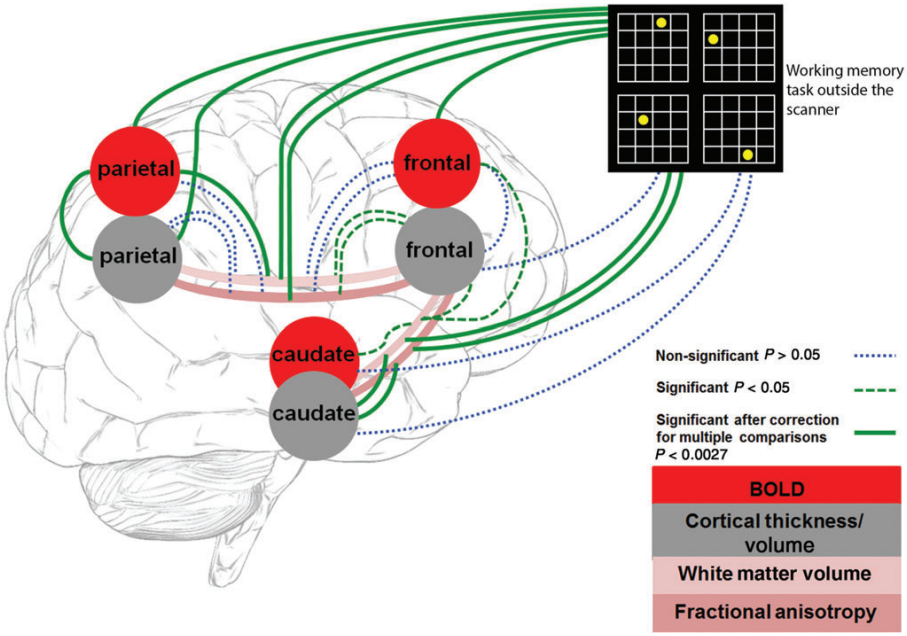

Figure 4. Cross-sectional analysis of correlations between brain–brain and brain–WM. The correlations include all 3 rounds of repeated measures for all variables. The dashed green and dotted blue lines show the significant and nonsignificant correlations, respectively, based on Tables 1 and 2. The thick green lines are those that survived the multiple comparisons correction.

Table 3
Prediction of future WM capacity based on measures collected 2 years earlier

Imaging measures	Regions	Estimated parameters	*F* (df)	*P*-value
BOLD contrast values	Superior frontal	2.33	2.68 (73.89)	0.11
	Parietal	1.67	2.98 (78.43)	0.09
	Caudate	6.30	7.58(73.43)	**7.4×10^{-3}**
Cortical thickness	Superior frontal	6.23	2.67 (93.51)	0.11
	Parietal	−2.72	0.39 (104.93)	0.53
	Caudate	0.01	1.84 (81.13)	0.18
White matter volume	Fronto-parietal	27.26	7.24 (48.07)	**0.010**
	Fronto-striatal	30.69	8.44 (47.73)	**5.55×10^{-3}**
Fractional anisotropy	Fronto-parietal **	105.57	17.96 (71.33)	**6.60×10^{-5}**
	Fronto-striatal**	156.96	26.96 (72.52)	**2.00×10^{-6}**

The *P*-values in bold correspond to the tests that survived correction for multiple comparisons.
**Significant after the effect of age was removed ($P < 0.05$, corrected for multiple comparisons).

predicted by white matter structural measures in both fronto-parietal and fronto-striatal pathways (for white matter volume: $P < 0.01$ and for FA: $P < 6.6 \times 10^{-5}$). Moreover, BOLD contrast in the caudate significantly predicted future WM performance ($P = 7.4 \times 10^{-3}$).

In a separate analysis, we corrected for sex and age at baseline. The FA values of both fronto-parietal and fronto-striatal pathways still significantly predicted future WM performance, $P < 6.8 \times 10^{-3}$ (significant after correction for multiple comparisons). However, white matter volume and caudate BOLD activity were not significant after controlling for age. This is consistent with the concurrent correlations after correcting for age, in which we found that only white matter FA values were age-independently correlated with WM.

We also analyzed the interaction with age in the prediction analyses. The only brain measure that showed significant interaction with age was the activity in caudate nucleus ($P = 1.8 \times 10^{-4}$). Then, we divided the subjects into 2 groups based on their age (below and above 16 years old) to test the predictive ability of caudate activity in these 2 subsets. The BOLD contrast values in caudate significantly predicted future WM capacity for younger subjects ($P = 9.0 \times 10^{-4}$) but not for older individuals ($P = 0.24$), after controlling for age and sex.

Discussion

In the present study, we investigated the relationship between brain structure and function in an anatomically predefined network related to WM performance, using both cross-sectional and longitudinal designs.

In the cross-sectional analysis, WM capacity correlated with BOLD contrast in both frontal and parietal regions, cortical thickness in the parietal cortex, and white matter structure (both FA and volume) of fronto-parietal and fronto-striatal tracts. These findings are consistent with previous developmental studies of BOLD activity (Klingberg et al. 2002; Kwon et al. 2002; Olesen, Nagy, et al. 2003; Crone et al. 2006; Klingberg 2006; Scherf et al. 2006). Cortical thinning of the supramarginal gyrus has previously been correlated with performance on a verbal WM task in a developmental sample, after correction for age (Østby et al. 2011).

Correlation between white matter structure and WM capacity is consistent with several previous developmental studies (Olesen, Nagy, et al. 2003; Nagy et al. 2004; Østby et al. 2011; Vestergaard et al. 2011). FA of the ventrofronto-striatal tract has previously been correlated with the development of response inhibition (Liston et al. 2006), but to our knowledge the fronto-striatal tract has not been associated with WM capacity.

ADHD is a neuropsychiatric disorder where WM deficits are thought to play an important role (Nigg 2001; Westerberg et al. 2004; Martinussen et al. 2005). The current associations with WM are largely overlapping with findings in ADHD subjects of thinner frontal and parietal cortex (Makris et al. 2007) as well as lower FA and fronto-parietal connections (Makris et al. 2008), suggesting that these anatomical deviations observed in ADHD could be related to cognitive impairments.

In this study, we provided results both with and without accounting for the effect of age, because correcting for age has both advantages and disadvantages. The key reason to correct for age would be to remove possible nonspecific effects of development. In the case of WM, that would be assuming that there is some factor outside the measured WM network of brain regions that is responsible for the increase in WM capacity, and that this unknown factor correlates with age. The disadvantage of correcting for age is that it only leaves variance that is independent of development, which defeats the purpose of using a developmental sample in the first place. We would thus argue that not co-varying out the effect of age gives a better estimate of the developmental aspect of WM development. The age-independent correlation, in this case the FA values of the fronto-parietal and fronto-striatal networks as well BOLD in parietal cortex, would be factors contributing to interindividual differences in WM capacity independent of development. This is also consistent with reports of such association in adult samples (Takeuchi et al. 2011).

Regarding the white matter measures and their relationship to current and future WM capacity, there was a difference in that FA values, but not volume, were significant after correcting for age. The white matter measures could be affected by many structural characteristics, such as the number, size, diameter, packing and organization of the axons, oligodendrocytes, and other extra-neuronal factors such as astrocyte changes and angiogenesis. In this study, we found that FA is less affected than white matter volume by age. If FA is less affected by age, one might speculate that the remaining relationship is influenced by some structural aspects, which do not increase with age and might be due to the genetic differences such as the number, packing, and organization of axons.

The cross-sectional analysis showed regional correlations of BOLD, cortical thickness, and FA. Correlations between fronto-parietal BOLD and FA values have previously been reported in developmental samples (Olesen, Nagy, et al. 2003; Østby et al. 2011) as well as adult samples (Burzynska et al. 2011). In another study, the relationship between the structural connection probabilities and its functional activation was trained in a least-squares linear regression model and could predict functional activation to faces in the fusiform gyrus (Saygin et al. 2011). It is also possible that the BOLD-cortical thickness correlations, as also found in adults studies (Takeuchi et al. 2014), reflect a causal influence of cortex thickness on brain activity. Regarding the relationship to white matter structures, it is difficult to directly interpret these as a causal relationship, since we did not include additional control regions outside of the WM network, and could not find evidence of any structural characteristics predicting other structural measures 2 years later (data not shown).

The longitudinal analysis provided a radically different pattern of associations. Despite being correlated with concurrent WM capacity, none of the cortical measures, neither BOLD nor thickness, predicted future WM. White matter structure, on the other hand, correlated with both concurrent measures of WM and WM capacity 2 years later. These results clearly show how the white matter integrity, specifically of fronto-parietal and fronto-striatal tracts, provides an important basis for the development of future WM capacity. The present data might suggest that the development of capacity would only emerge in connection with other regions, and the efficiency of those connections determine the rate of development.

The measures from the caudate nucleus provided a very different pattern of association with WM than all other structures: while neither volume nor activity correlated with concurrent WM, there was a significant correlation between caudal activity and WM capacity 2 years later. The importance of the caudate is also illustrated by the predictive function of the fronto-striatal connections. Moreover, there was a significant interaction of caudal activity by age, emphasizing its role in early development.

Although the caudate nucleus is connected to the prefrontal and parietal cortices (Alexander et al. 1991; Aosaki et al. 1995) and active during performance on a WM task in both nonhuman primates (Levy et al. 1997), children (Klingberg et al. 2002; Ziermans et al. 2012), and adults (McNab and Klingberg 2007), it has not specifically been related to childhood development of WM. Regarding memory and cognitive function, the caudate has mostly been linked to implicit learning and habit formation (Packard and Knowlton 2002; Graybiel 2008). In a study where nonhuman primates learned associations in a delay task, it was found that, after the rule changed, the activation of the caudate changed earlier than the cortical changes, where the latter matched the changes in behavior (Pasupathy and Miller 2005). This is consistent with the current finding where cortical activity and structure correlate with behavior, but are preceded in time by the activity of the caudate.

Studies of the neural basis of WM training (Klingberg et al. 2005; Klingberg 2010) might provide a link between the studies of implicit learning on the one hand, and cognitive development on the other. Two studies of training-induced improvements in WM have shown activity in the thalamus and caudate nucleus (Olesen, Westerberg, et al. 2003; Dahlin et al. 2008), and in one of those, the striatal activity predicted the amount of improvement seen after training (Dahlin et al. 2008). In a positron emission tomography study, improvements after WM training were associated with changes in D2 receptor occupancy of the caudate (Bäckman et al. 2011), while the change in capacity is associated with cortical D1 receptor density (McNab and Klingberg 2007). Genetic studies have found that polymorphisms related to the *DAT-1* transporter (Brehmer et al. 2009; Söderqvist et al. 2012) and *DRD2* receptor expression (Söderqvist et al. 2014) affect the amount of improvement during WM training. Both *DAT-1* and *DRD2* are preferentially expressed in the basal ganglia. Taken together, these findings suggest that there might be similarities between cognitive development during childhood, training of WM, and implicit learning, and that the caudate nucleus and the fronto-striatal

connections play a key role in the learning processes, while the capacity is more closely related to cortical processes.

In conclusion, these results suggest a dynamic of the neural systems underlying WM development, where cortical activity and structure are closely related to current WM, while the subcortical white matter tracts and activity in the caudate are preceding these changes and predict future WM capacity.

Notes

Conflict of Interest: None declared.

References

Alexander GE, Crutcher MD, DeLong MR. 1991. Basal ganglia-thalamocortical circuits: parallel substrates for motor, oculomotor, "prefrontal" and "limbic" functions. Prog Brain Res. 85:119–146.

Alloway T. 2007. Automated working memory assessment manual. Oxford: Harcourt.

Aosaki T, Kimura M, Graybiel A. 1995. Temporal and spatial characteristics of tonically active neurons of the primate's striatum. J Neurophysiol. 73:1234–1252.

Bäckman L, Nyberg L, Soveri A, Johansson J, Andersson M, Dahlin E, Neely AS, Virta J, Laine M, Rinne JO. 2011. Effects of working-memory training on striatal dopamine release. Science. 333:718.

Brehmer Y, Westerberg H, Bellander M, Fürth D, Karlsson S, Bäckman L. 2009. Working memory plasticity modulated by dopamine transporter genotype. Neurosci Lett. 467:117–120.

Brett M, Anton J-L, Valabregue R, Poline J-B. 2002. Region of interest analysis using the MarsBar toolbox for SPM 99. Neuroimage. 16: S497.

Burzynska AZ, Nagel IE, Preuschhof C, Li S-C, Lindenberger U, Bäckman L, Heekeren HR. 2011. Microstructure of frontoparietal connections predicts cortical responsivity and working memory performance. Cereb Cortex. 21:2261–2271.

Camos V. 2008. Low working memory capacity impedes both efficiency and learning of number transcoding in children. J Exp Child Psychol. 99:37–57.

Crone EA, Wendelken C, Donohue S, van Leijenhorst L, Bunge SA. 2006. Neurocognitive development of the ability to manipulate information in working memory. Proc Natl Acad Sci. 103:9315–9320.

Dahlin E, Neely AS, Larsson A, Bäckman L, Nyberg L. 2008. Transfer of learning after updating training mediated by the striatum. Science. 320:1510–1512.

Dale AM, Fischl B, Sereno MI. 1999. Cortical surface-based analysis: I. Segmentation and surface reconstruction. Neuroimage. 9:179–194.

Dumontheil I, Klingberg T. 2012. Brain activity during a visuospatial working memory task predicts arithmetical performance 2 years later. Cereb Cortex. 22:1078–1085.

Dumontheil I, Roggeman C, Ziermans T, Peyrard-Janvid M, Matsson H, Kere J, Klingberg T. 2011. Influence of the COMT genotype on working memory and brain activity changes during development. Biol Psychiatry. 70:222–229.

Fischl B, Dale AM. 2000. Measuring the thickness of the human cerebral cortex from magnetic resonance images. Proc Natl Acad Sci. 97:11050–11055.

Fitzmaurice GM, Laird NM, Ware JH. 2012. Applied longitudinal analysis. John Wiley and Sons.

Gathercole SE, Brown L, Pickering SJ. 2003. Working memory assessments at school entry as longitudinal predictors of National Curriculum attainment levels. Educ Child Psychol. 20:109–122.

Graybiel AM. 2008. Habits, rituals, and the evaluative brain. Annu Rev Neurosci. 31:359–387.

Klingberg T. 2006. Development of a superior frontal? Intraparietal network for visuo-spatial working memory. Neuropsychologia. 44:2171–2177.

Klingberg T. 2010. Training and plasticity of working memory. Trends Cogn Sci. 14:317–324.

Klingberg T, Fernell E, Olesen PJ, Johnson M, Gustafsson P, Dahlström K, Gillberg CG, Forssberg H, Westerberg H. 2005. Computerized training of working memory in children with ADHD—a randomized, controlled trial. J Am Acad Child Adolesc Psychiatry. 44:177–186.

Klingberg T, Forssberg H, Westerberg H. 2002. Increased brain activity in frontal and parietal cortex underlies the development of visuospatial working memory capacity during childhood. J Cogn Neurosci. 14:1–10.

Kwon H, Reiss AL, Menon V. 2002. Neural basis of protracted developmental changes in visuo-spatial working memory. Proc Natl Acad Sci. 99:13336–13341.

Leh SE, Johansen-Berg H, Ptito A. 2006. Unconscious vision: new insights into the neuronal correlate of blindsight using diffusion tractography. Brain. 129:1822–1832.

Levy R, Friedman HR, Davachi L, Goldman-Rakic PS. 1997. Differential activation of the caudate nucleus in primates performing spatial and nonspatial working memory tasks. J Neurosci. 17:3870–3882.

Liston C, Watts R, Tottenham N, Davidson MC, Niogi S, Ulug AM, Casey B. 2006. Frontostriatal microstructure modulates efficient recruitment of cognitive control. Cereb Cortex. 16:553–560.

Makris N, Biederman J, Valera EM, Bush G, Kaiser J, Kennedy DN, Caviness VS, Faraone SV, Seidman LJ. 2007. Cortical thinning of the attention and executive function networks in adults with attention-deficit/hyperactivity disorder. Cereb Cortex. 17:1364–1375.

Makris N, Buka SL, Biederman J, Papadimitriou GM, Hodge SM, Valera EM, Brown AB, Bush G, Monuteaux MC, Caviness VS. 2008. Attention and executive systems abnormalities in adults with childhood ADHD: a DT-MRI study of connections. Cereb Cortex. 18:1210–1220.

Martinussen R, Hayden J, Hogg-Johnson S, Tannock R. 2005. A meta-analysis of working memory impairments in children with attention-deficit/hyperactivity disorder. J Am Acad Child Adolesc Psychiatry. 44:377–384.

McLean JF, Hitch GJ. 1999. Working memory impairments in children with specific arithmetic learning difficulties. J Exp Child Psychol. 74:240–260.

McNab F, Klingberg T. 2007. Prefrontal cortex and basal ganglia control access to working memory. Nat Neurosci. 11:103–107.

Nagy Z, Westerberg H, Klingberg T. 2004. Maturation of white matter is associated with the development of cognitive functions during childhood. J Cogn Neurosci. 16:1227–1233.

Nigg JT. 2001. Is ADHD a disinhibitory disorder? Psychol Bull. 127:571.

Olesen PJ, Macoveanu J, Tegnér J, Klingberg T. 2007. Brain activity related to working memory and distraction in children and adults. Cereb Cortex. 17:1047–1054.

Olesen PJ, Nagy Z, Westerberg H, Klingberg T. 2003. Combined analysis of DTI and fMRI data reveals a joint maturation of white and grey matter in a fronto-parietal network. Cogn Brain Res. 18: 48–57.

Olesen PJ, Westerberg H, Klingberg T. 2003. Increased prefrontal and parietal activity after training of working memory. Nat Neurosci. 7:75–79.

Østby Y, Tamnes CK, Fjell AM, Walhovd KB. 2011. Morphometry and connectivity of the fronto-parietal verbal working memory network in development. Neuropsychologia. 49:3854–3862.

Packard MG, Knowlton BJ. 2002. Learning and memory functions of the basal ganglia. Annu Rev Neurosci. 25:563–593.

Pasupathy A, Miller EK. 2005. Different time courses of learning-related activity in the prefrontal cortex and striatum. Nature. 433:873–876.

Postle BR, Zarahn E, D'Esposito M. 2000. Using event-related fMRI to assess delay-period activity during performance of spatial and nonspatial working memory tasks. Brain Res Protoc. 5:57–66.

Reuter M, Fischl B. 2011. Avoiding asymmetry-induced bias in longitudinal image processing. Neuroimage. 57:19–21.

Reuter M, Rosas HD, Fischl B. 2010. Highly accurate inverse consistent registration: a robust approach. Neuroimage. 53:1181–1196.

Reuter M, Schmansky NJ, Rosas HD, Fischl B. 2012. Within-subject template estimation for unbiased longitudinal image analysis. Neuroimage. 61:1402–1418.

Saygin ZM, Osher DE, Koldewyn K, Reynolds G, Gabrieli JD, Saxe RR. 2011. Anatomical connectivity patterns predict face selectivity in the fusiform gyrus. Nat Neurosci. 15:321–327.
Scherf KS, Sweeney JA, Luna B. 2006. Brain basis of developmental change in visuospatial working memory. J Cogn Neurosci. 18:1045–1058.
Shaw P, Greenstein D, Lerch J, Clasen L, Lenroot R, Gogtay N, Evans A, Rapoport J, Giedd J. 2006. Intellectual ability and cortical development in children and adolescents. Nature. 440:676–679.
Söderqvist S, Bergman Nutley S, Peyrard-Janvid M, Matsson H, Humphreys K, Kere J, Klingberg T. 2012. Dopamine, working memory, and training induced plasticity: Implications for developmental research. Dev Psychol. 48:836.
Söderqvist S, Matsson H, Peyrard-Janvid M, Kere J, Klingberg T. 2004. Polymorphisms in the dopamine receptor 2 gene region influence improvements during working memory training in children and adolescents. J Cogn Neurosci. 26:56–62.
Söderqvist S, McNab F, Peyrard-Janvid M, Matsson H, Humphreys K, Kere J, Klingberg T. 2010. The SNAP25 gene is linked to working memory capacity and maturation of the posterior cingulate cortex during childhood. Biol Psychiatry. 68:1120–1125.
Sowell ER, Thompson PM, Leonard CM, Welcome SE, Kan E, Toga AW. 2004. Longitudinal mapping of cortical thickness and brain growth in normal children. J Neurosci. 24:8223–8231.
Szucs D, Devine A, Soltesz F, Nobes A, Gabriel F. 2013. Developmental dyscalculia is related to visuo-spatial memory and inhibition impairment. Cortex. 49:2674–2688.
Takeuchi H, Taki Y, Nouchi R, Hashizume H, Sassa Y, Sekuguchi A, Kotozaki Y, Nakagawa S, Nagase T, Miyauchi CM. 2014. Associations among imaging measures (2): The association between gray matter concentration and task-induced activation changes. Hum Brain Mapp. 35:185–198.
Takeuchi H, Taki Y, Sassa Y, Hashizume H, Sekiguchi A, Fukushima A, Kawashima R. 2011. Verbal working memory performance correlates with regional white matter structures in the frontoparietal regions. Neuropsychologia. 49:3466–3473.
Tamnes CK, Fjell AM, Østby Y, Westlye LT, Due-Tønnessen P, Bjørnerud A, Walhovd KB. 2011. The brain dynamics of intellectual development: Waxing and waning white and gray matter. Neuropsychologia. 49:3605–3611.
Tamnes CK, Østby Y, Walhovd KB, Westlye LT, Due-Tønnessen P, Fjell AM. 2010. Neuroanatomical correlates of executive functions in children and adolescents: a magnetic resonance imaging (MRI) study of cortical thickness. Neuropsychologia. 48:2496–2508.
Tamnes CK, Walhovd KB, Grydeland H, Holland D, Ostby Y, Dale AM, Fjell AM. 2013. Longitudinal working memory development is related to structural maturation of frontal and parietal cortices. J Cogn Neurosci. 25:1611–1623.
Ullman H, Almeida R, Klingberg T. 2014. Structural maturation and brain activity predict future working memory capacity during childhood development. J Neurosci.
Vestergaard M, Madsen KS, Baaré WF, Skimminge A, Ejersbo LR, Ramsøy TZ, Gerlach C, Åkeson P, Paulson OB, Jernigan TL. 2011. White matter microstructure in superior longitudinal fasciculus associated with spatial working memory performance in children. J Cogn Neurosci. 23:2135–2146.
Wendelken C, O'Hare ED, Whitaker KJ, Ferrer E, Bunge SA. 2011. Increased functional selectivity over development in rostrolateral prefrontal cortex. J Neurosci. 31:17260–17268.
Westerberg H, Hirvikoski T, Forssberg H, Klingberg T. 2004. Visuo-spatial working memory span: a sensitive measure of cognitive deficits in children with ADHD. Child Neuropsychol. 10: 155–161.
Ziermans T, Dumontheil I, Roggeman C, Peyrard-Janvid M, Matsson H, Kere J, Klingberg T. 2012. Working memory brain activity and capacity link MAOA polymorphism to aggressive behavior during development. Transl Psychiatry. 2:e85.